AD A102637

DTIC FILE COPY

REPORT DOCUMENTATION PAGE		READ INSTRUCTIONS BEFORE COMPLETING FORM
1. REPORT NUMBER N00014-77-C-0319	2. GOVT ACCESSION NO. AD-A102637	3. RECIPIENT'S CATALOG NUMBER
4. TITLE (and Subtitle) THIN FILMS, SURFACES AND INTERFACES: A FOURIER-TRANSFORM THEORY OF THEIR ELECTRONIC STRUCTURE		5. TYPE OF REPORT & PERIOD COVERED Final 5/1/77-4/30/80
		6. PERFORMING ORG. REPORT NUMBER
7. AUTHOR(s) Frank E. Harris		8. CONTRACT OR GRANT NUMBER(s) N00014-77-C-0319
9. PERFORMING ORGANIZATION NAME AND ADDRESS University of Utah Salt Lake City, Utah 84112		10. PROGRAM ELEMENT, PROJECT, TASK AREA & WORK UNIT NUMBERS 318-056
11. CONTROLLING OFFICE NAME AND ADDRESS Office of Naval Research 800 N. Quincy Street Arlington, Virginia 22217		12. REPORT DATE 15 May 1981
		13. NUMBER OF PAGES
14. MONITORING AGENCY NAME & ADDRESS(if different from Controlling Office) ONR Branch Office 1030 E. Green Street Pasadena, California 91106		15. SECURITY CLASS. (of this report) Unclassified
		15a. DECLASSIFICATION/DOWNGRADING SCHEDULE

16. DISTRIBUTION STATEMENT (of this Report)

Unlimited - Unclassified

DISTRIBUTION STATEMENT A
Approved for public release;
Distribution Unlimited

17. DISTRIBUTION STATEMENT (of the abstract entered in Block 20, if different from Report)

DTIC
AUG 1 0 1981
C

18. SUPPLEMENTARY NOTES

19. KEY WORDS (Continue on reverse side if necessary and identify by block number)

Film, Surface, Interface, Theory, Fourier, Electronic, Structure, Lattice, Sum, Hartree-Fock

20. ABSTRACT (Continue on reverse side if necessary and identify by block number)

Presents mathematical topics needed to carry out ab initio electronic structure calculations on surface or interfacial systems. Includes a study of methods for Brillouin-zone integrations, an analysis of electrostatic energies in periodic films, convergence acceleration techniques for lattice sums, and a general exposition of the formulation of the Hartree-Fock method for systems with two-dimensional periodicity.

DD FORM 1473 EDITION OF 1 NOV 65 IS OBSOLETE
1 JAN 73
S/N 0102-LF-014-6601

81 8 10 002

THIN FILMS, SURFACES AND INTERFACES: A FOURIER-TRANSFORM

THEORY OF THEIR ELECTRONIC STRUCTURE

Frank E. Harris
University of Utah
Salt Lake City, Utah 84112

15 May 1981

Final Report for Period 1 May 1977 - 30 April 1980.

Prepared for

Introduction

The general aim of the subject contract was to support studies in which Fourier representation techniques were used to facilitate ab initio studies of the electronic structures of thin-film, surface, and interfacial systems without the approximations ordinarily introduced to handle the exchange energy. The work is reported in detail in the eight technical publications produced under the contract.

Personnel

The work under the contract was supervised and contributed to by Dr. Frank E. Harris (Professor of Physics and Chemistry) and Dr. Hendrik J. Monkhorst (Research Associate Professor of Physics). For the first two years, Dr. Harris was the principal investigator; for the third and final year this responsibility was shared by Drs. Harris and Monkhorst. Major amounts of work were also performed by Dr. William A. Schwalm (Postdoctoral Research Associate). Effort for shorter periods of time was provided by Dr. Tomislav P. Zivkovic, Dr. Bogumil Jeziorski, and Mr. James D. Pack. Dr. K. Szalewicz collaborated with us in one technical report.

Narrative Summary

Much of the work under the contract involved the resolution of technical questions prerequisite to calculations on actual systems. The general methods to be used are described in technical publications 4, 5, and 6 (vide infra). Evaluation of the lattice sums describing the long-range electrostatic interactions are reported in publications 1 and 8. Techniques for sums over states are discussed in publication 2. Publications 3 and 7 deal with questions arising out of the mathematics of the analysis. These studies complete the material prerequisite to actual calculations; a study of hydrogen films (not reported here) has been completed subsequent to the expiration of this contract.

Technical Publications

1. "Convergence Acceleration Techniques for Lattice Sums Arising in Electronic Structure Studies of Crystalline Solids", F. E. Harris, J. Math. Phys. 18, 2377 (1977).

2. "Special Points for Brillouin-Zone Integrations--A Reply", J. D. Pack and H. J. Monkhorst, Phys. Rev. B 16, 1748 (1977).

3. "Analytic Connection between Configuration-Interaction and Coupled-Cluster Methods", T. P. Zivkovic and H. J. Monkhorst, J. Math. Phys. 19, 1007 (1978).

4. "Hartree-Fock Density-of-States for Extended Systems", H. J. Monkhorst, Phys. Rev. B 20, 1504 (1979).

5. "Exact LCAO Method for Two-Dimensional Crystals Using Fourier Transform Technique", H. J. Monkhorst (not published).

6. "Hartree-Fock Formalism for the Calculation of Total Energies and Charge Densities of Thin Films", F. E. Harris, H. J. Monkhorst, and W. A. Schwalm, J. Vac. Sci & Tech. 16, 1318 (1979).

7. "Analytic Continuation in Exchange Perturbation Theory", B. Jeziorski, W. A. Schwalm, and K. Szalewicz, J. Chem. Phys. 73, 6215 (1980).

8. "Electrostatics for Periodic Films of Atoms", H. J. Monkhorst and W. A. Schwalm, Phys. Rev. B 23, 1729 (1981).

Appendix A.

Copies of technical publications

Convergence acceleration technique for lattice sums arising in electronic-structure studies of crystalline solids[a]

Frank E. Harris[b]

Department of Chemistry, University of Hawaii at Manoa, 2545 The Mall, Honolulu, Hawaii 96822
(Received 24 June 1977)

Slowly convergent lattice summations arise when *ab initio* quantum-mechanical studies of electronic structure in crystalline solids are carried out by Fourier representation methods. Summations of this type are identified and discussed, and it is shown how a technique related to, but not identical with, that of Ewald can be used to accelerate their convergence. The presentation is illustrated with numerical examples.

I. INTRODUCTION

It is well known that lattice sums of electrostatic energy contributions (Madelung sums) converge so slowly that convergence acceleration schemes are of great importance. This observation is not only relevant for the conditionally convergent summations describing the potentials of charge arrays, but also applies to systems of higher-order multipoles for which there are no formal convergence difficulties. Illustrative of the problem is the summation of r^{-6} over the nonzero points of a simple cubic lattice. To obtain this sum to five significant figures, it is necessary to include points out to approximately $r = 10$, a total of over 4,000 points. Allowance for the crystal symmetry would reduce the sum to that of approximately 150 inequivalent points, but in actual applications the distances may be measured from a low-symmetry point or occur with an offset (e.g., $|r^2 + \delta^2|^{-4}$). We see that from a practical viewpoint the convergence difficulties of inverse power summations persist to surprisingly high powers.

The two best-known methods for accelerating convergence of Madelung sums are those of Evjen[1] and Ewald.[2] The Ejven method consists of grouping together the contributions of shells of points in such a way that the low-order multipole moments of each shell vanish. The result is that the contributions of shells fall off with increasing distance more rapidly than do the contributions of individual points. We shall not discuss the Evjen method further in this paper, because it is not directly applicable to summations where all points make contributions of the same sign. The Ewald method involves the introduction of an integral transform for the potential, followed by a division of the transform integration into two ranges, each of which is then treated separately. From one integration range there emerges a summation which converges more rapidly than the original sum. For the other integration range, the Poisson summation formula[3] is used to replace the summands by their Fourier transforms, after which that sum also becomes rapidly convergent.

When *ab initio* quantum-mechanical studies of the electronic structures of crystalline solids are developed

in a Fourier representation formulation,[4] there arise Madelung-type summations of the sorts and with the problems identified above. It is therefore highly desirable to apply convergence acceleration techniques to such summations, but they differ from those previously studied to an extent which renders impractical the usual acceleration techniques. The purpose of this paper is to present and illustrate a method by which the most time-consuming summations in *ab initio* quantum-mechanical calculations on solids can be evaluated more accurately and conveniently.

In succeeding sections of this paper we describe briefly the physical problems giving rise to the summations whose evaluations we seek, we give alternative (unaccelerated) forms of these sums, and we present an acceleration technique in the spirit of, but not identical with that of Ewald. Illustrative results indicate the effectiveness of the method.

II. PHYSICAL BACKGROUND

Fourier representation techniques have been used for the evaluation of the multicenter integrals arising in electronic structure calculations.[5] In such approaches a key quantity is the Fourier transform of a product of atomic orbitals. For example, the electron repulsion integral $\langle \varphi_a \varphi_c | r_{12}^{-1} | \varphi_b \varphi_d \rangle$ is given by the well-known formula

$$\langle \varphi_a \varphi_c | r_{12}^{-1} | \varphi_b \varphi_d \rangle = \frac{1}{2\pi^2} \int \frac{d\mathbf{q}}{q^2} \exp(-i\mathbf{q} \cdot \mathbf{R}_{ac})$$
$$\times \phi_{ab}^T(\mathbf{q}) \phi_{cd}^T(-\mathbf{q}), \qquad (1)$$

with $\mathbf{R}_{ac} = \mathbf{R}_c - \mathbf{R}_a$, $\mathbf{R}_a$ the center for orbital φ_a, and

$$\phi_{ab}^T(\mathbf{q}) = \langle \varphi_a(\mathbf{r}) | \exp(i\mathbf{q} \cdot \mathbf{r}) | \varphi_b(\mathbf{r} - \mathbf{R}_{ab}) \rangle. \qquad (2)$$

Equation (2) shows ϕ_{ab}^T to be the Fourier transform of $\varphi_a^* \varphi_b$ in a coordinate system with origin at $\mathbf{R}_a$. When φ_a and φ_b are Slater-type orbitals (STO's), the right-hand side of Eq. (2) is cumbersome to evaluate but can be reduced either to a single quadrature or to an infinite series of Bessel functions.[5] However, for $q = 0$, ϕ_{ab}^T assumes a simple form; it is then the overlap integral $\langle \varphi_a | \varphi_b \rangle$.

Expressions parallel to Eqs. (1) and (2) arise when Fourier representation methods are used for electronic-structure calculations on crystalline solids.[4] As an example, consider the use of Bloch-wave crystal

orbitals $|k_a\rangle$, defined as

$$|k_a\rangle = \exp(ik \cdot r)\sum_\mu \varphi_a(r - R_\mu), \qquad (3)$$

where k is the Bloch wave vector and the R_μ are the lattice vectors. The index "a" denotes the functional form of φ_a. This definition of $|k_a\rangle$ is of what we call "modulated plane wave" type, and shares with the usual linear-combination-of-atomic-orbital (LCAO) or "tight-binding" orbitals the calculational features described below. In terms of these crystal orbitals, the electron repulsion integrals of interest are $\langle k_a k_c' | r_{12}^{-1} | k_b k_d'\rangle$ and $\langle k_a k_c' | r_{12}^{-1} | k_b' k_d\rangle$; the first of these integrals diverges faster than the sample size increases, but the divergence is offset by those of the electron—nuclear attraction integrals $\langle k_a | \sum_\mu |r - R_\mu|^{-1} | k_b\rangle$ and the nuclear—nuclear repulsions.

The nondivergent (i.e., properly extensive) part of $\langle k_a k_c' | r_{12}^{-1} | k_b k_d'\rangle$ may be reduced to the form

$$\langle k_a k_c' | r_{12}^{-1} | k_b k_d'\rangle = \frac{4\pi N}{v_0}\sum_\mu{}' \frac{1}{q_\mu^2}\Phi_{ab}^T(q_\mu)\Phi_{cd}^T(-q_\mu), \qquad (4)$$

where N is the number of unit cells in the sample, the q_μ are the vectors of the lattice reciprocal to the R_μ, and v_0 is the unit-cell volume of the R_μ lattice. The prime on the summation sign indicates that the point $q_\mu = 0$ is to be omitted from the sum. The Φ^T are transforms of lattice sums of atomic—orbital products, and are therefore linear combinations of the ϕ^T appearing in Eq. (2):

$$\Phi_{ab}^T(q) = \sum_\mu \langle \varphi_a(r) | \exp(iq \cdot r) | \varphi_b(r - R_\mu)\rangle. \qquad (5)$$

The integrals $\langle k_a k_c' | r_{12}^{-1} | k_b' k_d\rangle$ and the nondivergent part of $\langle k_a | \sum_\mu |r - R_\mu|^{-1} | k_b\rangle$ also reduce to summations involving Φ^T. The overlap integral $\langle k_a | k_b\rangle$ assumes the simple form

$$\langle k_a | k_b\rangle = N\Phi_{ab}^T(0). \qquad (6)$$

Crystalline solids appear to be far more economically described when the atomic orbitals appearing in Eq. (3) are chosen to be STO's rather than the historially more popular Gaussian-type orbitals. Fortunately, an STO-based formulation is practical, as the quantities Φ_{ab}^T of Eq. (5) can be reduced to readily manipulable forms. Although the individual summands of Eq. (5) are difficult to calculate [cf. the discussion immediately following Eq. (2)], the equation can be made tractable by taking advantage of the presence of the lattice sum. A number of calculations based on Eqs. (4) and (5) have now been reported.

While the work done to date suffices to demonstrate the practicality of Fourier representation methods for solid-state electronic structure studies, it has also shown that the evaluation of Eq. (5) consumes the bulk of the required computational effort, and that the root of the problem is the slow rate of convergence of the lattice sum involved. We therefore turn our attention to methods for the evaluation of Eq. (5), and more specifically to the introduction of convergence acceleration techniques of the kinds already found to be useful in Madelung summations.

III. EVALUATION OF Φ_{ab}^T (q)

We now consider more specifically the evaluation of Eq. (5) when φ_a and φ_b are normalized 1s STO's:

$$\varphi_a = (\zeta_a^3/\pi)^{1/2}\exp(-\zeta_a r). \qquad (7)$$

Expressions involving STO's of higher quantum numbers can be derived by analogy or by differentiating the results given here with respect to the screening parameters ζ_a and ζ_b. Inserting Eq. (7) into Eq. (5),

$$\Phi_{ab}^T(q) = [(\zeta_a\zeta_b)^{3/2}/\pi]\sum_\mu\int dr$$

$$\times \exp(-\zeta_a r - \zeta_b|r - R_\mu| + iq \cdot r). \qquad (8)$$

The integral on the right-hand side of Eq. (8) is that which was earlier identified as cumbersome to evaluate. For simplicity we assume a simple cubic lattice.

The most straightforward evaluation of Φ_{ab}^T is obtained by using the Fourier convolution theorem to write

$$\Phi_{ab}^T(q) = [1/(2\pi)^3]\sum_\mu\int dp\, \varphi_a^T(q - p)[\varphi_b(r - R_\mu)]^T(p). \qquad (9)$$

Introducing the expression for the transform of the 1s STO,

$$\varphi_a^T(q) = 8\pi^{1/2}\zeta_a^{5/2}/(q^2 + \zeta_a^2)^2, \qquad (10)$$

and noting that

$$[\varphi(r - R_\mu)]^T(p) = \exp(iR_\mu \cdot p)\varphi^T(p), \qquad (11)$$

we have

$$\Phi_{ab}^T(q) = \frac{8(\zeta_a\zeta_b)^{5/2}}{\pi^2}\sum_\mu\int dp$$

$$\times \frac{1}{(|q - p|^2 + \zeta_a^2)^2}\frac{\exp(iR_\mu \cdot p)}{(p^2 + \zeta_b^2)^2}. \qquad (12)$$

Next, we interchange the order of summation and integration in Eq. (12), reaching thereby a lattice sum satisfying[7]

$$\sum_\mu \exp(iR_\mu \cdot p) = (8\pi^3/v_0)\sum_\mu \delta(p - p_\mu), \qquad (13)$$

where the p_μ are reciprocal-lattice vectors. Equation (13) is sometimes referred to as a "lattice orthogonality relation", and is a special case of a Poisson summation formula, the summands on its right-hand side being Fourier transforms of those on its left. When the right side of Eq. (13) is substituted into Eq. (12), the p integration reduces to a lattice sum, and we have the final result

$$\Phi_{ab}^T(q) = \frac{64\pi(\zeta_a\zeta_b)^{5/2}}{v_0}$$

$$\times \sum_\mu \frac{1}{(|q - p_\mu|^2 + \zeta_a^2)^2(p_\mu^2 + \zeta_b^2)^2}. \qquad (14)$$

Equations (8) and (14) may be regarded as the two "standard" ways to express Φ_{ab}^T as a lattice sum. To simplify further discussion, we recapitulate these equations in a dimensionless notation in which the summations are over a unit lattice of vectors μ, and write $v_0 = a^3$, $\delta_i = a\zeta_i/2\pi$, $q = 2\pi\nu/a$:

$$\Phi_{ab}^T(\nu) = \frac{(\delta_a\delta_b)^{3/2}}{\pi}\sum_\mu\int dr$$

$$\times \exp(-\delta_a r - \delta_b |\mathbf{r} - 2\pi\mu| + i\nu\cdot\mathbf{r}) \qquad (15)$$

$$= \frac{8(\delta_a\delta_b)^{5/2}}{\pi^2}\sum_\mu \frac{1}{(|\nu-\mu|^2+\delta_a^2)^2(\mu^2+\delta_b^2)^2}. \qquad (16)$$

Leaving aside for the moment the very real differences in ease of evaluation of the summands of Eqs. (15) and (16), we note that the summation of Eq. (15) will converge rapidly when δ_a or δ_b is large, but only slowly when both δ_a and δ_b are small. We note also that the convergence will be exponential (as that of a three-dimensional *geometric series*). On the other hand, Eq. (16) will converge rapidly when δ_a or δ_b is small, but will become inappropriate when δ_a and δ_b are both large. The summation of Eq. (16) approaches for large μ that of μ^{-8}, with the disadvantages identified for such sums in the introduction.

Remembering now that the summands of Eq. (15) are relatively difficult to evaluate, we may appreciate the real problem in the evaluation of Φ_{ab}^T. We should like to have at least part of the convenience of Eq. (16), but in a context improving its convergence, particularly for large δ_a and δ_b. We cannot really afford to use Eq. (15) unless δ_a and δ_b are so large that extremely few terms are required.

IV. ACCELERATION OF CONVERGENCE

Following the general idea of the Ewald method, we introduce integral transforms for φ_a and φ_b in Eq. (5), planning to divide the integrations into regions each of which will receive optimal further processing. The transform we have found most suitable is that suggested by Kikuchi[8] and subsequently used by Shavitt and Karplus[9]:

$$\exp(-\delta r) = \frac{\delta}{\pi^{1/2}}\int_0^\infty dx\, x^{-1/2}\exp(-x\delta^2 - r^2/4x). \qquad (17)$$

Insertion of Eq. (17) for $\exp(-\delta_a r)$ and $\exp(-\delta_b|\mathbf{r}-2\pi\mu|)$ in Eq. (15) [the dimensionless equivalent of Eq. (5)] yields

$$\Phi_{ab}^T(\nu) = \frac{(\delta_a\delta_b)^{5/2}}{\pi^2}\sum_\mu\int_0^\infty dx\int_0^\infty dy (xy)^{-1/2}$$
$$\times \exp(-\delta_a^2 x - \delta_b^2 y)\int d\mathbf{r}\exp\left(-\frac{r^2}{4x}-\frac{|\mathbf{r}-2\pi\mu|^2}{4y}\right.$$
$$\left. + i\nu\cdot\mathbf{r}\right). \qquad (18)$$

The $\mathbf{r}$ integration may now be carried out, leading to the result

$$\Phi_{ab}^T(\nu) = \frac{8(\delta_a\delta_b)^{5/2}}{\pi^{1/2}}\sum_\mu\int_0^\infty dx\int_0^\infty dy\frac{xy}{(x+y)^{3/2}}$$
$$\times \exp\left(-\delta_a^2 x - \delta_b^2 y - \frac{\nu^2 xy}{x+y}-\frac{\pi^2\mu^2}{x+y}+\frac{2\pi i x\mu\cdot\nu}{x+y}\right). \qquad (19)$$

We next notice that the μ summation will converge at a rate mainly determined by the magnitude of $x+y$. We therefore change variables from x, y to s, t, where $s = x+y$, $t = (x-y)/(x+y)$, with limits $0 \leq s < \infty$, $-1 \leq t \leq 1$, and with $dx\,dy = \frac{1}{2}s\,ds\,dt$:

$$\Phi_{ab}^T(\nu) = \frac{(\delta_a\delta_b)^{5/2}}{\pi^{1/2}}\sum_\mu\int_0^\infty ds\int_{-1}^1 dt\, s^{3/2}(1-t^2)$$
$$\times \exp(-\gamma s - \pi^2\mu^2/s + \pi i(1+t)\mu\cdot\nu), \qquad (20)$$

with

$$\gamma = \tfrac{1}{2}\delta_a^2(1+t) + \tfrac{1}{2}\delta_b^2(1-t) + \tfrac{1}{4}\nu^2(1-t^2). \qquad (21)$$

We are now ready to divide the range of s into the two intervals $(0, Z)$ and (Z, ∞), where Z is arbitrary and will be specified later. For the first of these intervals the μ sum will be strongly convergent, in fact converging as $\exp(-\pi^2\mu^2/Z)$. For the remaining interval, the convergence is poor, but can be improved by use of the Poisson summation formula

$$\sum_\mu\exp(-\pi^2\mu^2/s + \pi i(1+t)\mu\cdot\nu)$$
$$= \left(\frac{s}{\pi}\right)^{3/2}\sum_\mu\exp[-s|\mu - \tfrac{1}{2}(1+t)\nu|^2]. \qquad (22)$$

After substitution of Eq. (22) for (Z, ∞), the integrations in both s and t may be carried out, leading to the final result

$$\Phi_{ab}^T(\nu) = \frac{(\delta_a\delta_b)^{5/2}}{\pi^{1/2}}\sum_\mu\int_0^Z ds\int_{-1}^1 dt\, s^{3/2}(1-t^2)$$
$$\times \exp[-\gamma s - \pi^2\mu^2/s + \pi i(1+t)\mu\cdot\nu]$$
$$+ \frac{8(\delta_a\delta_b)^{5/2}}{\pi^2}\sum_\mu\left[\frac{\exp(-\alpha Z)}{\alpha(\alpha-\beta)^2}\left(\frac{2}{\alpha-\beta}-\frac{1}{\alpha}+Z\right)\right.$$
$$\left. + \frac{\exp(-\beta Z)}{\beta(\beta-\alpha)^2}\left(\frac{2}{\beta-\alpha}+\frac{1}{\beta}+Z\right)\right], \qquad (23)$$

with

$$\alpha = |\mu-\nu|^2 + \delta_a^2, \qquad (24)$$

$$\beta = \mu^2 + \delta_b^2. \qquad (25)$$

If there is a μ value such that $\alpha = \beta$, the square bracket on the right-hand side of Eq. (23) must be replaced for that μ value by

$$\left[\quad\right] = \frac{\exp(-\alpha Z)}{\alpha}\left(\frac{Z^3}{6}+\frac{Z^2}{2\alpha}+\frac{Z}{\alpha^2}+\frac{1}{\alpha^3}\right) \quad (\alpha=\beta). \qquad (26)$$

We note that the portion of Eq. (23) corresponding to the interval (Z, ∞) now exhibits convergence as $\exp(-\mu^2 Z)$.

Equation (23) possesses the convergence acceleration properties we seek. The value of Z remains to be chosen; it determines the relative importance of the two μ summations. In the limit $Z \to 0$, the first sum vanishes while the second approaches that of Eq. (16); in the limit $Z \to \infty$ only the first sum survives, and it can be shown equivalent to Eq. (15). Intermediate values of Z give pairs of series corresponding roughly to Eqs. (15) and (16), but each converging more rapidly than the limiting series to which it corresponds. Remembering that the first summation contains summands which are harder to evaluate than those of the second sum, we may choose Z small enough that very few terms of the first summation are needed, but with Z sufficiently far from zero that we have effective exponential convergence in the second sum.

V. NUMERICAL EXAMPLES

For illustrative purposes we elect to aim for seven significant figures and to choose Z small enough that in the first sum of Eq. (23) we will need to keep only $\mu = 0$ and the six members of the $(1, 0, 0)$ star

$[\mu = (1, 0, 0), (-1, 0, 0), (0, 1, 0), (0, -1, 0), (0, 0, 1),$ $(0, 0, -1)]$. The leading terms omitted from the first sum will have $\mu^2 = 2$, and can be expected to be smaller than the $\mu = 0$ term by approximately the factor $\exp(-2\pi^2/Z)$, ignoring any additional convergence which may be produced by large values of δ_a or δ_b. We therefore tentatively take $Z = 1$, causing the six omitted terms with $\mu^2 = 2$ to aggregate to about 10^{-8} or less of the leading term. Details of the calculation of the above-described terms are given in an appendix.

In evaluating the second sum, we note that the $\exp(-\alpha Z)$ portion of the summand is maximal when $\mu \approx \nu$, while the $\exp(-\beta Z)$ portion peaks at $\mu = 0$. We therefore reorganize the sum so as to keep for each portion a set of terms radiating spherically out from its respective maximum. With $Z = 1$ our accuracy requirements will be met if we keep μ values within spheres of radius $\sqrt{18+}$ about the maxima. There are 20 stars of μ values within such a sphere.

For the purpose of presenting numerical results, we write Eq. (23) in the form

$$\Phi_{ab}^{T}(\nu) = SZ(0) + SZ(1, 0, 0) + LZ, \qquad (27)$$

where $SZ(0)$ and $SZ(1, 0, 0)$ are the respective contributions of the $\mu = 0$ and $(1, 0, 0)$ stars to the first (small-Z) summation, and LZ is the contribution of the second (large-Z) summation. Table I gives the results of a number of calculations for various δ_a, δ_b, and ν values, both for $Z = 1$ and for other Z values. The accuracy of the results is attested to by their substantial independence of Z; the effectiveness of the formulation is indicated by the fact that some of the quoted results would have required thousands of terms if evaluated without a convergence acceleration technique.

ACKNOWLEDGMENTS

APPENDIX: EVALUATION OF "SMALL-Z" SUMMANDS

The $\mu = 0$ term, denoted $SZ(0)$ in Eq. (27), can be completely reduced to a closed expression involving the error function. It is convenient to introduce the definitions

$$F(u) = u^{-1/2} \, \text{erf}(u^{1/2}) = \frac{2}{\sqrt{\pi}} \int_0^1 \exp(-uv^2) \, dv, \qquad (A1)$$

$$G(u) = u^{-1/2} e^u \, \text{erf}(u^{1/2}) = \frac{2e^u}{\sqrt{\pi}} \int_0^1 \exp(-uv^2) \, dv. \qquad (A2)$$

In the material to follow, $G(u)$ occurs for negative u, and therefore involves error functions of imaginary argument. We have prepared a computer program for rapid and accurate evaluation of $G(u)$ with negative u.

The actual reduction of $SZ(0)$ is tedious, but can be accomplished with a judicious choice of standard procedures. The results can be expressed in terms of the auxiliary quantities $\alpha = \frac{1}{2}\nu(1 + d)$, $\beta = \frac{1}{2}\nu(1 - d)$, $a = \frac{1}{2}(\delta_a^2 + \delta_b^2) + \frac{1}{4}\nu^2$, $b = \frac{1}{4}(\delta_a^2 - \delta_b^2)$, $c = \frac{1}{2}(\delta_a^2 + \delta_b^2 + \alpha^2 + \beta^2)$, and $d = (\delta_b^2 - \delta_a^2)/\nu^2$. The final formulas depend upon whether ν or b vanish; we distinguish three cases as set forth below:

$$SZ(0) = [4(\delta_a \delta_b)^{5/2} Z^{1/2}/\pi^{1/2} c \nu^3]$$
$$\times ((\pi^{1/2}\nu/2c)\{[\alpha^2 + d\delta_a^2]F(\delta_a^2 Z) + [\beta^2 - d\delta_b^2]F(\delta_b^2 Z)\}$$
$$+ \exp(-\delta_a^2 Z)\{\beta - \alpha[c - (4\alpha\beta/\nu^2)(1 + Zc)] G(-\alpha^2 Z)\}$$
$$+ \exp(-\delta_b^2 Z)\{\alpha - \beta[c - (4\alpha\beta/\nu^2)$$
$$\times (1 + Z_c)] G(-\beta^2 Z)\} \quad (\nu \neq 0) \qquad (A3)$$

$$= [(\delta_a \delta_b)^{5/2} Z^{1/2}/2b^3]$$

TABLE I. Lattice sums $\Phi_{ab}^{T}(\nu)$ of Eqs. (23) and (27) and the "small-Z" and "large-Z" contributions thereto for various values of the convergence acceleration parameter Z.

δ_a	2.0	2.0	2.0	2.0	2.0	2.0	2.0	2.0	2.0
δ_b	1.0	1.0	1.0	1.0	1.0	1.0	1.0	1.0	1.0
ν_x	0.0	0.0	0.0	0.0	0.0	1.0	1.0	1.0	8.0
ν_y	0.0	0.0	0.0	0.0	0.0	0.0	0.0	0.0	6.0
ν_z	0.0	0.0	0.0	0.0	0.0	0.0	0.0	0.0	4.0
Z	0.50	0.75	1.00	1.10	1.20	0.80	1.00	1.20	1.00
$SZ(0)$	0.13143383	0.25054432	0.36571232	0.40785898	0.44726064	0.24930055	0.32635939	0.39299372	3.9222328(−3)
$SZ(1,0,0)$	0.00000000	0.00000027	0.00001192	0.00003330	0.00007819	0.00000036	0.00000615	0.00004025	0.0000146(−3)
LZ	0.75903396	0.63993161	0.52475204	0.48258395	0.44313733	0.45821558	0.38115115	0.31448285	0.5628282(−3)
$\Phi_{ab}^{T}(\nu)$	0.89046779	0.89047620	0.89047628	0.89047623	0.89047615	0.70751649	0.70751669	0.70751681	4.3850756(−3)

δ_a	2.0	6.0	6.0	6.0	0.2	0.2	0.2	0.2
δ_b	1.0	1.0	1.0	1.0	0.1	0.1	0.1	0.1
ν_x	8.0	0.0	0.0	0.0	0.0	0.0	8.0	8.0
ν_y	6.0	0.0	0.0	0.0	0.0	0.0	6.0	6.0
ν_z	4.0	0.0	0.0	0.0	0.0	0.0	4.0	4.0
Z	1.20	0.80	1.00	1.20	0.50	1.00	0.50	1.00
$SZ(0)$	3.9458438(−3)	0.22931254	0.25550774	0.27513503	0.00000	0.00002	0.0049480(−5)	0.0072523(−5)
$SZ(1,0,0)$	0.0000892(−3)	0.00000024	0.00000333	0.00001895	0.00000	0.00000	0.0000000(−5)	0.0000000(−5)
LZ	0.4391423(−3)	0.12086336	0.09466506	0.07502213	286.57986	286.57985	3.6241185(−5)	3.6218148(−5)
$\Phi_{ab}^{T}(\nu)$	4.3850753(−3)	0.35017614	0.35017613	0.35017610	286.57986	286.57986	3.6290665(−5)	3.6290671(−5)

$$\times \{(1/\pi^{1/2}Z)[\exp(-\delta_b^2 Z) - \exp(-\delta_a^2 Z)]$$

$$+ (a-b)F(\delta_b^2 Z) - (a+b)F(\delta_a^2 Z)\} \quad (\nu = 0, \ b \neq 0) \quad (A4)$$

$$= (\delta_a^5 Z^{1/2}/a^2)\{F(\delta_a^2 Z) - (2/\pi^{1/2})(1 + 2aZ/3)$$

$$\times \exp(-\delta_a^2 Z)] \quad (\nu = b = 0). \quad (A5)$$

The other contribution we require is that when μ is a member of the $(1, 0, 0)$ star; this contribution was denoted $SZ(1, 0, 0)$. Starting from Eq. (23), we proceed by expanding $\exp(-\gamma s)$ in a Taylor series about $s = Z$, after which the s and t integrations separate in each term:

$$SZ(1, 0, 0) = \frac{(\delta_a \delta_b)^{5/2}}{\pi^{1/2}} \sum_{n=0}^{\infty} A_n(Z) \int_{-1}^{1} dt \, \gamma^n (1 - t^2) \exp(-\gamma Z)$$

$$\times \{\cos[\pi(1 + t)\nu_x] + \cos[\pi(1 + t)\nu_y]$$

$$+ \cos[\pi(1 + t)\nu_z]\}, \quad (A6)$$

with

$$A_n(Z) = \frac{2}{n!} \int_0^Z ds \, s^{3/2}(Z - s)^n \exp(-\pi^2/s). \quad (A7)$$

The quantities $A_n(Z)$ depend only upon n and Z, so that once Z is fixed they may be determined once and for all. For $Z = 1$ they decrease rapidly with increasing n; for seven-significant-figure results they are not needed beyond $n = 4$.

The t integration could be reduced analytically to error functions of complex argument, but it is never needed with an accuracy of more than about four significant figures and is easily handled by numerical integration. We have obtained satisfactory results both from the use of Simpson's rule and from Lobatto quadratures.[10]

[1]H. M. Evjen, Phys. Rev. 39, 675 (1932).
[2]P. P. Ewald, Ann. Physik 64, 253 (1921).
[3]See, for example, F. Oberhettinger, *Fourier Expansions, A Collection of Formulas* (Academic, New York, 1973), p. 5.
[4]See, for example, F. E. Harris, in *Advances in Theoretical Chemistry*, edited by D. Henderson and H. Eyring (Academic, New York, 1975), Vol. 1, pp. 147—218.
[5]R. A. Bonham, J. L. Peacher, and H. L. Cox, Jr., J. Chem. Phys. 40, 3083 (1964).
[6]H. J. Monkhorst and F. E. Harris, Int. J. Quantum Chem. 6, 601 (1972).
[7]See, for example, J. Callaway, *Quantum Theory of the Solid State* (Academic, New York, 1974), pp. 352ff.
[8]R. Kikuchi, J. Chem. Phys. 22, 148 (1954).
[9]I. Shavitt and M. Karplus, J. Chem. Phys. 43, 398 (1965).
[10]*Handbook of Mathematical Functions*, edited by M. Abramowitz and I. A. Stegun (Nat. Bur. Stds., Washington, D.C., 1964), p. 888.

"Special points for Brillouin-zone integrations"—a reply*

James D. Pack and Hendrik J. Monkhorst

Department of Physics. University of Utah, Salt Lake City. Utah 84112

(Received 19 April 1977)

It is again emphasized that for all cubic lattices the method of Monkhorst and Pack generates not only point sets identical to those obtained by Chadi and Cohen, but also intermediate sets with the same properties. In addition, a comparison of these two methods for the hexagonal lattice reveals our method to be more flexible and efficient.

In reply to the preceding comments[1] by Chadi on "Special points for Brillouin-zone integrations," we feel the following remarks should be presented. The formalism which we have given[2] is completely general and can be applied to any of the 5 two-dimensional Bravais lattices or any of the 14 three-dimensional Bravais lattices. However, each lattice is unique, and the method must be tailored to fit the symmetry requirements of that particular lattice. This consideration will result in a reduction in the number of special k points required by a factor roughly equal to the order of the point group at a lattice site (at least it will approach that limit as $q \to \infty$).

The special treatment required for the body-centered-cubic (bcc) lattice has already been presented in the Appendix of our previous paper.[2] Again we emphasize that when $q = 2^n$ the bcc point sets generated by the procedure outlined in the Appendix are identical to those given by Chadi and Cohen[3] (CC). These point sets are more efficient than those obtained by a straightforward application of the general formalism to the primitive bcc lattice whose translation vectors are not mutually perpendicular.

To efficiently treat the hexagonal Bravais lattice we agree that our method must be slightly modified. We suggest the following alterations. Let u_p assume the values

$$u_p = (p - 1)/q_a, \quad p = 1, 2, 3, \ldots, q_a. \tag{1}$$

Assign the same values to u_r, while retaining the original definition for u_s

$$u_s = (2s - q_c - 1)/2q_c, \quad s = 1, 2, 3, \ldots, q_c. \tag{2}$$

Using the primitive translation vectors given by CC for the hexagonal lattice, these special $\vec{k}$ points occupy a rhombus-prism Brillouin zone (BZ), but reciprocal-lattice translations can bring them into a hexagonal-prism BZ. The D_{6h} symmetry reduces the region of interest to an irreducible zone (whose volume is $\frac{1}{24}$ that of the BZ) defined by

$$0 < 2u_p + u_r < 1, \quad 0 \le u_r \le u_p \le \tfrac{1}{2}, \quad 0 \le u_s < \tfrac{1}{2}. \tag{3}$$

To have orthogonal functions $A_m(\vec{k})$ the following

restrictions must be imposed on the components of $\vec{R}$:

$$0 \le 2R_2 \le R_1, \quad 2R_1 - R_2 \le q_a, \quad 0 \le R_3 < \tfrac{1}{2} q_c. \tag{4}$$

Such stars will satisfy the orthogonality relationships

$$\frac{1}{q_a^2 q_c} \sum_{j=1}^{P(q)} w_j A_m(\vec{k}_j) A_n(\vec{k}_j) = \delta_{mn}, \tag{5}$$

where the weights, w_j, are obtained from symmetry considerations,[4] and

$$P(q) = P_a(q_a) P_c(q_c). \tag{6}$$

It can be shown that

$$P_a(q_a) = (\alpha + 1)(3\alpha + \beta) + \delta_{\beta 0}, \tag{7}$$

where

$$\beta = q_a \bmod 6, \quad \alpha = \tfrac{1}{6}(q_a - \beta), \tag{8}$$

and

$$P_c(q_c) = \begin{cases} \tfrac{1}{2} q_c & \text{if } q_c \text{ is even}, \\ \tfrac{1}{2}(q_c + 1) & \text{if } q_c \text{ is odd}. \end{cases} \tag{9}$$

In other words, as q assumes values 1 through 10, $P_a(q)$ assumes, respectively, the values 1, 2, 3, 4, 5, 7, 8, 10, 12, 14; while $P_c(q)$ takes on the values 1, 1, 2, 2, 3, 3, 4, 4, 5, 5. The parameters q_a and q_c are chosen to best suit the problem and need not be equal. *It is advantageous to restrict q_c to even values.*

Using this method we get point sets somewhat similar to those of CC. To compare the two methods it is helpful to consider the two-dimensional hexagonal lattice. Cunningham has applied the method of CC to two dimensions.[5] Using the criteria of CC that a point set is more efficient if it eliminates more nearest shells (rings in this case) of direct lattice points, let us compare the two methods. The first set of CC has three special $\vec{k}$ points and fails at the fifth nearest ring. Our method yields a three-point set which also fails at the fifth ring, though the point sets are different. The next set of CC has six points and fails at the 12th ring. Our method does not give a set

with six points, but the one with five points fails at the 11th ring and the one with seven points fails at the 15th ring. The next set of CC has 18 points and fails at the 31st ring, while our 12-point set fails at that same 31st ring. As the number of points increases our method becomes increasingly more efficient, and also gives many more point sets from which to choose.

---

*Research sponsored in part by the NSF under Grant No. GP-31373X.

[1] D. J. Chadi, Phys. Rev. B **16**, 1746 (1977).

[2] H. J. Monkhorst and J. D. Pack, Phys. Rev. B **13**, 5188 (1976).

[3] D. J. Chadi and M. L. Cohen, Phys. Rev. B **8**, 5747 (1973).

[4] G. F. Koster, in *Solid State Physics*, edited by F. Seitz and D. Turnbull (Academic, New York, 1957), Vol. 5, pp. 173–256.

[5] S. L. Cunningham, Phys. Rev. B **10**, 4988 (1974).

Analytic connection between configuration–interaction and coupled-cluster solutions[a]

Tomislav P. Živković[b] and Hendrik J. Monkhorst

Department of Physics, University of Utah, Salt Lake City, Utah 84112
(Received 17 May 1977)

The coupled-cluster (CC) equations in the work of Coester, Kümmel, Čížek, Paldus, and others are inhomogeneous, nonlinear and algebraic in the cluster operators to be determined. If taken to all orders, they are equivalent to complete configuration–interaction (CI) equations, except for states orthogonal to the reference state Φ. However, if taken only to nth order, they are not equivalent to the nth order CI equations, and due to their nonlinear form, the existence and the number of the solutions is not guaranteed. Also, the reality of the associated energy values is not certain since these values do not arise as eigenvalues of a Hermitian operator. We show that the equations can be cast in the form of perturbed CI equations, with the "perturbations" being non-Hermitian and nonlinear in the CI-like coefficients to be calculated. In the case of a finite number of single-particle states, we construct the solutions to the CC equations by analytic continuation from the CI solutions. Singularities peculiar to the method are identified and studied, and conditions for reality and the maximum multiplicity of solutions are given. In general, the energy will be real, and the number of solutions equals that of the associated CI problem. Singularities or instabilities in the coupled-cluster equations can be traced to unphysical assumptions in the basis set Hamiltonian, or a poor description to highly excited states.

I. INTRODUCTION

In their landmark publications of 1957, Goldstone[1] and Hubbard[2] proved the existence of the now-famous linked-cluster theorem for interacting fermion systems. The theorem, in effect, states that the perturbation corrections to the wavefunction and total energy beyond the independent-particle approximation can be represented by linked Feynman graphs. Earlier Brueckner[3] had proved this to hold for a few orders in the interaction strength by explicit computation. Goldstone and Hubbard generalized this to all orders. The significance of the linked-cluster theorem stems, in part, from the proportionality of the energy corrections for a crystal, plasma or nuclear matter fermions at a given density with the number of particles. It also provides a nice bookkeeping device for the myriad of perturbation correction terms.

Both Goldstone's and Hubbard's proofs use the interaction representation, thereby introducing time dependence in an intrinsically time-independent physical problem. Through the "time" integrations (resulting from the adiabatic switching of the interaction), the energy denominators of perturbation theory appear, and a cancellation of unlinked terms in both the exact wavefunction and correlation energy results. Even for bound states the Feynman diagrammatic language of "forward" and "backward" scattering of particles is kept, although this notion has only physical realism in scattering phenomena.

Notwithstanding its rigor and elegance, there are a number of disturbing aspects about the way the linked-cluster theorem was introduced and, subsequently, has been interpreted and applied. The first objection concerns the introduction of time dependence in the deriva-

tion. It certainly has made understanding of the proof more opaque from a mathematical standpoint, and even Goldstone admits that in his paper. Later Brandow[4] made the same point. In fact, it even leaves many authors still worrying to this date about the different types of cancellations of terms that we seem to have to distinguish.[5]

The second objection is the emphasis on the order-by-order feature of the theorem and, most importantly, its implementation. Yet it is well known that for Coulombic forces in extended systems perturbation theory diverges in all orders except the first one. The standard cure is partial summations of the most divergent terms to all orders, thereby eliminating this unphysical singularity. It is claimed as one of the strengths of the linked-cluster theorem to find, through topological arguments, which diagrams should be summed to infinite order. At the same time, in most cases, one lacks physical insight into the meaning of the particular partial summation. An infinite number of infinite-valued diagrams is always ignored thus casting doubt on the choice of those that are kept.

The third and main objection is the diversion of the attention away from the physical basis of the linked-cluster theorem to the algebraic and particularly topological meaning of linkedness or connectedness. In a sense, it is a question of representation in which one prefers to describe correlation effects. Its choice is inconsequential only when calculations can be carried to completion in the particular representation. Unfortunately this is almost never the case, so we are left with the choice of the "most efficient" representation leading to the "most favorable" convergence. (Of course, we entirely ignore the practical problem of our limitation to handle only a finite number of excitations in the zeroth order spectrum. But this applies to any representation.)

In a many-fermion configuration space, the exact

wavefunction is "most of the time" well described by an independent-particle form. The probability for two or more particles to come close is small, and diminishes rapidly when an increasing number of them are involved. This is even attenuated by the Pauli exclusion principle that causes all fermions to carry a Fermi hole, even in the independent-particle model. Therefore, the energetic effect of this clustering of fermions, described by so-called linked terms, should decrease rapidly as their size increases. There is a significant probability for many pairs of fermions to cluster (or correlate) with antiparallel spin with no correlation of their relative positions. This leads to so-called unlinked terms in the wavefunction, expressible as the product of linked terms. Their occurrence is overwhelmingly important in large systems, and their neglect causes serious errors.

The importance of the linked-cluster theorem from a wavefunction point of view is its recognition of the fast convergence of the energetic effect from above linked-cluster type terms beyond the independent-particle approximation. At the same time, it includes products of these linked terms to higher orders in a most convenient manner. Goldstone and Hubbard were aware of this fact, and in Hubbard's paper it is brought out to some extent. However, the overall emphasis remained on the connection with the quantum-electrodynamical methods of Feynman, leading to the order-by-order view of many-body effects and scattering pictures.

Almost simultaneously, Coester[6] proposed a radically different approach to the same linked-cluster theory that does not suffer from any of the above disadvantages. It is time independent; it is algebraically simple; and it makes the physically significant corrections to the independent-particle wavefunction very explicit. The crucial idea is to express the exact wavefunction in occupation number formalism as

$$\Psi = e^T \Phi = (1 + T + T^2/2! + T^3/3! + \cdots)\Phi, \quad (1)$$

where the reference state Φ is defined by

$$\Phi = \prod_{\alpha=1} b_\alpha |vac\rangle, \quad b_\alpha = a^*_\alpha, \quad (2)$$

$|vac\rangle$ is the vacuum state and b_α are the creation operators for the fermions in the reference state. We denote with α the occupied states, and with r the unoccupied states. The *cluster operator* T is defined by

$$T = \sum_{s=1} T_s, \quad (3)$$

where

$$T_1 = \sum_{r\alpha} t^r_\alpha b_r a_\alpha,$$
$$T_2 = \sum_{(rr')(\alpha\alpha')} t^{rr'}_{\alpha\alpha'} b_r b_{r'} a_{\alpha'} a_\alpha, \quad (4)$$

and the general s-particle cluster operator T_s is given by

$$T_s = \sum_{R\Delta} t^R_\Delta b_{r_1} \cdots b_{r_s} a_{\alpha_s} \cdots a_{\alpha_1}, \quad (5)$$

where R is the ordered set of s "particle" indices $\{r_1, r_2, \cdots\}$, and Δ is that for the s "hole" indices $\{\alpha_1, \alpha_2, \cdots\}$. Here and in the following we will use the notation

$$\Phi^R_\Delta(s) = b_{r_1} \cdots b_{r_s} a_{\alpha_s} \cdots a_{\alpha_1} \Phi. \quad (6)$$

We sometimes write Φ^R_Δ when no confusion will arise. T_s creates s-particle-hole pairs, which makes Eq. (1) a nonunitary transformation of Φ. Its exponential form keeps track of the counting over distinct corrections to Φ only, expressed as replacements of one-particle states by cluster functions and their products, and represented by T_s and products thereof. The power of this description results from two aspects. First, without loss of generality, we can assume that the T_s describe linked clusters, meaning that these operators cannot be written as the product of two or more operators. This assumption is consistent with the equations that determine the cluster operators.

The second advantage is that we can perform a simple algebraic trick. When the Schrödinger equation is in our cluster expansion form

$$H(e^T \Phi) = E(e^T \Phi) \quad (7)$$

we can obtain its solution from the equivalent expression[6]

$$(e^{-T} H e^T)\Phi = E\Phi. \quad (8)$$

But now we can express the left-hand side of Eq. (8) as a *finite* commutation series,

$$e^{-T} H e^T = H + [H, T] + \tfrac{1}{2}[[H, T], T]$$
$$+ \cdots + (1/4!)[[[[H, T], T], T], T]. \quad (9)$$

The series terminates after five terms since H contains at most two particle operators. Using simple commutator algebra[7] one can reduce those expressions even further. In order to obtain equations for E and T_s one premultiplies Eq. (8) with $\langle\Phi|$ and $\langle\Phi^R_\Delta|$ and gets:

$$\langle\Phi|e^{-T} H e^T|\Phi\rangle = E, \quad T = \sum_{s=1}^n T_s, \quad (10)$$

$$\langle\Phi^R_\Delta(s)|e^{-T} H e^T|\Phi\rangle = 0 \quad (s = 1, 2, \ldots, n). \quad (11)$$

Each wavefunction nonorthogonal to Φ can be expressed in the form (1). However, usually one includes only up to n-particle cluster operators which leads to an approximation of the exact wavefunction. The corresponding equations are of the order n, as indicated in Eqs. (10) and (11). Moreover, we assume that the number of single-particle states is finite. This implies that both the number of particles K and the number of holes N is finite. Solutions of Eqs. (10) and (11) are hence approximate solutions of the Schrödinger equation for K particles in a finite dimensional Hilbert space. Obviously $n \leq N$. However, the case $n = N$ is of no practical interest. As shown in the Appendix, provided $n = N$, Eqs. (10) and (11) are equivalent to the corresponding finite dimensional configuration-interaction (CI) equations for all states nonorthogonal to Φ. Also, as n increases, the number of excitations increases so rapidly that it soon becomes impractical to solve these equations. Hence we assume $n < N$.

In actual calculations, Hartree—Fock or Brueckner orbitals for α and r states were used and a very limited number of nonzero T_s were kept. Obviously as many Eqs. (11) are needed as nonzero t^R_Δ amplitudes. It was found that in all electron systems considered, the pair

T.P. Zivkovic and H.J. Monkhorst

approximation $T = T_2$ leads to about 99% of the attainable correlation energy.[9] This is a very reassuring result which, as indicated above, can be well understood on statistical grounds.

In a long series of publications since 1960, Coester, Kümmel *et al.*[3] have used this method (named by them the exp-S method) for nuclear ground-state energies and properties. Čížek and Paldus[4,10] were the first to apply the method to a few atoms and molecules in calculations of ground-state correlation energies. Because of their pair approximations, the latter authors adopted the terms coupled-pair many electric theory (CPMET) and extended CPMET. To stress the general cluster aspects of the method, and the significant coupling between the clusters which results in nonlinear terms in Eqs. (11), we propose the name coupled-cluster (CC) method.

As expected, it turns out that by iteration of the algebraic equations (10) and (11) one generates all Goldstone-type linked perturbation terms, provided linked clusters to all orders are included. The marvel of this method seems to be that it zeros in directly to the heart of the correlation corrections in a most compact, yet transparent manner. This applies to fermion systems with any kind of interaction.

Even since its inception, Coester and Kümmel's approach has been largely ignored by the many-body theoretical community for a number of reasons. From a formal standpoint, it seemed to address itself only to calculating the ground-state correlation effects. These were not considered as very interesting quantities compared to response phenomena of many-body systems, which quite naturally shifted the attention to Green's function methods. Diagrammatic perturbation methods are used to compute these functions in a more or less systematic way. In a recent paper,[11] we have shown that one can indeed use the CC method to compute properties, both time dependent and time independent, by casting it in Green's functionlike form. Yet we can preserve the algebraic and conceptual simplicity, and we get easily solvable equations.

A serious objection was also the relative messiness of the coupled algebraic equations (11). These are nonlinear, inhomogeneous, and, if not carefully handled, of considerable complexity. Moreover, they are not in some eigenvalue form, thus not guaranteeing the reality and a definite multiplicity of their solutions. Coester[12] made some attempts to answer these questions.

We have now eliminated this objection by casting the CC method in the form of a perturbed configuration-interaction (CI) method. The perturbation is a non-Hermitian, unbounded operator with polynomial dependence on the CI-like coefficients to be determined.[13] Algebraically it is somewhat like the Hartree—Fock method, except that there the Coulomb and exchange operator are Hermitian and bounded. With the help of the analytic continuation method we will show a one-to-one correspondence of the CC solutions with CI solutions, and reality of E values for real Hamiltonians. Moreover, many mathematical properties such as the appearance of singularities will be derived. As we will

see, these are more of numerical than physical significance.

In the next section we will present the derivation of the CI-like representation of the CC method followed by a section with numerical examples to illustrate some analytic properties of the formulation. In Sec. IV a summary is given of the mathematical analysis of the general CC equations, the details of which are given in the Appendix. We close with a section in which we point out the significance of the findings for the CC equations, and for the problem of solutions to coupled, nonlinear algebraic equations in general. As a byproduct, we obtain the number of Hartree—Fock solutions in a particular atomic orbital basis.

II. GENERAL

The most general state Ψ in cluster expansion form nonorthogonal to Φ can be written as

$$\Psi = e^T \Phi = (1 + C)\Phi, \tag{12}$$

where T is given by Eqs. (3)—(5), and

$$C = \sum_s C_s, \tag{13}$$

$$C_s = \sum_{R\Delta} C_\Delta^R b_r b_{r'} \cdots a_{\alpha'} a_\alpha. \tag{14}$$

Here R and Δ are, as before, the ordered sets of s "particle" and "hole" indices. In order to cast the CC equations in a form more accessible to mathematical analysis, we make use of the formal identities

$$e^T = 1 + C, \tag{15}$$

$$T = \ln(1 + C), \tag{16}$$

expressing T_s in CI-like operators C_s and vice versa. According to Theorem 1 in the Appendix, the CC equations (11), including up to n-tuple excitations, can be written as

$$\langle \Phi_\Delta^R(s) | (H - E)\{1 + C_1 + \cdots + C_n$$
$$+ [C_{n+1}(n) + C_{n+2}(n)]\} | \Phi \rangle = 0, \quad s = 0, 1, 2, \ldots, n, \tag{17}$$

where

$$C_{n+1}(n) = \sum_{k=2}^{n+1} \frac{(-)^k}{k} \sum_{\{s_i\}} \delta(s_1 + \cdots + s_k, n+1) \prod_{i=1}^{k} C_{s_i},$$

$$C_{n+2}(n) = \sum_{k=2}^{n+1} \frac{(-)^k}{k} \sum_{\{s_i\}} \delta(s_1 + \cdots + s_k, n+1)$$
$$\times C_1 \prod_{i=1}^{k} C_{s_i} - \sum_{k=3}^{n+2} \frac{(-)^k}{k} \sum_{\{s_i\}} \delta(s_1 + \cdots + s_k, n-2)$$
$$\times \sum_{i=1}^{k} C_{s_i}, \tag{18}$$

and $\sum_{\{s_i\}}$ is the summation over all possible choices of $s_1, s_2, \cdots$ such that their sum is in accord with the δ function. Instead of the CC Eqs. (17) we observe the following somewhat more general equations,

$$\{H + \lambda V(\Psi)\}\Psi = E\Psi, \tag{19}$$

where

$$H_{R\Delta, R'\Delta'} = \langle \Phi_\Delta^R | H | \Phi_{\Delta'}^{R'} \rangle, \tag{20}$$

$$V_{R\Delta, R'\Delta'} = V_{R\Delta} \delta_{R'\Delta', 00}$$
$$= \langle \Phi_\Delta^R | H \{C_{n+1}(n) + C_{n+2}(n)\} | \Phi \rangle \delta_{R'\Delta', 00}, \tag{21}$$

$$\Psi_{R\Delta} = \langle \Psi_\Delta^R | 1 + \cdots + C_n | \Phi \rangle. \tag{22}$$

It can easily be shown that in the case of $\lambda = 1$ Eq. (19) reduces to Eq. (17). The above equation is, however, written in the matrix form, where H is a Hermitian matrix with matrix elements given by Eq. (20). On the other hand, V is basically a non-Hermitian matrix with matrix elements depending on the components $\Psi_{R\Delta}$ of the column vector Ψ. As pointed out in the Introduction, we assume that the number of single-particle states is finite.

Equation (19) where λ is a parameter will be called the characteristic equation (CE). For the case $\lambda = 0$, this equation reduces to the usual CI equation of order n with the subsidiary condition $\Psi_{00} = \langle \Psi | \Phi \rangle = 1$. In this case Eq. (19) is a Hermitian equation, eigenvalues E are real, and the number of independent solutions Ψ is less than or equal to the dimension of the space involved. Our idea is to use this well-known property of Eq. (19) in the case $\lambda = 0$, and by analytic continuation to extend the corresponding solutions to the whole complex λ plane. The particular case in point is $\lambda = 1$ where the solution of the nth order CC Eqs. (17) should come. Thus, by that process, from the existence and reality of the solutions of CI equations, we hope to infer the existence and reality of the solutions to the CC equations. If, however, this fails, we are at least in the position to trace down the reason why it is so.

III. EXAMPLE

In order to get a clearer insight into the structure of the CE and the different possibilities which can emerge, we shall give an example of a CE which is simple enough to be solved analytically, yet incorporates all the characteristic features.

We consider a system consisting of two particles which can be distributed among four different states. In this case, there are six two-particle states; one non-excited, four singly excited, and one double excited state (see Fig. 1). If only single excitations are explicitly taken into account, the CE for the above system reads:

$$\langle \Phi_\Delta^R(s) | (H - E)\{1 + C_1 + \lambda[C_2(1) + C_3(1)]\} | \Phi \rangle = 0,$$

$$C_2(1) = \tfrac{1}{2} C_1^2, \quad C_3(1) = \tfrac{1}{6} C_1^3, \quad s = 0,1, \tag{23}$$

which can be easily deduced from Eqs. (17) and (18). The single excitation operator C_1 can be written in the form
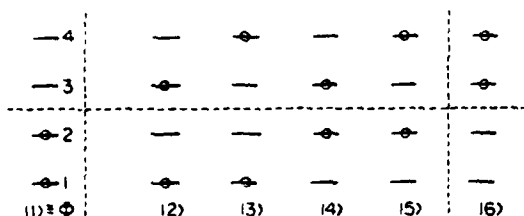
FIG. 1. Schematic representation of the ground state $|1\rangle \equiv \Phi$ and excited states $|2\rangle$ through $|6\rangle$ constructed from four one-particle states (denoted by 1 to 4), as used in examples of Sec. III. $|2\rangle$ to $|5\rangle$ are monoexcited states, and $|6\rangle$ is a doubly excited state.

$$C_1 = x_2 b_2 a_2 + x_3 b_4 a_2 + x_4 b_3 a_1 + x_5 b_4 a_1, \tag{24}$$

where

$$x_i = \langle i | C_1 | \Phi \rangle.$$

This gives

$$C_2(1) | \Phi \rangle = (x_2 x_5 + x_3 x_4) | 6 \rangle, \quad C_3(1) | \Phi \rangle = 0. \tag{25}$$

We can now insert Eq. (25) into Eq. (23) and write the resulting equation in a matrix form,

$$\begin{pmatrix} h_{11} & \cdots & h_{15} \\ \cdot & & \cdot \\ \cdot & & \cdot \\ \cdot & & \cdot \\ h_{51} & & h_{55} \end{pmatrix} + \lambda(x_2 x_5 + x_3 x_4) \begin{pmatrix} h_{16} & 0 & \cdots & 0 \\ \cdot & & & \cdot \\ \cdot & & & \cdot \\ \cdot & & & \cdot \\ h_{56} & 0 & \cdots & 0 \end{pmatrix} = E \begin{bmatrix} 1 \\ x_2 \\ \vdots \\ x_5 \end{bmatrix},$$

$$h_{ij} = \langle i | H | j \rangle, \quad i,j = 1,\ldots,6. \tag{26}$$

Equation (26) incorporates some correlation effects since two particles are involved. On the other hand, only single excitations are explicitly taken into account, and hence the corresponding CC method is not equivalent to the CI method, which is known to have six linearly independent solutions with real eigenvalues. Thus Eq. (26) is the simplest nontrivial example of the CE. This model example will prove quite useful in the demonstration of the different properties of the CE.

So far, matrix elements h_{ij} are restricted only by the hermiticity condition $h_{ij} = h_{ji}^*$. We shall now solve Eq. (26) for some special choices of those elements.

Our first example is

$$\begin{pmatrix} u & 0 & v & v & 0 \\ 0 & 0 & 0 & 0 & 0 \\ v^* & 0 & 0 & 0 & 0 \\ v^* & 0 & 0 & 0 & 0 \\ 0 & 0 & 0 & 0 & 0 \end{pmatrix} + \lambda(x_2 x_5 + x_3 x_4) \begin{pmatrix} 0 & 0 & 0 & 0 & 0 \\ 0 & 0 & 0 & 0 & 0 \\ q & 0 & 0 & 0 & 0 \\ q & 0 & 0 & 0 & 0 \\ 0 & 0 & 0 & 0 & 0 \end{pmatrix} \begin{bmatrix} 1 \\ x_2 \\ x_3 \\ x_4 \\ x_5 \end{bmatrix}$$

$$= E \begin{bmatrix} 1 \\ x_2 \\ x_3 \\ x_4 \\ x_5 \end{bmatrix}. \tag{27}$$

We assume u, v, and q to be all nonzero and obviously $u^* = u$. Matrix equation (27) leads to a set of five equations in five unknowns:

$$u + vx_3 + vx_4 = E,$$

$$0 = Ex_2,$$

$$v^* + \lambda q(x_2 x_5 + x_3 x_4) = Ex_3, \tag{27'}$$

$$v^* + \lambda q(x_2 x_5 + x_3 x_4) = Ex_4,$$

$$0 = Ex_5,$$

If we put $E = 0$ in Eq. (27') we obtain solutions satisfying

$$x_3(u + vx_3) - vx_2 x_5 = vv^*/\lambda q,$$

$$x_4 = -(u/v + x_3), \quad E = 0. \tag{28}$$

For each $\lambda \neq 0$ those solutions form a three-dimensional variety in the four-dimensional space spanned by x_2, x_3, x_4, and x_5. We can arbitrarily choose three eigenfunctions satisfying Eq. (28), and one possibility is

$$\Psi_1 = \begin{bmatrix} 1 \\ x \\ 0 \\ -u/v \\ x \end{bmatrix}, \quad \Psi_2 = \begin{bmatrix} 1 \\ 0 \\ (-u+D)/2v \\ (-u-D)/2v \\ 0 \end{bmatrix}, \quad \Psi_3 = \begin{bmatrix} 1 \\ 1/\lambda \\ (-u+D)/2v \\ (-u-D)/2v \\ 0 \end{bmatrix},$$

(29)

where

$$x = [(-v^*/\lambda q)]^{1/2}, \quad D = [(u^2 + 4v^2 v^*/\lambda)]^{1/2}.$$

We note that the space of the eigenfunctions (28) is not linear. If Ψ_1 and Ψ_2 are eigenvectors of Eq. (27) with the corresponding eigenvalue $E = 0$, their linear combination $\Psi = \Psi_1 + \beta \Psi_2$ such that $\langle \Psi | \Phi \rangle = 1$ (i.e., $\alpha + \beta = 1$) is generally not an eigenfunction to Eq. (27). This is the consequence of the nonlinear character of the equations (27), namely of the dependence of the matrix V on the eigenfunction Ψ. We can enlarge the notion of degenerate states to the general case that more than one eigenvector Ψ corresponds to a given eigenvalue E without those eigenvectors necessarily forming a linear space. In this sense, the solutions (28) are triply degenerate, forming a three-dimensional hypersurface in the four-dimensional space spanned by x_2 to x_5. As λ tends to zero, at least one of the components $x_i = \langle \Psi | i \rangle$ tends to infinity. Since $\langle \Psi | \Phi \rangle \equiv \langle \Psi | 1 \rangle = 1$, this means that Ψ tends to be orthogonal to the nonexcited state Ψ. In particular if in our case we take a limit of Ψ_1, Ψ_2, and Ψ_3 as λ tends to zero we obtain, up to the normalization constant:

$$\Psi_1 \to \begin{bmatrix} 0 \\ 1 \\ 0 \\ 0 \\ 1 \end{bmatrix}, \quad \Psi_2 \to \begin{bmatrix} 0 \\ 0 \\ 1 \\ -1 \\ 0 \end{bmatrix}, \quad \Psi_3 \to \begin{bmatrix} 0 \\ 1 \\ 0 \\ 0 \\ 0 \end{bmatrix}.$$

(30)

Those three vectors are orthogonal to the vector Φ and though they are not eigenvectors of the CE, they are eigenvectors of the corresponding CL. This behavior of the above solutions of Eq. (27) reflects a general property of the solutions of CI. Since $\langle \Psi | \Phi \rangle = 1$, no state orthogonal to Φ can be an eigenfunction of CE.

Besides degenerate eigenfunctions (28) corresponding to the eigenvalue $E = 0$, Eq. (27) has in addition two non-degenerate eigenfunctions Ψ_4 and Ψ_5:

$$\Psi_4(\lambda) = \begin{bmatrix} 1 \\ 0 \\ x(\lambda) \\ x(\lambda) \\ 0 \end{bmatrix}, \quad \Psi_5(\lambda) = \begin{bmatrix} 1 \\ 0 \\ x'(\lambda) \\ x'(\lambda) \\ 0 \end{bmatrix},$$

(31)

$$E_4(\lambda) = \{u(v - \lambda q) + v([u^2 + 4v^*(2v - \lambda q)])^{1/2}\}/(2v - \lambda q),$$

$$E_5(\lambda) = \{u(v - \lambda q) - v([u^2 + 4v^*(2v - \lambda q)])^{1/2}\}/(2v - \lambda q),$$

where

$$x(\lambda) = \{-u + ([u^2 + 4v^*(2v - \lambda q)])^{1/2}\}/(4v - 2\lambda q),$$

$$x'(\lambda) = \{-u - ([u^2 + 4v^*(2v - \lambda q)])^{1/2}\}/(4v - 2\lambda q).$$

It should be observed that those two eigenfunctions represent one and the same analytic function in the complex λ plane, and that components of Ψ_4 and Ψ_5, as well as E_4 and E_5, lie on two different Riemann sheets of this function. There are two singular points of which one is

a pole (for Ψ_5) and the other is a branch point,

$$\lambda_p = 2v/q, \quad \lambda_b = (u^2 + 8vv^*)/4v^*q.$$

(32)

In the case of $\lambda = 0$, which represents CI, vectors Ψ_4 and Ψ_5 reduce to

$$\Psi_4(0) = \begin{bmatrix} 1 \\ 0 \\ x \\ x \\ 0 \end{bmatrix}, \quad \begin{aligned} x &= [-u + (u^2 + 8vv^*)^{1/2}]/4v, \\ E_4 &= [u + (u^2 + 8vv^*)^{1/2}]/2, \end{aligned}$$

(33)

$$\Psi_5(0) = \begin{bmatrix} 1 \\ 0 \\ x' \\ x' \\ 0 \end{bmatrix}, \quad \begin{aligned} x' &= [-u - (u^2 + 8vv^*)^{1/2}]/4v, \\ E_5 &= [u - (u^2 + 8vv^*)^{1/2}]/2. \end{aligned}$$

If we start with the vector $\Psi_4(\lambda)$ for $\lambda = 0$ and move along the line which encircles the branch point λ_b and then come back to the point $\lambda = 0$, we arrive at the vector $\Psi_5(0)$ as indicated on Fig. 2. $\Psi_4(0)$ and $\Psi_5(0)$ are mutually orthogonal and their associated eigenvalues are real, which is not generally true for $\Psi_4(\lambda)$ and $\Psi_5(\lambda)$. Obviously, $\Psi_4(\lambda)$ and $\Psi_5(\lambda)$ cannot always remain orthogonal, since they are analytic continuations to each other, and in the branch point, λ_b, they coincide. Concerning reality of the corresponding eigenvalues, in the case of the real Hamiltonian (i.e., v and q real), energy as a function of (real) λ is real, as long as we do not pass a branch point. Once $\lambda > \lambda_b$ (for the case $\lambda_b > 0$, and $\lambda < \lambda_b$ if $\lambda_b < 0$), energy $E(\lambda)$ starts to be complex due to the negative number under the square root in Eq. (31). If, however, H is not real, energy $E(\lambda)$ is generally complex for each $\lambda \neq 0$. Hence the reality and nonreality of the eigenvalues of the CC equations depends on the basis in which matrix elements are written. If these matrix elements are complex, the eigenvalue is generally complex. If, however, these elements are real, the eigenvalue is real at least in some neighborhood of the point $\lambda = 0$. This is to be compared with the CI method which always gives real eigenvalues for any choice of the basis vectors. We see that the most sensible basis choice for CC equations is a real basis where there is much more reason to believe that the corresponding eigenvalues will be real. As is well known, in the case of velocity-independent Hamil-
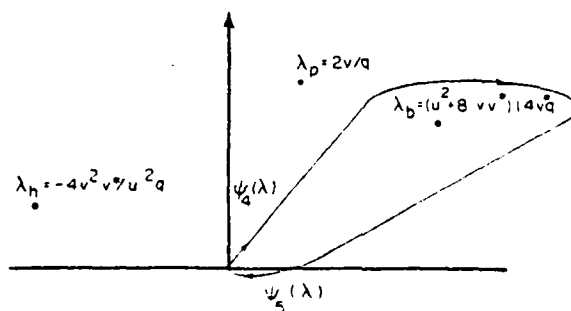

FIG. 2. Singular points in the complex λ plane and a path analytically connecting the solutions $\Psi_4(\lambda)$ and $\Psi_5(\lambda)$ of the examples of Sec. III. $\Psi_4(\lambda)$ and $\Psi_5(\lambda)$ belong to different Riemann sheets, and coincide in the branchpoint λ_b. λ_p and λ_h are a pole and hidden singularity, respectively.

tonians, such a basis always exists. It should be noted, however, that even in the case when H is complex, the eigenvalues are not completely without meaning: The imaginary part of the energy is a small quantity of first order in λ and as long as λ is small, the predominant contribution to $E(\lambda)$ is given by its real part, and the imaginary part can be considered as an error since, in any case, the CC method is only an approximation.

One can easily see that if H is real and if $\lambda_b < 0$ the CC equations will always have real eigenvalues. If, however, $\lambda_b > 0$, the reality will be insured by the requirement $\lambda_b \geq 1$, i.e.,

$$(u^2 + 8v^2)/4vq \geq 1. \tag{34}$$

This holds particularly true if q is small with respect to v or, from Eq. (27), if the mutual interaction of the states which are explicitly taken into account is big with respect to the interaction of those states with the states which are taken into account implicitly through the matrix V. That is, however, in accord with our intuitive feeling of the validity of the CC method.

Our next example is the CE,

$$\begin{pmatrix} 0 & 0 & u & 0 & 0 \\ 0 & 0 & 0 & 0 & 0 \\ u^* & 0 & 0 & 0 & 0 \\ 0 & 0 & 0 & 0 & 0 \\ 0 & 0 & 0 & 0 & 0 \end{pmatrix} + \lambda(x_2 x_5 + x_3 x_4) \begin{pmatrix} 0 & 0 & 0 & 0 & 0 \\ 0 & 0 & 0 & 0 & 0 \\ 2v & 0 & 0 & 0 & 0 \\ v & 0 & 0 & 0 & 0 \\ 0 & 0 & 0 & 0 & 0 \end{pmatrix} \begin{bmatrix} 1 \\ x_2 \\ x_3 \\ x_4 \\ x_5 \end{bmatrix}$$

$$= E \begin{bmatrix} 1 \\ x_2 \\ x_3 \\ x_4 \\ x_5 \end{bmatrix}, \tag{35}$$

where u and v are supposed to be different from zero. Equation (35) is equivalent to a set of equations:

$$ux_3 = E,$$
$$0 = Ex_2,$$
$$u^* + 2\lambda v(x_2 x_5 + x_3 x_4) = Ex_3, \tag{35'}$$
$$\lambda v(x_2 x_5 + x_3 x_4) = Ex_4,$$
$$0 = Ex_5.$$

Concerning (35') it can be shown that there are two possibilities: Either $\lambda \neq u/v$ or $\lambda = u/v$. If $\lambda \neq u/v$, there are two solutions to (35'): $\lambda \neq u/v$,

$$\Psi_1 = \begin{bmatrix} 1 \\ 0 \\ (u^*/u)^{1/2} \\ 0 \\ 0 \end{bmatrix}, \quad \Psi_2 = \begin{bmatrix} 1 \\ 0 \\ -(u^*/u)^{1/2} \\ 0 \\ 0 \end{bmatrix}, \quad \begin{aligned} E_1 &= (uu^*)^{1/2}, \\ E_2 &= -(uu^*)^{1/2}. \end{aligned}$$

$$\tag{36}$$

If, however, $\lambda = u/v$, there is an infinite number of solutions to (35'),

$$\Psi(\lambda = u/v) = \begin{bmatrix} 1 \\ 0 \\ E/u \\ x \\ 0 \end{bmatrix}, \quad E = ux \pm (u^2 x^2 + uu^*)^{1/2}. \tag{37}$$

Note that each energy E can be an eigenvalue, except for $E = 0$. Later we shall see that it is a general property of the CE that sometimes, for particular values of λ, an infinite number of eigenvalues are possible. We shall call such a point in a complex λ plane a resonance point.

The two examples above illustrate different types of anomalies which can be expected for the CE. We shall now examine the CE in more detail in order to show that the above two examples exhaust all but one of the anomalies which can be expected.

IV. GENERAL STRUCTURE OF CE

In the previous section we gave some examples of the CE in order to illustrate possible types of solutions. Now we are going to observe the CE from a general point of view.

Observe the CE

$$[H + \lambda V(x)]x = Ex, \quad x_1 = 1, \tag{38}$$

where $x = \{x_1, \ldots, x_m\}$ stands for a vector Ψ whose components $\Psi_{R\Delta}$ are renumerated in the order $1, 2, \ldots, m$ (see the Appendix). The two basic questions we want to answer are the existence of solution (E, x) and the reality of the eigenvalue E.

In order to reach these answers in the most complete sense, we must carefully analyze the mathematical structure of the CE. In particular, we have to identify singularities in the complex λ plane. In this section, we summarize the results of this analysis. Most of the details are given in the Appendix, particularly the proof of important theorems. We proceed by first discussing the special λ points for which the CE is singular in character, followed by rigorous answers to the above questions of existence, reality, and multiplicity of solutions (E, x).

(a) Resonance points

As illustrated by Example 2, the CE may have some points λ for which it has an infinite number of distinct eigenvalues. We called such a point a resonance point. It is shown in the Appendix that if λ_r is a resonance point, each E, except for a finite number of them, is an eigenvalue of the Eq. (38) where $\lambda = \lambda_r$. Thus, between resonance and nonresonance points there is a complete symmetry. In a nonresonance point there is a finite number of eigenvalues E; in a resonance point there is a finite number of E which are not eigenvalues.

Another question concerns the distribution of resonance points in a λ plane. This question is answered by Theorem 4 to the effect that there is either a finite number of resonance points, or there is a finite number that are not resonance points. If the first case occurs, we call the CE normal. However, the possibility that the CE is not normal is very unlikely. It would mean that for almost every λ Eq. (38) would have each E, except a finite number of them, as an eigenvalue. Physically it would imply that the CC equations, which correspond to the point $\lambda = 1$, are void of any significance, since even if $\lambda = 1$ were not a resonance point, each point infinitesimally close to it would be. However, we

1012   J. Math. Phys., Vol. 19, No. 5, May 1978

T.P. Zivkovic and H.J. Monkhorst   1012

were not able to rule out this possibility, although we believe that it actually does not take place. In any event, if the CC equations are to be given any physical significance, the corresponding CE should have, at most, a finite number of resonance points and hence it should be normal.

The solutions which are "specific" for a resonance point we call resonance solutions. Besides resonance solutions in a resonance point, we can also have non-resonance solutions—the distinction being that resonance solutions cannot be extended in the region outside the resonance point. Obviously, if each resonance solution could be extended continuously to some neighborhood $N(\lambda_r)$ of a point λ_r, then in each point of $N(\lambda_r)$ there would be an infinite number of distinct eigenvalues, and hence this point should be resonance as well. But this would imply that each λ except a finite number of them, is resonance, which would mean that the CE is not normal. Hence, in the case of a normal CE, only a finite number of the solutions in a resonance point λ_r can be extended continuously outside this point and those solutions we call nonresonance. Thus resonance solutions do exist only in a resonance point and cannot be extended outside it. They are isolated, and since the corresponding eigenvalue E can assume almost any value, be it real or complex, they are void of any physical meaning.

Note that the point $\lambda = 0$, by the very definition, cannot be a resonance point, and hence in the case of normal CE there is a small neighborhood $N(0)$ of the point $\lambda = 0$ where there is no resonance point. This is in accord with the intuitive idea that for small λ the term $\lambda V(x)$ should be considered as a perturbation, and hence should not destroy the "good" feature of the CE in the point $\lambda = 0$. One must, however, be careful in such conclusions since, although $V(x)$ is continuous, it is not a bounded operator as shown in Lemma 7 of the Appendix. Hence there is no *a priori* reason why λV for infinitesimal λ should be infinitesimal.

(b) Singular points

CE (38), for a given (E, x) and a given λ, is well characterized by the Jacobian

$$D(\lambda, E, x)$$

$$= \begin{vmatrix} 1 & (h_{12} + \lambda \partial^2 V_1(x)) & \cdots & (h_{1m} + \lambda \partial^m V_1(x)) \\ x_2 & (h_{22} - E + \lambda \partial^2 V_2(x)) & \cdots & \cdot \\ & \cdot & & \cdot \\ & \cdot & & \cdot \\ x_m & (h_{m2} + \lambda \partial^2 V_m(x)) & \cdots & (h_{mm} - E + \lambda \partial^m V_m(x)) \end{vmatrix},$$

$$\partial^i = \frac{\partial}{\partial x_i}. \tag{39}$$

As shown in the Appendix (Theorem 5), if (E_0, x_0) is a solution of the CE in a point λ_0, and if a corresponding Jacobian $D(\lambda_0, E_0, x_0)$ is different from zero, then this solution can be analytically extended in the whole λ plane with the exception of a finite number of points. The solution $[E(\lambda), x(\lambda)]$, which is obtained by this

process of analytic extension, we call normal. Our main concern, however, are those normal solutions which are defined in the point $\lambda = 0$, which corresponds to the CI. Such solutions we call regular. They can bridge the gap between CI and CC, since they can be extended out of the point $\lambda = 0$, to the whole λ plane, and provided they are defined in the point $\lambda = 1$, they connect CI and CC solutions in a natural way. The normal solution $[E(\lambda), x(\lambda)]$, which is the extension of the solution (E_0, x_0) in the point $\lambda = \lambda_0$, is by the very definition non-resonant. Moreover, it is an algebraic function of λ, and as such it may have poles and branch points. As shown by Lemma 10, if $\lambda = \lambda_b$ is a branch point of a normal solution $[E(\lambda), x(\lambda)]$, the Jacobian $D[\lambda_b, E(\lambda_b), x(\lambda_b)]$ should be equal to zero. Also, according to Lemma 8, vanishing of the Jacobian can be due to a continuous degeneracy of the solution at this point (see Definition 3). If $\lambda = \lambda_d$ is such a point, we call it the point of accidental degeneracy. It is shown in the Appendix that vanishing of the Jacobian in a point $\lambda = \lambda'$ indicates instability of the normal solution $[E(\lambda'), x(\lambda')]$. Thus in a branch point and in the accidental degeneracy point the corresponding solution is unstable. It may also happen that the solution $[E(\lambda), x(\lambda)]$ is unstable in some point $\lambda = \lambda_h$ (i.e., the corresponding Jacobian is zero), but it is neither a branch nor an accidental degeneracy point. In this case, we say that $\lambda = \lambda_h$ is a hidden singularity of a normal solution $[E(\lambda), x(\lambda)]$.

It should be noted, however, that although $[E(\lambda), x(\lambda)]$ is not defined in a pole $\lambda = \lambda_p$, the corresponding Jacobian may well be defined in this point. $D(\lambda) \equiv D[\lambda, E(\lambda), x(\lambda)]$ is an analytic function in λ, and there is a possibility that there exists an analytic continuation of this function in a point $\lambda = \lambda_p$ which is a pole of a solution $[E(\lambda), x(\lambda)]$. It may happen that the Jacobian vanishes in this point; hence poles can also cause disappearance of the Jacobian.

In conclusion then, if $[E(\lambda), x(\lambda)]$ is a regular (normal) solution, it may have four types of singular points. First there are poles which are those points where $[E(\lambda), x(\lambda)]$ is not defined. Second there are branch points, third there are accidental degeneracies, and fourth there are hidden singularities.

(c) Examples of singular points

The above possibilities are illustrated in Sec. III. The regular eigenfunction $\Psi_5(\lambda)$ Eq. (31) has a pole in a point $\lambda_p = 2v/q$ and a branch point in $\lambda_b = (u^2 + 8vv^*)$ $4v^*q$. In addition, there is a hidden singularity in a point $\lambda_h = -4v^2 v^*/u^2 q$. This last singular point can be found if we observe the corresponding Jacobian, which is

$$D(\lambda) = D[\lambda, E(\lambda), \Psi(\lambda)]$$

$$= \begin{vmatrix} 1 & 0 & v & v & 0 \\ x_2 & -E & 0 & 0 & 0 \\ x_3 & \lambda q x_5 & \lambda q x_4 - E & \lambda q x_3 & \lambda q x_2 \\ x_4 & \lambda q x_5 & \lambda q x_4 & \lambda q x_3 - E & \lambda q x_2 \\ x_5 & 0 & 0 & 0 & -E \end{vmatrix}. \tag{40}$$

Both eigenfunctions $\Psi(\lambda)$ in Eq. (31) satisfy $x_2 = x_5 = 0$ and $x_3 = x_4 = x$. Hence

$$D(\lambda) = E^3[E + 2x(v - \lambda q)]. \tag{41}$$

Thus $D(\lambda) = 0$ if either $E = 0$ or $E + 2x(v - \lambda q) = 0$. The first possibility yields

$$E = 0 \Rightarrow \lambda_1 = \lambda_h = -4v^2 v^*/u^2 q, \quad \lambda_2 = \lambda_p = 2v/q. \tag{42}$$

The point λ_2 is a pole while the point λ_1, being neither a pole nor a branch point, is a hidden singularity. Another possibility yields

$$E + 2x(v - q) = 0 \Rightarrow \lambda = \lambda_b = (u^2 + 8vv^*)/4v^*q, \tag{43}$$

which is a branch point.

Concerning the eigenfunctions Ψ_1, Ψ_2, and Ψ_3, Eq. (29), one finds $D(\lambda) \equiv 0$ in accord with Lemma 8. Thus the vanishing of the Jacobian is due to a continuous degeneracy. However, no point λ is a point of accidental degeneracy, since the above eigenfunctions are degenerate identically, i. e., for each λ. Hence they are not normal eigenfunctions (see Theorem 5). In the same way, one finds $D(\lambda = u/v) = 0$ in the case of a resonance solution (37). This is in accord with Lemma 9.

(d) Physical meaning of singular points

The solutions close to a pole or a branch point can obviously have no physical meaning. Close to a pole, for example, at least one component of a vector $x(\lambda)$ tends to infinity. This, however, means that the operator V cannot be treated as a perturbation anymore. However, in the CC equation, V is introduced as an approximation which takes into account only some of the excited states. Hence, if a pole is close to a point $\lambda = 1$, the corresponding regular solution is not of much value. Formally, close to a pole a state $x(\lambda)$ tends to be orthogonal to a state Φ, and thus if $\langle x | \Phi \rangle$ is small for some solution (E, x) of the CC equations, we should regard this solution as poorly representing the real state. Hence the CC formalism is good only for a few low-lying states, expecially for a ground state which is likely to have significant overlap with a state Φ.

On the other hand, close to a branch point we have two different solutions with eigenfunctions whose overlap approaches to 1. However, at the point $\lambda = 0$, those two eigenfunctions are mutually orthogonal and hence distinct. Thus if operator V is to be considered as a perturbation, the solution close to a branch point can also have no physical meaning.

(e) Reality of solutions

The question of the reality of the solutions, especially, the reality of the eigenvalue E, is answered by Lemma 12. Provided Hamiltonian H is real, each regular solution $[E(\lambda), x(\lambda)]$ is real along the real λ axis, as long as we don't meet some branch point. It means that if there is no branch point between the points $\lambda = 0$ and $\lambda = 1$, the corresponding solution of CC equations ($\lambda = 1$) should be real. Note that the essential requirement is the reality of the Hamiltonian. As is well known, provided Hamiltonian H is velocity independent, there exists a real basis.

It is interesting to note that the reality and the nonreality of eigenvalues E depends to some extent on the basis in which matrix elements of the Hamiltonian H

(and hence of the operator V) are written. Different orthonormal bases can be connected by unitary transformations and eigenvalues of CC equations are generally not invariant with respect to them. This can be illustrated using as an example the CE (27). The full Hamiltonian of the system described by this equation is a six-by-six matrix. Observe now the infinitesimal unitary transformation,

$$U = I + i\epsilon A, \quad a_{36} = a_{46} = a_{63} = a_{64} = 1 \tag{44}$$
$$\text{otherwise,} \quad a_{ij} = 0, \quad i,j = 1, 2, \ldots, 6$$

and assume that H is real,

$$h_{13} = h_{14} = v = v^*, \quad h_{36} = h_{46} = q = q^*. \tag{45}$$

To first order in ϵ the transformed CE reads

$$\begin{pmatrix} u & 0 & v & v & 0 \\ 0 & 0 & 0 & 0 & 0 \\ v & 0 & 0 & 0 & 0 \\ v & 0 & 0 & 0 & 0 \\ 0 & 0 & 0 & 0 & 0 \end{pmatrix} + \lambda(x_2 x_5 + x_3 x_4) \begin{pmatrix} -2i\epsilon v & 0 & 0 & 0 & 0 \\ 0 & 0 & 0 & 0 & 0 \\ q + i\epsilon P & 0 & 0 & 0 & 0 \\ q + i\epsilon P & 0 & 0 & 0 & 0 \\ 0 & 0 & 0 & 0 & 0 \end{pmatrix} \begin{bmatrix} 1 \\ x_2 \\ x_3 \\ x_4 \\ x_5 \end{bmatrix}$$

$$= E \begin{bmatrix} 1 \\ x_2 \\ x_3 \\ x_4 \\ x_5 \end{bmatrix}, \tag{46}$$

where

$$P = h_{66} = \langle 6 | H | 6 \rangle.$$

Due to (45) the eigenvalues of the nontransformed CE (27) are real for real λ values as long as $\lambda \le \lambda_b$. This is obvious from Eqs. (31) and (32). However, the eigenvalues associated with the transformed CE (46) are complex, which results from the appearance of complex terms in the operator V.

It should be noted that the eigenvalues of CI equations are also generally not invariant with respect to unitary transformations. However, in the case of CI equations, eigenvalues remain always real, while in the case of CC equations they can, as shown above, assume complex values as well.

Unitary transformation (44) mixes singly excited states $|3\rangle$ and $|4\rangle$ with the doubly excited state $|6\rangle$. However, we can consider unitary transformations of one-particle type, which only mix occupied and unoccupied one-particle states among themselves. Such transformations express new creation (annihilation) operators as linear combinations of old creation (annihilation) operators, and they change the reference state Φ only up to the phase. Obviously CC equations (11), and hence the CE, are invariant with respect to those transformations. Usually, however, a velocity-independent Hamiltonian is written either in the real basis or in some basis which can be connected by the above type of unitary transformation with a real basis. We conclude that, provided Hamiltonian H is velocity independent, eigenvalues E are generally real. The reality of the eigenvalue can be violated only if the corresponding regular solution of the CE has a branch point of the real λ axis between real points $\lambda = 0$ and $\lambda = 1$.

(f) Modified characteristic equation

As mentioned above, regular solutions of the CE are our main concern, since only those solutions can connect CI and CC. However, a given CE can have very few or no regular solutions at all. In order that a solution $[E(\lambda), x(\lambda)]$ be regular, it is essential that the corresponding Jacobian is not identical to 0. This is a serious limitation, and we would like to extend the notion of a regular solution to as many solutions of the characteristic equation as possible.

This can be done by a slight modification of the characteristic equation. Instead of Eq. (38) we observe the equation

$$\{H + \epsilon A + \lambda[V(x) - \epsilon A]\}x = Ex, \quad x_1 = 1, \qquad (47)$$

where operator A satisfies requirement (A45). We call this equation the modified characteristic equation (MCE). For $\epsilon = 0$ it reduces to the usual CE, while for $\lambda = 1$ it represents the CC equations. Formally, Eq. (47) can be considered as a characteristic equation of the CC method and a "modified" CI where Hamiltonian H is replaced with $H' = H + \epsilon A$, while at the same time operator V is replaced with $V' = V - \epsilon A$.

All the conclusions concerning the behavior and structure of the solutions of CE do apply to the solutions of MCE as well. As shown in the Appendix, for small enough ϵ, which we assume to be the case, MCE has exactly m regular solutions $[E(\lambda), x(\lambda)]$. Each of those solutions can have a finite number of singular points which are of four types: pole, branch point, accidental degeneracy, and hidden singularity. In a pole the solution $[E(\lambda), x(\lambda)]$ is not defined and at least one component of a vector $x(\lambda)$ blows up. Thus the pole corresponds to an eigenfunction which is formally orthogonal to Φ. In each neighborhood of a branch point there are at least two solutions which smoothly approach each other. In an accidental degeneracy point there are at least two solutions with the same energy. Finally, if the point λ is a hidden singularity point, none of the above holds, but the solution $[E(\lambda), x(\lambda)]$ is unstable and the corresponding Jacobian vanishes.

(g) Geometric interpretation of solutions

For each λ the CE is a set of m equations in m unknowns. Geometrically we can think of those equations as describing m hypersurfaces in an m-dimensional space X^m. Each solution is then a common intersection of those hypersurfaces. Such a picture can help us to understand the nature of resonance points and different types of singular points. In Fig. 3 are shown those different possibilities and their geometrical meaning. This figure deals with the simple case where we have only two hypersurfaces, $f_1(\lambda, E, x) = 0$ and $f_2(\lambda, E, x) = 0$. In Fig. 3 those hypersurfaces for a given λ value are shown. Figure 3(a) corresponds to a crossing of all hypersurfaces in a given point. In this point, $D \neq 0$ and hence it is a nonresonance solution. In Fig. 3(b) the two hypersurfaces do not cross; or, if one prefers, they meet in infinity. Hence there is no solution. However, the Jacobian still can be defined as the analytic continuation of the Jacobian in some neighboring λ point.
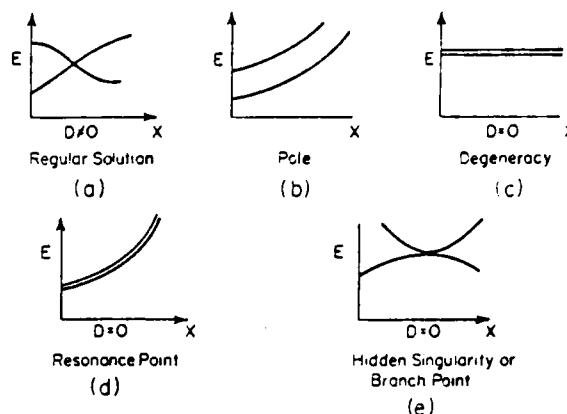

FIG. 3. Graphical depictions of possible solutions as intersections of m hypersurfaces in m-dimensional space, and their associated values of the Jacobian D.

In Figs. 3(c) and 3(d) both hypersurfaces do coincide which corresponds in a more general case to the dependence of hypersurfaces. In the former case, since E is always constant, we have degeneracy, while in the latter case it is a resonance point. Finally, Fig. 3(e) can describe either a hidden singularity or a branch point. In order to distinguish those two possibilities, we should draw at least a three-dimensional diagram including λ axes as well. In the first case (hidden singularity) the two hypersurfaces should only touch in some point. In a branch point, as we proceed along the λ axes starting from a point of touch, we should continuously arrive at two distinct crossing points corresponding to two solutions. It should be noted, however, that in reality two axes correspond to each axis: One for a real part and another for an imaginary part. Figure 3 is hence only approximate.

V. DISCUSSION

Exploiting the analytic connection of the CC with the CI method, we have come to the following main conclusions concerning the solutions of CC equations.

(1) Each MCE has as many regular solutions as the corresponding CI. Here, there are, in general, as many solutions to the CC equations as the number of solutions to the associated CI equations. The particular CI solution can be "lost" only if the point $\lambda = 1$ is a pole or a branch point of a corresponding regular solution of MCE.

(2) Unless a branch point exists on the real axis in the complex λ plane between 0 and 1 the energy eigenvalue will be real for a real Hamiltonian. If the Hamiltonian matrix is complex, the energy might become complex.

(3) Solutions to the CC equations associated with highly excited states tend to become more and more orthogonal to Φ. They will also describe these states poorly. Therefore, it becomes more likely that those excited CC solutions will show singularities close to $\lambda = 1$. Whether this causes the CC solution to be not defined ($\lambda = 1$ is a pole) or has a complex energy value (branch point between 0 and 1 on a real axis) is dependent on the Hamiltonian matrix elements.

J. Math. Phys., Vol. 19, No. 5, May 1978

T.P. Zivkovic and H.J. Monkhorst   1015

The reader will have noticed that little use was made of the actual algebraic form of Eqs. (38), peculiar for the CC equations. This is particularly the case when discussing the occurrence of resonance points, poles, and branch points. As evidenced by Lemmas 6 and 9 in the Appendix, it is important for proving the reality of the solution, but only to the extent that

$$V(\mathbf{x}^*) = V^*(\mathbf{x}).$$

This suggests that the developed procedure of analytically constructing the solutions to nonlinear, algebraic equations from a known problem (in this case the linear CI equations), is quite general. Thus, with some modification this method can be applied to Hartree–Fock (HF) equations as well. The modification is required since HF equations are not analytic in the unknowns. This follows from the fact that the HF potential depends on the products of the components of the eigenvectors Ψ_i with complex conjugates of those components. However, this difficulty can be overcome, and essentially the same method of the characteristic equation can be applied. One finds that, if HF equations describe a system consisting of N particles, and if there are M one-particle states (occupied plus unoccupied), then the characteristic equation corresponding to this HF has $\binom{M}{N}$ regular solutions. In order to obtain this result, it is necessary to redefine the characteristic equations and the definition of the regular solution in an appropriate way. This will be done elsewhere.[14]

APPENDIX

Lemma 1: Let T and C be cluster and configuration operators defined by

$$T = \sum_{s=1} T_s, \quad C = \sum_{s=1} C_s, \tag{A1}$$

where T_s and C_s,

$$T_s = \sum_{\alpha_1 \cdots \alpha_s, r_1 \cdots r_s} t^{r_1 \cdots r_s}_{\alpha_1 \cdots \alpha_s} b_{r_1} \cdots b_{r_s} a_{\alpha_s} \cdots a_{\alpha_1},$$

$$C_s = \sum_{\alpha_1 \cdots \alpha_s, r_1 \cdots r_s} c^{r_1 \cdots r_s}_{\alpha_1 \cdots \alpha_s} b_{r_1} \cdots b_{r_s} a_{\alpha_s} \cdots a_{\alpha_1}, \tag{A2}$$

are operators creating linear combinations of s-tuple p-h excitations. Further, let T and C be connected by the operator relation

$$e^T = 1 + C. \tag{A3}$$

The following two operator relations hold:

$$C_s = \sum_{k=1}^{s} \frac{1}{k!} \sum_{\{s_i\}} \delta(s_1 + \cdots + s_k, s) \prod_{i=1}^{k} T_{s_i}, \tag{A4}$$

$$T_s = \sum_{k=1}^{s} \frac{(-)^{k-1}}{k} \sum_{\{s_i\}} \delta(s_1 + \cdots + s_k, s) \prod_{i=1}^{k} C_{s_i}. \tag{A4'}$$

In Eq. (A4) and (A4') the sum "$\sum_{\{s_i\}}$" extends over all possible combinations of k numbers $s_1, s_2, \ldots, s_k$ such that $s_1 + s_2 + \cdots + s_k = s$.

Proof: Due to (A2) we have

$$[C_s, C_p] = [T_s, T_p] = 0, \quad s, p = 1, 2, \cdots \tag{A5}$$

and hence

$$e^T = \sum_{i=0} T^i / i! = \sum_{i=0} \left(\sum_{p=1} T_p \right)^i / i!$$

$$= 1 + T_1 + (T_2 + T_1^2/2) + (T_3 + T_1 T_2 + T_1^3/6) + \cdots$$

$$= 1 + \sum_{s=1} \left[\sum_{k=1} \frac{1}{k!} \sum_{\{s_i\}} \delta(s_1 + \cdots + s_k, s) \prod_{i=1}^{k} T_{s_i} \right]. \tag{A6}$$

where the last expression can be obtained by a simple combinatorial analysis. Comparison with (A3) proves (A4) now.

The inverse relation (A4') can be proven along the same lines using the operator relation

$$T = \ln(1 + C) = \sum_{i=1} \frac{(-)^i}{i} C^i. \tag{A7}$$

(A7) is formally valid only if $|C| < 1$. However, if the right-hand side in (A7) is applied to any state Ψ consisting of a finite number of excitations this series is finite and hence (A7) holds. Thus (A4') deduced from (A7) is valid for all finite-dimensional cases.

Theorem 1: Let

$$\langle \Phi^R_\Delta(s) | e^{-T}(H - E)e^T | \Phi \rangle = 0,$$

$$T = T_1 + \cdots + T_n, \quad s = 0, 1, \ldots, n, \tag{A8}$$

be a set of CC equations including up to n excitations. This set of equations is equivalent to the CI-like equations,

$$\langle \Phi^R_\Delta(s) | (H - E)\{1 + C + [C_{n+1}(n) + C_{n+2}(n)]\} | \Phi \rangle = 0,$$

$$C = C_1 + \cdots + C_n, \quad s = 0, 1, \ldots, n, \tag{A9}$$

where

$$C_{n+1}(n) = \sum_{k=2}^{n+1} \frac{(-)^k}{k} \sum_{\{s_i\}} \delta(s_1 + \cdots + s_k, n+1) \prod_{i=1}^{k} C_{s_i},$$

$$C_{n+2}(n) = \sum_{k=2}^{n+1} \frac{(-)^k}{k} \sum_{\{s_i\}} \delta(s_1 + \cdots + s_k, n+1) C_1 \prod_{i=1}^{k} C_{s_i} \tag{A10}$$

$$- \sum_{k=3}^{n+2} \frac{(-)^k}{k} \sum_{\{s_i\}} \delta(s_1 + \cdots + s_k, n+2) \prod_{i=1}^{k} C_{s_i}.$$

Operators C_s and T_s for $s \leqslant n$ are connected by the relations (A4) and (A4').

Proof: Let the space of states consist of, at most, N-tuple excitations. Observe (A3). Formally $T_s = C_s = 0$ if $s > N$, while for the case $s \leqslant N$ the connection between C_s and T_s is given by (A4) and (A4'). Now let T terminate after the nth term $T = T_1 + T_2 + \cdots + T_n$, and let us express C_s in terms of such T. In order to denote that C_s depends on n we will write $C_s(n)$. From (A4) it follows that $C_s(n) = C_s$ if $s \leqslant n$. Let us now look at $C_{n+1}(n)$. This operator has the same dependence on T_s as the operator C_{n+1}, provided we put $T_{n+1} = 0$ in (A4). Hence, from (A4),

$$C_{n+1}(n) = C_{n+1} - T_{n+1}. \tag{A11}$$

By the same argument, we obtain

$$C_{n+2}(n) = C_{n+2} - (T_{n+2} + T_1 T_{n+1}). \tag{A12}$$

From (A4),

$$T_{n+1} = C_{n+1} + \sum_{k=2}^{n+1} \frac{(-)^{k-1}}{k} \sum_{\{s_i\}} \delta(s_1 + \cdots + s_k, n+1) \prod_{i=1}^{k} C_{s_i},$$

$$T_{n+2} = C_{n+2} - C_1 C_{n+1} + \sum_{k=3}^{n+2} \frac{(-)^{k-1}}{k} \sum_{\{s_i\}} \delta(s_1 + \cdots + s_k, n+2)$$

$$\times \prod_{i=1}^{k} C_{s_i}, \tag{A13}$$

and hence Eq. (A10) follows. This proves that (A8) is equivalent to

$$\Phi_\Delta^R(s) \left| e^{-T}(H - E)\{1 + C + [C_{n+1}(n) + C_{n+2}(n)]\} \right| \Phi\rangle = 0,$$
$$C = C_1 + \cdots + C_n, \quad s = 0, 1, \ldots, n, \tag{A14}$$

where $C_{n+1}(n)$ and $C_{n+2}(n)$ are given by (A10). Operators C_{n+3}, C_{n+4}, etc., creating $(n+3)$-, $(n+4)$-tuple excitations do not enter into (A14), since Hamiltonian H destroys at most two excitations, operator $\exp(-T)$ can only create excitations and the state $\langle \Phi_\Delta^R(s)|$ contains at most n excitations.

By induction, we now conclude that operator $\exp(-T)$ can be omitted in (A14). First, observe the case $s = 0$. Obviously,

$$\langle \Phi | e^{-T}(H - E)\{1 + C + [C_{n+1}(n) + C_{n+2}(n)]\} | \Phi \rangle$$

$$\equiv \langle \Phi | (H - E)\{1 + C + [C_{n+1}(n) + C_{n+2}(n)]\} | \Phi \rangle = 0, \tag{A15}$$

since $\exp(-T) = 1 - T + T^2/2! + \cdots$ can only create excitations and there is no excitation in $\langle \Phi |$. Second, we have

$$\langle \Phi_\Delta^R(1) | e^{-T}(H - E)\{1 + C + [C_{n+1}(n) + C_{n+2}(n)]\} | \Phi \rangle$$

$$\equiv \langle \Phi_\Delta^R(1) | (H - E)\{1 + C + [C_{n+1}(n) + C_{n+2}(n)]\} | \Phi \rangle$$

$$- \langle \Phi_\Delta^R(1) | T(H - E)\{1 + C + [C_{n+1}(n) + C_{n+2}(n)]\} | \Phi \rangle = 0. \tag{A16}$$

Operator T, when acting on any ket $|\Psi\rangle$, creates at least one more particle-hole pair in it. Therefore, according to (A15) the second term in (A16) is zero and hence

$$\langle \Phi_\Delta^R(1) | (H - E)\{1 + C + [C_{n+1}(n) + C_{n+2}(n)]\} | \Phi \rangle = 0. \tag{A17}$$

By induction it follows

$$\langle \Phi_\Delta^R(s) | (H - E)\{1 + C + [C_{n+1}(n) + C_{n+2}(n)]\} | \Phi \rangle = 0,$$
$$s = 0, 1, \ldots, n. \tag{A18}$$

This set of equations is equivalent to (A14) and hence to (A8). Theorem 1 is thus proved.

A kind of inverse theorem also holds:

Theorem 2: Let

$$\Phi_\Delta^R(s) | (H - E)(1 + C) | \Phi \rangle = 0,$$
$$C = C_1 + \cdots + C_n, \quad s = 0, 1, \ldots, n \tag{A19}$$

be a set of CI equations including up to n-tuple excitations. This set of equations is equivalent to the CC-like equations

$$\Phi_\Delta^R(s) | e^{-T(n)}(H - E)e^{T(n)} | \Phi \rangle = 0, \quad s = 0, 1, \ldots, n, \tag{A20}$$

where

$$T(n) = T_1 + \cdots + T_n + T_{n+1}(n) + T_{n+2}(n),$$

$$T_{n+1}(n) = -\sum_{k=2}^{n} \frac{1}{k!} \sum_{\{s_i\}} \delta(s_1 + \cdots + s_k, n+1) \prod_{i=1}^{k} T_{s_i},$$

$$T_{n+2}(n) = \sum_{k=2}^{n} \frac{1}{k!} \sum_{\{s_i\}} \delta(s_1 + \cdots + s_k, n+1) T_1 \prod_{i=1}^{k} T_{s_i} \tag{A21}$$

$$- \sum_{k=3}^{n} \frac{1}{k!} \sum_{\{s_i\}} \delta(s_1 + \cdots + s_k, n+2) \prod_{i=1}^{k} T_{s_i}.$$

Operators C_s and T_s for $s \le n$ are connected by the relations (A4) and (A4'). The above theorem can be proven along the same lines as Theorem 1. Both theorems express a formal symmetry between CI and CC equations.

Observe the equations:

$$\langle \Phi_\Delta^R(s) | (H - E)\{1 + C + \cdots + C_n$$

$$+ \lambda[C_{n+1}(n) + C_{n+2}(n)]\} | \Phi \rangle = 0, \tag{A22}$$

$$s = 0, 1, \ldots, n.$$

These equations explicitly include up to n-tuple excitations while $(n+1)$ and $(n+2)$-tuple excitations are included through the operators $C_{n+1}(n)$ and $C_{n+2}(n)$, which depend on C_1 to C_n, according to (A10). For $\lambda = 1$ this set of equations reduces to (A9), hence it is equivalent to CC equations including up to nth order clusters T_s. For $\lambda = 0$, Eqs. (A24) reduce to a usual CI problem including up to n-tuple excitations.

Lemma 2: Equations (A22) can be written in the matrix form

$$[H + \lambda V(\Psi)]\Psi = E\Psi, \quad \Psi_{00} = 1, \tag{A23}$$

where H and V are matrices with elements

$$H_{R\Delta, R'\Delta'} = \langle \Phi_\Delta^R | H | \Phi_{\Delta'}^{R'} \rangle,$$

$$V_{R\Delta, R'\Delta'} = V_{R\Delta} \delta_{R'\Delta', 00} \tag{A24}$$

$$= \langle \Phi_\Delta^R | H[C_{n+1}(n) + C_{n+2}(n)] | \Phi \rangle \delta_{R'\Delta', 00},$$

and Ψ is a column vector with components

$$\Psi_{R\Delta}(s) = \langle \Phi_\Delta^R(s) | C_s | \Phi \rangle = c_{\alpha_1 \cdots \alpha_s}^{r_1 \cdots r_s}, \quad s = 0, 1, \ldots, n. \tag{A25}$$

Lemma 2 follows directly from (A22). The requirement $\Psi_{00} = 1$ fixes the norm and phase of Ψ. Formally (A23) is an eigenvalue equation. Note that according to (A24), operator V is not Hermitian, and hence the reality of E is not guaranteed. We will call Eqs. (A22) and (A23) characteristic equations (CE). We shall analyze the solutions (eigenvectors and eigenvalues) of the CE as a function of λ. Besides CE (A23) we will sometimes consider the equation

$$\{H + \epsilon A + \lambda[V(\Psi) - \epsilon A]\}\Psi = E\Psi, \quad \Psi_{00} = 1, \tag{A23'}$$

where A is a real Hermitian operator. Later on [see Eq. (A45)] we will impose some additional requirements on A. We will call Eq. (A23') the modified characteristic equation (MCE). Obviously, for $\epsilon = 0$ this equation reduces to CE. Note also that for $\lambda = 1$ it reduces to CC equations. In what follows, we will refer mainly to CE. However, all the conclusions, unless otherwise specified, apply to MCE as well.

We now first examine some properties of the operator V and its matrix elements $V_{R\Delta}$.

Lemma 3: Each $V_{R\Delta}$ is either identically zero or it is a polynomial in the components of the vector Ψ.

(a) All matrix elements $V_{R\Delta}(s)$, corresponding to the s-tuple excitations where $s < n - 1$ are identically zero.

(b) If there is no $(n + 1)$-tuple excitation $|\Phi_{\Delta'}^{R'}(n+1)\rangle$ such that

$$\langle \Phi_\Delta^R(n-1)|H|\Phi_{\Delta'}^{R'}(n+1)\rangle \neq 0, \tag{A26}$$

the matrix element $V_{R\Delta}(n-1)$ corresponding to $(n-1)$-tuple excitations $|\Phi_\Delta^R(n-1)\rangle$ is identically zero. Otherwise $V_{R\Delta}(n-1)$ is polynomial in the components of Ψ of degree $(n+1)$ and with smallest power 2.

(c) If there is no $(n+1)$-tuple excitations $|\Phi_{\Delta'}^{R'}(n+1)\rangle$ such that

$$\langle \Phi_\Delta^R(n)|H|\Phi_{\Delta'}^{R'}(n+1)\rangle \neq 0 \tag{A27}$$

and at the same time no $(n+2)$-tuple excitations $|\Phi_{\Delta'}^{R'}(n+2)\rangle$ such that

$$\langle \Phi_\Delta^R(n)|H|\Phi_{\Delta'}^{R'}(n+2)\rangle \neq 0 \tag{A28}$$

matrix element $V_{R\Delta}(n)$ corresponding to n-tuple excitations $|\Phi_\Delta^R(n)\rangle$ is identically zero. If only (A26) holds, $V_{R\Delta}$ is a polynomial in the components of Ψ of the degree $(n+1)$ with smallest power 2 [same case as (b)]. If (A29) holds $V_{R\Delta}(n)$ is polynomial in components of Ψ of degree $(n+2)$ with smallest power 2.

Summarizing, Lemma 3 states that unless $V_{R\Delta}$ is identically zero, it is a polynomial of Ψ components of degree at most $(n+2)$ and at least 2.

Lemma 4: Polynomial $V_{R\Delta}$ contains each component of Ψ with power of at most 1.

Lemma 5: If the Hamiltonian H is real, matrix elements $V_{R\Delta}(\Psi)$ satisfy

$$[V_{R\Delta}(\Psi)]^* = V_{R\Delta}(\Psi^*) \tag{A29}$$

Lemma 6: If the Hamiltonian H is real, and if $\langle E_0, \Psi_0\rangle$ is a solution of CE for $\lambda = \lambda_0$, then (E_0^*, Ψ_0^*) is a solution of the same CE in the point $\lambda = \lambda_0^*$.

All these Lemmas follow from (A10) and (A24). For example,

$$V_{R\Delta}(n-1) = \langle \Phi_\Delta^R(n-1)|H[C_{n+1}(n) + C_{n+2}(n)]|\Phi\rangle$$

$$= \sum_{k=2}^{n+1} \frac{(-)^k}{k} \sum_{\{s_i\}} \delta(s_1 + \cdots + s_k, n+1)$$

$$\times \sum_{R'\Delta'} \langle \Phi_\Delta^R(n-1)|H|\Phi_{\Delta'}^{R'}(n+1)\rangle$$

$$\times \langle \Phi_{\Delta'}^{R'}(n+1) \prod_{i=1}^{k} C_{s_i}|\Phi\rangle. \tag{A30}$$

If in the above expressions there is at least one vector $|\Phi_{\Delta'}^{R'}(n+1)\rangle$ such that relation (A26) holds, the term in (A30) corresponding to $k = n+1$ gives rise to the highest power $(n+1)$ in the components of Ψ. The lowest power is 2, corresponding to the term with $k = 2$ in (A30). In the same way, matrix elements $V_{R\Delta}(n)$ can be analyzed. Lemma 4 follows from the fact that $a_i^2 = 0$ for each Fermion annihilation operator a_i^2. Since operators C_s can only create particle-hole pairs and never destroy them, once such pairs are created the repeated application of the same $p - h$ creation operators on the new

state gives zero. Lemma 5 can be deduced straightforwardly from the explicit expressions for $V_{R\Delta}$, such as (A30), and from the assumed reality of the matrix elements of H. Lemma 6 follows from Lemma 5. The following lemma is also of some interest.

Lemma 7: Operator V is either identically zero or it is nonbounded.

Proof: Observe first that according to (A23) operator V is defined only for Ψ such that $\Psi_{00} = 1$. From Eq. (A24) it follows that

$$\Psi_{R\Delta}' = (V\Psi)_{R\Delta} = V_{R\Delta}(\Psi). \tag{A31}$$

Assume now that V is not identically zero. According to Lemma 3, there is $(R'\Delta')$ such that $V_{R'\Delta'}$ is a polynomial in the components of Ψ of the degree at least 2. Hence

$$\frac{|V\Psi|^2}{|\Psi|^2} = \frac{\sum_{R\Delta} |V_{R\Delta}(\Psi)|^2}{\sum_{R\Delta} |\Psi_{R\Delta}|^2} \geq \frac{|V_{R'\Delta'}(\Psi)|^2}{\sum_{R\Delta} |\Psi_{R\Delta}|^2}. \tag{A32}$$

However, $|V_{R'\Delta'}(\Psi)|^2$ is a polynomial of at least fourth degree, while $\sum_{R\Delta} |\Psi_{R\Delta}|^2$ is a polynomial of a degree 2, and hence the right-hand side in Eq. (A32) is not bounded. It follows that V is not bounded either.

Observe that although V is not bounded it is continuous since its matrix elements are polynomial (continuous) functions of the components of a vector Ψ.

We would now like to examine the properties of CE as a function of the parameter λ. Examples given in Sec. III suggest the following definitions:

Definition 1: Point λ_r in a complex λ plane is a resonance point of a CE if for $\lambda = \lambda_r$ the CE has an *infinite* number of eigenvalues.

Definition 2: Point λ_n in a complex λ plane is a nonresonance point of a CE if, for $\lambda = \lambda_n$ the CE has a finite number of eigenvalues.

The emphasis in Definitions 1 and 2 is on the number of eigenvalues and not on the number of eigenfunctions, which can be infinite due to degeneracy. It is clear that $\lambda = 0$ is a nonresonance point.

We now prove the following theorem.

Theorem 3: Let λ_r be a resonance point of a CE. Each value E, except a finite number of them, is an eigenvalue of the CE.

Proof: In order to prove this theorem, it is more convenient to renumerate the components $\Psi_{R\Delta}$ of a vector Ψ in such a way that we first take component $\Psi_{00} = 1$, then in some definite order all components corresponding to single excitations, then all components associated with double excitations, etc., up to n-tuple excitations. We denote the renumerated components by x_i, $i = 1, \ldots, m$. With this enumeration understood, we write, instead of Ψ, the vector x. Thus (A23) reads

$$[H + \lambda V(x)] = Ex, \quad x_1 = 1, \tag{A33}$$

where H and V are $m \times m$ square matrices with elements given by (A24), using the correspondence $\Psi_{R\Delta} \to x_i$. The matrix equation (A33) is a system of m equations in m unknowns:

$$f_1 \equiv h_{11} + h_{12}x_2 + \cdots + h_{1m}x_m + \lambda V_1(x) - E = 0,$$

$$f_2 \equiv h_{21} + h_{22}x_2 + \cdots + h_{2m}x_m + \lambda V_2(x) - Ex = 0,$$

$$\vdots$$

$$\text{(A34)}$$

$$f_m \equiv h_{m1} + h_{m2}x_2 + \cdots + h_{mm}x_m + \lambda V_m(x) - Ex_m = 0,$$

where the unknowns are $E, x_2, \ldots, x_m$. Each polynomial f_i can be uniquely factorized in a set of $k(i)$ irreducible polynomials $f_i^{j_i}$, $j_i = 1, \ldots, k(i)$. For example, the polynomial

$$f = x_1^3 - x_2^3 + x_1 x_2^2 - x_1^2 x_2 + x_2 - x_1 = 0$$

can be factorized as

$$f \equiv (x_1^2 - x_2^2 - 1)(x_1 - x_2) = 0.$$

Hence the set (A34) is equivalent to $K \equiv \prod_i k(i)$ sets of equations

$$f_1^{j_1} = 0, \quad j_1 = 1, 2, \ldots, k(1),$$

$$f_2^{j_2} = 0, \quad j_2 = 1, 2, \ldots, k(2), \qquad \text{(A35)}$$

$$f_m^{j_m} = 0, \quad j_m = 1, 2, \ldots, k(m).$$

Each equation in (A35) represents a hypersurface in the m-dimensional space X^m spanned by $E, x_2, \ldots, x_m$. Geometrically, the solution of (A34) is the joint intersection of all hypersurfaces $f_1^{j_1} \cdots f_m^{j_m}$. Assume now that the point $\lambda = \lambda_r$ is a resonance point of (A34). In this case, there is at least one set (A35) which has an infinite number of intersections in X^m with different values of E. Due to the algebraic structure of the $f_i^{j_i}$ this can happen only if this set is dependent. But this means that it can be solved step by step to lead finally to an equation of the type

$$g[E, x_2(x_i), \ldots, x_{i-1}(x_i), x_i, x_{i+1}(x_i), \ldots, x_m(x_i)] = 0, \quad \text{(A36)}$$

which is algebraic in $E, x_2, \ldots, x_m$, where all $x_s(x_i)$ are algebraic in x_i. Therefore (A36) is algebraic in E and x_i, and, being satisfied for a denumerable number of distinct E values, it is satisfied for each E except, possibly, for a finite number of them. This proves Theorem 3.

Related to this Theorem is the following theorem.

Theorem 4: Each CE has either a finite number of resonance points, or each λ is a resonance point except for a finite number of them.

This theorem is proven along the same lines as the preceding one. Assume namely that a given CE has an infinite number of resonance points. From this infinite number, we can extract a denumerable subset of them. According to Theorem 3, for each resonance point the CE is satisfies for all E except for a finite number of them. It follows that for a denumerable number of resonance points there is a set consisting of all E except for, at most, a denumerable number of them. However, due to the algebraic character of the CE exclusion can apply only to a finite number of them. This means that the equations

$$f_i(\lambda, E, x) = 0 \qquad \text{(A37)}$$

are satisfied for a denumerable number of λ values and for all E with the possible exception of a finite num-

ber of them. But then, since f_i are polynomials, (A37) should be satisfied for all λ with the exception of a finite number. This proves Theorem 4.

It is very likely that the number of resonance points can only be finite, meaning that the second possibility in Theorem 4 does not apply for realistic cases. However, we were unable to prove that.

Besides resonance points, the CE can also have singular points. In order to define these points, we first introduce the Jacobian of the CE which is defined for a given λ, E, and x_i:

$$D(\lambda, x, E) = \begin{vmatrix} \partial' f_1 \cdots \partial^m f_1 \\ \partial' f_m \cdots \partial^m f_m \end{vmatrix}, \qquad \text{(A38)}$$

where

$$\partial' = \frac{\partial}{\partial E}, \quad \partial^i = \frac{\partial}{\partial x_i}, \quad i = 2, \ldots, m.$$

In the case of CE we have

$$D(\lambda, x, E) = - \begin{vmatrix} 1 & (h_{12} + \lambda\partial^2 V_1) & \cdots & (h_{1m} + \lambda\partial^m V_1) \\ x_2 & (h_{22} - E + \lambda\partial^2 V_2) & \cdots & (h_{2m} + \lambda\partial^m V_2) \\ \cdot & & & \\ \cdot & & & \\ \cdot & & & \\ x_m & (h_{m2} + \lambda\partial^2 V_m) & \cdots & (h_{mm} - E + \lambda\partial^m V_m) \end{vmatrix}$$

$$\text{(A38')}$$

and similarly for the MCE. Now the following theorem can be proven.

Theorem 5: Let the CE

$$[H + \lambda V(x)]x = Ex \qquad \text{(A39)}$$

for $\lambda = \lambda_0$ have a solution (E_0, x_0). Further let the corresponding Jacobian be different from zero:

$$D(\lambda_0, E_0, x_0) \neq 0. \qquad \text{(A40)}$$

Then there is $E(\lambda)$ and $x(\lambda)$ such that:

1. $E(\lambda)$ as well as each component of $x(\lambda)$ are analytic functions in the whole complex λ plane, with possible exceptions of, at most, a finite number of points.

2. $[E(\lambda), x(\lambda)]$ is a solution of a CE (A39) and for $\lambda = \lambda_0$ it concides with (E_0, x_0).

This solution $[E(\lambda), x(\lambda)]$ we shall call a *normal* solution. If $[E(\lambda), x(\lambda)]$ is defined in the point $\lambda = 0$ we shall call it *regular*. Also, eigenvalue $E(\lambda)$ and eigenfunction $x(\lambda)$ we shall call a normal (regular) eigenvalue and a normal (regular) eigenfunction, respectively. Note that by the very definition for each normal solution there is at least one point λ such that the corresponding Jacobian is different from zero.

Proof: The proof of the above Theorem 5 is based on the following Theorem 6.

Theorem 6: Let $g(x, y) = \{g_1, \ldots, g_n\}$ be continuous for vector x in a neighborhood of x_0 in R_m, and for vector y in a neighborhood of y_0 in R_n, with $g(x_0, y_0) = 0$. Suppose g is continuously differentiable in y and that the determinant

$$J \equiv \left| \frac{\partial g_i(x_0, y_0)}{\partial y_j} \right| \neq 0. \qquad \text{(A41)}$$

Then there is a neighborhood $N_1(x_0)$ in R_m and a neighborhood $N_2(y_0)$ in R_n such that for every x in N_1 there is a unique $y = \varphi(x)$ in N_2 for which $g[x, \varphi(x)] = 0$. If $g(x, y)$ is k times continuously differentiable in x and y, then $\varphi(x)$ is k times continuously differentiable $(k \geq 1)$.

The above theorem is proven in Ref. 15 for the case of real spaces R_m and R_n. However, it holds for the case of complex spaces as well, which can be proven along the same lines.

Putting $x \equiv \lambda$ and $y \equiv (E, x)$ the above theorem can immediately be applied to the CE. Since $V(x)$ is analytic in some neighborhood of a point $x = x_0$, $E(\lambda)$ and $x(\lambda)$ are analytic as well in some neighborhood $N(\lambda_0)$ of a point $\lambda = \lambda_0$ where a solution exists. Due to the algebraic character of the CE this solution shall be algebraic as well, and we can make an analytic continuation of the function $E(\lambda)$ and $x(\lambda)$ in the whole λ plane. Since these functions are algebraic in a small neighborhood $N(\lambda_0)$, they are algebraic in the whole λ plane as well. We have only to show that $[E(\lambda), x(\lambda)]$ is a solution of CE. In $N(\lambda_0)$ the solution $[E(\lambda), x(\lambda)]$ satisfies

$$f_i[\lambda, E(\lambda), x(\lambda)] = 0. \tag{A42}$$

Since $E(\lambda)$ and $x(\lambda)$ are analytic in λ, and since f_i is analytic in λ, E, and x, it is analytic in λ as well. On the other hand, f_i is identically zero in $N(\lambda_0)$ and, being analytic in λ, should therefore be identically zero for all λ. This proves that $[E(\lambda), x(\lambda)]$ satisfies CE for each λ where it is defined. However, $E(\lambda)$ and $x(\lambda)$ are algebraic functions of λ; hence they are defined for each λ with a possible exception of a finite number of poles and branch points.

It is interesting to see the meaning of the requirement (A40) in the above theorem. For that purpose, we use the following geometric interpretations:

Each equation $f_i(\lambda_0, E, x) = 0$ for a given $\lambda = \lambda_0$ represents a finite number of hypersurfaces in the m-dimensional space X^m spanned by E and $x_2, \ldots, x_m$. The vector $\nabla f_i(\lambda_0, E, x) = \{\partial^1 f_i, \partial^2 f_i, \ldots, \partial^m f_i\}$ is orthogonal to the hypersurface in the point (E, x). The Jacobian (A38) consists of vectors $\nabla f_1, \nabla f_2, \ldots, \nabla f_m$ and hence the vanishing of this quantity implies a linear dependence of these vectors. $D \neq 0$ thus means that ∇f_1 to ∇f_m are not linearly dependent. If the point (E_0, x_0) satisfies $f_i(\lambda_0, E_0, x_0) = 0$ it should lie on a common intersection of all hypersurfaces $f_i = 0$. Moreover, if the corresponding ∇f_i are linearly independent, the vectors orthogonal to $f_i = 0$ are linearly independent. Hence there is some neighborhood of point (E_0, x_0) in X^m where there is no other common intersection of hypersurfaces $f_i = 0$. Thus the nonvanishing of the Jacobian [Eq. (A40)] implies that the solution (E_0, x_0) should be isolated in the space X^m.

Definition 3: Let (E_0, x_0) be a solution of the CE in the point $\lambda = \lambda_0$. Further, in each neighborhood of (E_0, x_0) let $(E_0, x_0') \neq (E_0, x_0)$ exist such that it is a solution of the CE for $\lambda = \lambda_0$ as well. We say that (E_0, x_0) is a continuously degenerate solution of the CE in the point $\lambda = \lambda_0$.

According to the definition, a continuously degenerate solution is not isolated. Also, Eq. (A36) implies that a

resonance solution cannot be isolated. Hence, and in connection with the above conclusion, we did prove the following Lemmas.

Lemma 8: If (E_d, x_d) is a continuously degenerate solution of the CE for $\lambda = \lambda_d$, the corresponding Jacobian $D(\lambda_d, E_d, x_d)$ is equal to zero.

Lemma 9: If (E_r, x_r) is a resonance solution of the CE in a resonance point $\lambda = \lambda_r$, the corresponding Jacobian $D[\lambda_r, E(\lambda_r), x(\lambda_r)]$ is equal to zero.

Lemma 10: If $\lambda = \lambda_b$ is a branch point of a normal solution $[E(\lambda), x(\lambda)]$, the corresponding Jacobian $D(\lambda_b, E(\lambda_b), x(\lambda_b))$ is equal to zero.

Namely if $D(\lambda_b) \neq 0$, by Theorem 5 the solution $[E(\lambda), x(\lambda)]$ should be analytic in the point $\lambda = \lambda_b$ which contradicts the assumption that this is a branch point.

The inverse is not true: Vanishing of the Jacobian does not necessarily mean that the point $\lambda = \lambda'$ is either a branch point, a resonance point, or a point of continuous degeneracy. The above geometrical interpretation implies that if $D(\lambda_0) = 0$ the solution (E_0, x_0) should be unstable. Namely, if ∇f_i are linearly dependent, the point (E_0, x_0) is the common intersection of all $f_i = 0$ to at least first order. Hence there are some vectors (E, x) in a space X^m which differ to the first order from (E_0, x_0), but also satisfy the CE to at least second order. Note that by the very definition, continuously degenerate solutions, solutions in a branch point, and resonance solutions are unstable as well.

Theorem 5 now provides a basis for the definition and classification of different types of singular points. Intuitively, each point where the normal solution $[E(\lambda), x(\lambda)]$ is not analytic, or is unstable due to any reason, we consider as singular. Thus singular points are singular points of a given normal solution $[E(\lambda), x(\lambda)]$, and each normal solution can have a different set of singular points. On the other hand, resonance points are characteristic of the CE as a whole. We can have the following singular points:

1. Point $\lambda = \lambda_p$ where solution $[E(\lambda), x(\lambda)]$ is not defined. Since $[E(\lambda), x(\lambda)]$ is algebraic in λ, such a point is a pole. As we approach $\lambda = \lambda_p$ at least one component of a vector $x(\lambda)$ tends to infinity. Hence

$$\lim_{\lambda \to \lambda_0} \frac{\langle x(\lambda) | \Phi \rangle}{[\langle x(\lambda) : x(\lambda) \rangle]^{1/2}} = 0. \tag{A43}$$

This means that $x(\lambda)$ is more and more orthogonal to Φ. No vector orthogonal to Φ can be a solution to CE.

2. Point $\lambda = \lambda_b$ which is a branch point of the solution $[E(\lambda), x(\lambda)]$. Obviously, if λ_b is a branch point, $D(\lambda_b)$ should be equal to zero. If it were not, there would exist, according to Theorem 6, a unique analytic continuation of the solution $[E(\lambda_b), x(\lambda_b)]$ in some neighborhood of this point, which is contrary to the definition of a branch point. We call such a singularity a branch singularity.

3. Point $\lambda = \lambda_d$ where the normal solution $[E(\lambda), x(\lambda)]$ is continuously degenerate. According to Lemma 8, Jacobian $D(\lambda)$ vanishes in this point. We say that $\lambda = \lambda_d$ is a point of accidental degeneracy.

1020   J. Math. Phys., Vol. 19, No. 5, May 1978

T.P. Zivkovic and H.J. Monkhorst   1020

4. Point $\lambda = \lambda_h$ where the normal solution $[E(\lambda), x(\lambda)]$ is defined, the corresponding Jacobian is zero but the vanishing of the Jacobian is not due to any of the former reasons (branch point or accidental degeneracy). Such a point we call a point of a hidden singularity. As shown above, the solution $[E(\lambda), x(\lambda)]$ is unstable in this point.

In short, $\lambda = \lambda_0$ is a singular point of a normal solution $[E(\lambda), x(\lambda)]$ if either $[E(\lambda), x(\lambda)]$ is not defined in this point (pole) or, provided $[E(\lambda), x(\lambda)]$ is defined in $\lambda = \lambda_0$, the corresponding Jacobian vanishes (branch point, accidental degeneracy, and hidden singularity). Due to the algebraic character of the solution $[E(\lambda), x(\lambda)]$ and Jacobian $D(\lambda)$, there can be only a finite number of singular points. If it were not so, $D(\lambda)$ would be identically zero, contrary to the assumption that $[E(\lambda), x(\lambda)]$ is a normal solution.

The above definition of singular points applies only to the normal solution $[E(\lambda), x(\lambda)]$, i.e., such that there exist $\lambda = \lambda'$ with the property $D(\lambda') \neq 0$. However, we have no guarantee that in any point, including $\lambda = 0$, there exists a solution with nonvanishing Jacobian. In order to overcome this limitation, instead of the CE (A23) we observe MCE (A23'). We chose a real Hermitian operator A in such a way that no eigenfunction of the equation

$$Ax = ax \qquad (A44)$$

is orthogonal to Φ, and that all corresponding Jacobians are different from zero. In other words, A satisfies

$$Ax = ax - \begin{cases} \langle x \mid \Phi \rangle \neq 0, \\ D(E, x) = - \begin{vmatrix} 1 & a_{12} & \cdots & a_{1m} \\ x_2 & a_{22} - E & \cdots & a_{2m} \\ \cdot & & & \\ \cdot & & & \\ \cdot & & & \\ x_m & a_{m2} & \cdots & a_{mm} - E \end{vmatrix} \neq 0, \end{cases}$$
$$(A45)$$

and

$$a_{ij} = a_{ij}^* = a_{ji}.$$

Obviously such an operator always exists which can be demonstrated by construction. We now prove Lemma 11.

Lemma 11: There exists $\epsilon_0 \neq 0$ such that if $|\epsilon| \leqslant \epsilon_0$ and $\epsilon \neq 0$ no eigenfunction of the equation

$$(H + \epsilon A)x = Ex \qquad (A46)$$

is orthogonal to Φ, and all corresponding Jacobians are different from zero.

Proof: If ϵ is big enough Eq. (A46) is close enough to Eq. (A44) and since A and H are bounded operators, each solution of Eq. (A46) is close enough to some solution of Eq. (A44), and vice versa. Hence for big enough ϵ, no solution of (A46) is orthogonal to Φ and all corresponding Jacobians are different from zero. However Eq. (A46) has the structure of a CE and, by Theorem 5, all those solutions are analytic in ϵ, with the possible exception of a finite number of ϵ points. It follows that overlaps $\langle x(\epsilon) \mid \Phi \rangle$ are analytic in ϵ, and hence can become zero only in a finite number of points. The

same holds true for the corresponding Jacobians. Hence there is a small circle in the complex ϵ plane around a point $\epsilon = 0$ where no solution of Eq. (A46) is orthogonal to Φ and where all the corresponding Jacobians are different from zero, with the possible exception of the point $\epsilon = 0$. This proves Lemma 11.

We will consider the condition $\epsilon \neq 0$ and $\epsilon < \epsilon_0$ as a part of a definition of MCE. Also, without loss of generality, ϵ can be assumed real. With that in mind, and in combination with Theorem 5, the above Lemma proves the following Theorem 7.

Theorem 7: The modified characteristic equation has m regular solutions, i.e., the same number as the corresponding CI. This means that in each point $\lambda = \lambda'$ an MCE has m solutions which are analytically connected with m solutions of the CI equations (point $\lambda = 0$), unless $\lambda = \lambda'$ happens to either be a pole or a branch point of some regular solution.

We can now state something about the reality of the solutions $[E(\lambda), x(\lambda)]$.

Lemma 12: Let the Hamiltonian H be real and let $[E(\lambda), x(\lambda)]$ be a regular solution of the CE. Assume furthermore that $[E(\lambda), x(\lambda)]$ has no branch point on the real axis between the real points $\lambda = 0$ and $\lambda = \lambda_0$. Provided λ_0 is not a pole, the solution $[E(\lambda_0), x(\lambda_0)]$ exists and it is real.

Proof: Since $[E(\lambda), x(\lambda)]$ is regular, it is defined in $\lambda = 0$. Since H is real, $[E(0), x(0)]$ will be real. We can now reach $\lambda = \lambda_0$ starting from $\lambda = 0$ along some path P in the complex λ plane. P can always be chosen such that it avoids all possible singular points, and that the area enclosed by P and the real axis does not contain branch points [see Fig. 4]. Along P, we have the solution $[E(\lambda), x(\lambda)]$ which smoothly changes from $[E(0), x(0)]$ to $[E(\lambda_0), x(\lambda_0)]$. Now we can reach λ_0 as well along path P^* which is a complex conjugate of P. From Lemma 6, and because there are no branch points between P and the real axis, there is no branch point between P^* and the real axis either. Therefore, there is no branch point in the whole area enclosed by P and P^*. Hence the analytic continuation of $[E(0), x(0)]$ along either path will yield the same solutions in the point λ_0. However, from Lemma 6 and the reality of $[E(0), x(0)]$, it follows that

$$[E(\lambda), x(\lambda)] = [E^*(\lambda^*), x^*(\lambda^*)]$$

and hence, for $\lambda = \lambda_0 = \lambda_0^*$,

$$[E(\lambda_0), x(\lambda_0)] = [E^*(\lambda_0), x^*(\lambda_0)] \qquad (A47)$$
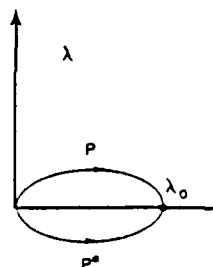
expressing the reality of the solution.

FIG. 4. Paths P and P^* in the complex λ plane connecting a configuration-interaction solution $(\lambda = 0)$ with that in point $\lambda = \lambda_0$ on the real axis. Solution $[E(\lambda_0), x(\lambda_0)]$ is real provided there is no branch-point on the real axis between 0 and λ_0.

Note in the above proof that the condition that there is no branch point between $\lambda = 0$ and $\lambda = \lambda_0$ on the real axis is essential since, if such a point would exist, the analytic continuations along P and P^* would give two different solutions—say, $[E_1(\lambda_0), x_1(\lambda_0)]$ and $[E_2(\lambda_0), x_2(\lambda_0)]$. All we could then infer is that $E_1(\lambda_0) = E_2^*(\lambda_0)$ and $x_1(\lambda_0) = x_2^*(\lambda_0)$. However, the absence of poles between 0 and λ_0 is not essential.

[1]J. Goldstone, Proc. R. Soc. London A 239, 267 (1957).
[2]J. Hubbard, Proc. R. Soc. London A 240, 539 (1957); 243, 336 (1957).
[3]K.A. Brueckner, Phys. Rev. 100, 36 (1955).
[4]B.H. Brandow, Rev. Mod. Phys. 39, 771 (1967).
[5]P.W. Langhof and A.J. Hernandez, Int. J. Quant. Chem. S10, 337 (1976).
[6]F. Coester, Nucl. Phys. 7, 421 (1958).
[7]H.J. Monkhorst, F.E. Harris, and D.L. Freeman (unpublished).
[8]J. Čižek, J. Chem. Phys. 45, 4256 (1966); Adv. Chem. Phys. 14, 35 (1969); see also Ref. 10.
[9]H. Kümmel, K.H. Lührmann, and J.G. Zabolitzky, "Many-Fermion Theory in exp-S Form," Phys. Rep. (in print) and references cited therein.
[10]J. Paldus, J. Čižek, and I. Shavitt, Phys. Rev. A 5, 50 (1972) and references therein to their earlier work; J. Paldus in "Proceedings of Boulder Conference on Theoretical Chemistry," June 1972, Boulder, Colorado; J. Paldus and J. Čižek, in Energy, Structure and Reactivity, edited by D.W. Smith and W.B. Rae (Wiley, New York, 1973), p. 198.
[11]H.J. Monkhorst, Int. J. Quant. Chem. S11, 421 (1977).
[12]F. Coester, Lectures in Theoretical Physics, Vol. 11, edited by K.T. Mahanthappa (Gordon & Breach, New York, 1969).
[13]T.P. Živković, Int. J. Quant. Chem. S11, 413 (1977).
[14]T.P. Živković (unpublished).
[15]T.L. Saaty and G. Bram, Nonlinear Mathematics (McGraw-Hill, New York, 1964), p. 39.

Hartree-Fock density of states for extended systems

Hendrik J. Monkhorst*

Department of Physics, University of Utah, Salt Lake City, Utah 84112

(Received 12 December 1978)

The density of states (DOS) of extended systems, calculated at the rigorous Hartree-Fock (HF) level, can have a number of unphysical features. It is shown analytically that in partially filled band systems (crystals, thin films, polymers) the HF DOS vanishes at the Fermi energy, regardless of Fermi-surface shape. HF DOS will also vanish, in the (rare) event that an equienergetic surface S for an energy different from the Fermi energy coincides with the Fermi surface S_F. Additional features such as shoulders, peaks, or near gaps can occur at energies with surfaces S close to S_F. No HF-related zero DOS arises in filled-band extended systems. Published HF DOS are discussed. A detailed summary of expressions for crystal HF matrix elements in momentum representation is given. Their modification for thin films and polymers is indicated.

I. INTRODUCTION

Since 1969 several calculations have appeared in the literature that aim towards obtaining rigorous Hartree-Fock (HF) results for crystalline solids. These calculations differed from previous work to the extent that full, nonlocal exchange was taken into account, and that integrals were calculated accurately or approximated carefully. Because only limited basis sets were used in Bloch orbital expansions no calculation can be considered to have reached the HF limit. Nevertheless, there are indications that several have come pretty close.

Two fundamentally different approaches to rigorous HF have been used. One of these can be characterized as a configuration-space (CS) approach, since the HF matrix elements are expressed as real (or direct) lattice sums over multicenter integrals. A formulation, using Adams-Gilbert local orbitals,[1] was first given by Kunz.[2] Applications were made to the optical properties of solid rare gases,[3] alkali halides,[4] and lithium hydride.[5] The linear-combination-of-atomic-orbitals (LCAO) version of this approach was applied to diamond,[6] LiF, and Ne.[7] More recently, the CS approach was applied to some "open-shell" solids (with partially filled bands) such as calcium,[8] lithium,[9] and TiO.[10]

The other approach can be described as a momentum-space (MS) approach, because reciprocal lattice summations are used to compute HF matrix elements. First introduced by Harris and Monkhorst,[11] the MS (or Fourier) method has also been used for diamond by Mauger and Lannoo,[12] employing Slater-type orbitals for atomic basis functions. Very recently the MS approach has been analyzed by Cox and Fry[13] and Fry et al.[14] (hereafter referred to by FBB). Applications to properties of several simple metals have also appeared.[15]

The CS and MS formulations are totally different in their analytic and computational details, although, when carried to their limits, the two approaches are identical. We already indicated that the CS and MS methods are based on direct and reciprocal lattice summations, respectively. This difference has several consequences of great practical import. To name a few:

(i) The CS approach is most appropriate for insulating crystals, whereas the MS approach converges best for conductors.

(ii) The Madelung-type conditional convergence problem that troubles the CS method is eliminated in the MS method through a rigorous cancellation of singularities. As a result, total HF energies with the CS method can oscillate seriously with assumed unit cell cluster size (implicit in the real lattice sum truncation), whereas in the MS method these energies are stable.

(iii) The most significant difference is that the CS method requires the calculation and manipulation of horrendous numbers of many-center integrals, particularly when Gaussian-type orbitals are used. The MS method, however, allows the reductions to reciprocal lattice sums involving Fourier transforms of basis functions only. Consequently, when n orbitals occur per unit cell, the computing effort of the CS method scales like n^4, and the MS method scales more like n^2.

In physical terms one can say that the CS approaches emphasize the calculation of the *total* wave function and charge distribution, whereas the MS approach emphasizes the deviation from a uniform charge distribution and associated wave functions. It can thus be understood that the methods have different ranges of applicability.

The successes of the crystal HF calculations are based on the precise definition of the HF method. This situation allows us to draw well-founded conclusions on the correlation effects in band widths,

gaps, and density of states (DOS). Moreover, and possibly most significantly, its variational character admits realistic geometry optimization. Finally, with the inclusion of proper basis functions, the method gives excellent charge distributions, with which many properties can be obtained.

Yet, the HF method has been discarded by many band theorists because of its "unphysical" aspects. They often refer to the vanishing DOS at the Fermi level in the electron gas and the enormous widening of the occupied band. Indeed, even the valence and conduction bands of alkali halides and diamond are substantially wider than those inferred from experiments.[4-6, 10, 12] In some instances correlation corrections have been made, and invariably the bandwidths become more "realistic."[3, 6, 10, 16] Whether the DOS vanishes at the Fermi level in crystals with partially filled bands had not been clearly established so far. Jennison[9] and FBB[14] discuss this question, but admit that it would be difficult to see in a DOS calculation with the conventional methods.

We wish to present a rigorous proof that, indeed, the DOS at the Fermi level vanishes rigorously whenever partially filled bands occur, regardless of the shape and the connectivity of the Fermi surface. We will also show that this is the case for extended systems periodic in one or two dimensions, such as polymers and thin films. No special features are expected in the DOS for filled and empty bands, except for widening of bands and gaps near the Fermi level. Finally, we raise the warning that unphysical features might occur in the DOS as conventionally calculated. These are related to the sudden drop to zero of the DOS at the top of the Fermi sea.

The above behavior of the DOS is associated with the extensiveness of the systems. Therefore, it is not surprising that it can be most elegantly shown with the MS approach. In Sec. II we summarize the basic formulas of crystal HF in the MS representation. This enables us to most easily discuss the analytic behavior of the band energies (Sec. III). Then follows the proof that the DOS vanishes for partially filled band systems (Secs. IV and V). A discussion of its consequences can be found in Sec. VI.

II. HARTREE-FOCK IN MOMENTUM REPRESENTATION

Consider a crystalline solid with A atoms per unit cell, with nuclear charges $Z_1, Z_2, \ldots, Z_A$ and position vectors $\vec{s}_1, \vec{s}_2, \ldots, \vec{s}_A$ relative to the unit-cell origin. The unit cell volume is v_0. The lattice vectors are indicated by $\vec{R}, \vec{R}'$, etc., and the associated reciprocal lattice vectors are denoted $\vec{K}, \vec{K}'$, etc.

We assume that the HF Bloch wave functions $|\nu \vec{k}\rangle$ can be expressed in the LCAO form

$$|\nu \vec{k}\rangle = \sum_p |p\vec{k}\rangle C_{p\nu}(\vec{k}), \tag{1}$$

where the basis Bloch orbitals $|p\vec{k}\rangle$ in $\vec{r}$ representation are given by

$$\langle \vec{r}|p\vec{k}\rangle = N^{-1/2} \sum_{\vec{R}} \exp(i\vec{k}\cdot\vec{R})\langle \vec{r}-\vec{R}|p\rangle \tag{2}$$

as a real lattice summation, or

$$\langle \vec{r}|p\vec{k}\rangle = \frac{N^{-1/2}}{v_0} \sum_{\vec{K}} \exp[i(\vec{K}+\vec{k})\cdot\vec{r}]\langle \vec{k}+\vec{K}|p\rangle \tag{3}$$

as a reciprocal lattice sum. N is the number of unit cells, and $\vec{k}$ is the Bloch vector in the Brillouin zone (BZ). $|p\rangle$ are the atomic orbitals.

The $|\nu \vec{k}\rangle$ are assumed to satisfy the orthonormality condition

$$\langle \mu \vec{k}|\nu \vec{k}\rangle = \delta_{\mu\nu}, \tag{4}$$

or, using Eq. (1) and the identification

$$S_{pq}(\vec{k}) \equiv \langle p\vec{k}|q\vec{k}\rangle, \tag{5}$$

we can write

$$\sum_{pq} C^*_{\mu p}(\vec{k})S_{pq}(\vec{k})C_{q\nu}(\vec{k}) = \delta_{\mu\nu}. \tag{6}$$

For later developments it is convenient to write $\underline{M}(\vec{k})$ for a matrix with elements $M_{pq}(\vec{k})$, and $\underline{C}_\nu(\vec{k})$ for a vector with components $C_{p\nu}(\vec{k})$. We can now compactly write, instead of Eq. (6),

$$\underline{C}^\dagger_\mu(\vec{k})\underline{S}(\vec{k})\underline{C}_\nu(\vec{k}) = \delta_{\mu\nu}. \tag{7}$$

We will need the density matrix $\underline{D}(\vec{k})$, with elements

$$D_{pq}(\vec{k}) = \sum_\nu n_\nu(\vec{k})C^*_{p\nu}(\vec{k})C_{q\nu}(\vec{k}). \tag{8}$$

The occupation number $n_\nu(\vec{k})$ is defined as

$$n_\nu(\vec{k}) = \begin{cases} 1, & \text{if } E_\nu(\vec{k}) \leq E_F, \\ 0, & \text{if } E_\nu(\vec{k}) > E_F, \end{cases} \tag{9}$$

where $E_\nu(\vec{k})$ and E_F are the HF band energies and Fermi energy as calculated below. Adopting a restricted HF scheme (double occupancy of the orbitals), we have the charge neutrality condition

$$\sum_i^{BZ} \sum_{pq} D_{pq}(\vec{k})S_{pq}(\vec{k}) = N\left(\sum_{m=1}^A Z_m\right), \tag{10}$$

where the $\vec{k}$ sum is over the BZ. Using the equivalence, as $N \to \infty$,

$$\sum_i \to \frac{Nv_0}{(2\pi)^3}\int d^3k \tag{11}$$

we can equivalently write, thanks to (7) and (8),

$$2 \sum_{\nu} \frac{\upsilon_0}{(2\pi)^3} \int_{BZ} d^3k\, n_\nu(\vec{k}) = \sum_{m=1}^{A} Z_m .$$

(12)

The HF equations can now be cast in the form

$$[\underline{F}(\vec{k}) - E_\nu(\vec{k}) \underline{S}(\vec{k})]\underline{C}_\nu(\vec{k}) = 0 .$$

(13)

As usual, these equations are obtained by minimizing the HF energy with constraints of Eqs. (7) and (10) [or (12)]. Indeed, the latter condition implicitly defines the Fermi energy E_F. The Fock matrix has the following structure:

$$F_{pq}(\vec{k}) \equiv \langle p\vec{k} | \hat{F} | q\vec{k} \rangle ;$$

(14)

$$\hat{F} = \hat{T} + \hat{V} + \hat{C} + \hat{X} .$$

(15)

$\hat{T}$, $\hat{V}$, $\hat{C}$, and $\hat{X}$ are the kinetic energy, nuclear attraction, electron-electron repulsion, and exchange operators, respectively.

We are now ready to discuss the expression for the various matrix elements over the operators in $\hat{F}$. As we indicated, we introduced the momentum representation for all integrals. This was followed by an interchange of the integrations and lattice sums, wherever admissible. Subsequently, use was made of the lattice orthogonality relation; as $N \to \infty$,

$$\sum_{\vec{R}} \exp(i\vec{Q} \cdot \vec{R}) = \frac{(2\pi)^3}{\upsilon_0} \sum_{\vec{K}} \delta(\vec{Q} - \vec{K}) .$$

(16)

For $\hat{V}$ and $\hat{C}$, singularities arise for $\vec{K} = 0$, due to the long-range nature of the Coulomb potential. A careful analysis reveals that these singularities rigorously cancel, provided that, besides charge neutrality, the unit cells have no dipole, quadrupole, or second moments.[17] (This condition is generally overlooked in conventional applications of Ewald-type lattice summations, and its non-satisfaction can cause shifts in the band energies and total energies of the CS approach.[18]) The expressions below are therefore the remainders after this long-range cancellation. These leftovers can be interpreted as resulting from a deviation from a uniform-charge distribution.

Casting the formulas in forms convenient for further discussion we have

$$S_{pq}(\vec{k}) = \frac{1}{\upsilon_0} \sum_{\vec{K}} \langle p | \vec{K} + \vec{k} \rangle \langle \vec{K} + \vec{k} | q \rangle ;$$

(17)

$$\langle p\vec{k} | \hat{T} | q\vec{k} \rangle = \frac{1}{\upsilon_0} \sum_{\vec{K}} \langle p | \vec{K} + \vec{k} \rangle \frac{(\vec{K} - \vec{k})^2}{2} \langle \vec{K} + \vec{k} | q \rangle ;$$

(18)

$$\langle p\vec{k} | \hat{V} | q\vec{k} \rangle = \frac{1}{\upsilon_0^2} \sum_{\vec{K}, \vec{K}'} {}' \langle p | \vec{K} + \vec{k} \rangle V(\vec{K} - \vec{K}') \langle \vec{K}' + \vec{k} | q \rangle ;$$

(19)

with the definitions

$$V(\vec{Q}) = -\frac{4\pi}{Q^2} Z(\vec{Q}) ;$$

(20)

$$Z(\vec{Q}) = \sum_{m=1}^{A} Z_m \exp(i\vec{Q} \cdot \vec{s}_m) ;$$

(21)

$$\langle p\vec{k} | \hat{C} | q\vec{k} \rangle = \frac{1}{\upsilon_0^2} \sum_{\vec{K}, \vec{K}'} {}' \langle p | \vec{K} + \vec{k} \rangle C(\vec{K} - \vec{K}') \langle \vec{K}' + \vec{k} | q \rangle$$

(22)

with the definition

$$C(\vec{Q}) = \frac{2\upsilon_0}{(2\pi)^3} \int d^3k' \sum_{rs} D_{rs}(\vec{k}')$$

$$\times \left[\frac{1}{\upsilon_0} \sum_{\vec{K}''} \langle r | \vec{K}'' + \vec{Q} + \vec{k}' \rangle \left(\frac{4\pi}{Q^2} \right) \right.$$

$$\left. \times \langle \vec{K}'' + \vec{k}' | s \rangle \right] .$$

(23)

Finally,

$$X_{pq}(\vec{k}) \equiv \langle p\vec{k} | \hat{X} | q\vec{k} \rangle$$

$$= \frac{1}{\upsilon_0^2} \sum_{\vec{K}, \vec{K}'} \langle p | \vec{K} + \vec{k} \rangle X(\vec{K} + \vec{k}, \vec{K}' + \vec{k}) \langle \vec{K}' + \vec{k} | q \rangle ,$$

(24)

where we have used the definition

$$X(\vec{Q}, \vec{Q}') = -\frac{\upsilon_0}{(2\pi)^3} \int d^3k' \sum_{rs} D_{rs}(\vec{k}')$$

$$\times \left(\frac{1}{\upsilon_0} \sum_{\vec{K}''} \frac{\langle r | \vec{K}'' + \vec{Q} - \vec{Q}' - \vec{k}' \rangle \langle \vec{K}'' - \vec{k}' | s \rangle}{|\vec{K}'' + \vec{Q} - \vec{k}'|^2} \right) .$$

(25)

The primes to the $\vec{K}, \vec{K}'$ sums of Eqs. (19) and (21) indicate the exclusion of $\vec{K} = \vec{K}'$. It is understood that $\vec{Q} - \vec{Q}'$ is a reciprocal lattice vector. Notice that the nonlocal character of $\hat{X}$ is reflected by the fact that $X(\vec{Q}, \vec{Q}')$ is not a function of $\vec{Q} - \vec{Q}'$ alone.

At this point it is well to remind the reader that Eqs. (17)–(24) are not always most convenient in actual calculations. We have found various alternative expressions more conducive to exploitation of convergence characteristics.[11,17] In particular, when $|p\rangle$ and/or $|q\rangle$ are corelike orbitals, direct-lattice sums give more rapid convergence. In practice, therefore, we have used a mixture of

direct and reciprocal lattice sums.[11]

The HF total energy per unit cell E_{HF} can be obtained from the expression

$$E_{HF} = \frac{v_0}{(2\pi)^3} \int d^3k \left[\sum_\nu n_\nu(\vec{k}) E_\nu(\vec{k}) \right.$$

$$\left. + \sum_{pq} [T_{pq}(\vec{k}) + V_{pq}(\vec{k})] D_{pq}(\vec{k}) \right] + C .$$

(26)

T and V are given by Eqs. (18)–(20), and C is a constant characteristic of the lattice structure and cell size

$$C = \left(\frac{1}{2} \right) \left(\frac{1}{2\pi^2} \right) \left[\frac{(2\pi)^3}{v_0} \sum_{\vec{K}}' \frac{|Z(\vec{K})|^2}{K^2} - Z^2(0) \int \frac{d^3q}{q^2} \right].$$

(27)

The sum in C excludes $K = 0$, and the integral is over all momentum values. This term appears when the singularity from the V contribution to (26) is balanced against that arising from the nuclear-nuclear repulsion.[17] Of course, the same condition applied to this cancellation as discussed below Eq. (16); the singularities have the same origin. The constant C can be interpreted as the electrostatic energy between the nuclei with charges Z_m and positions $\tilde{s}_m$ within the unit cell and a uniform compensating background of negative charge. It is easy to show that C vanishes if, in addition, the (positive) nuclear charge is spread out uniformly. This is the situation in the electron-gas model for a solid.

From Eqs. (17)–(25) it should be clear that the MS formulation is really advantageous for valence and conduction bands: the $\vec{K}, \vec{K}'$ sums will converge fast. A few such expressions can be found in FBB.

In conventional band calculations C has been usually ignored. This is unfortunate because it is easy to compute for any lattice structure,[17] and its inclusion allows a realistic total-energy evaluation.

Finally, we wish to point out that *all* $\vec{K}$ sums are accompanied by a factor $1/v_0$. This will prove important when discussing extended systems with lower dimensionality (see Sec. V).

III. AN EXPRESSION FOR $\vec{\nabla} E_\nu(\vec{k})$

For our analysis of the HF DOS we need the gradient of the band energies. Starting from (13) and dropping the $\vec{k}$ dependence from the expression, we get

$$(\vec{\nabla}\underline{F} - E_\nu\vec{\nabla}\underline{S})\underline{C}_\nu + (\underline{F} - E_\nu\underline{S})\vec{\nabla}\underline{C}_\nu - \vec{\nabla}E_\nu\underline{S}\,\underline{C}_\nu = 0 .$$ (28)

When we now premultiply with $\underline{C}_\nu^\dagger$; using the hermiticity of $\underline{F}, \underline{S}$ and the orthonormality condition of

Eq. (7), we readily arrive at

$$\vec{\nabla}E_\nu(\vec{k}) = \underline{C}_\nu^\dagger(\vec{k})[\vec{\nabla}\underline{F}(\vec{k}) - E_\nu(\vec{k})\vec{\nabla}\underline{S}(\vec{k})]\underline{C}_\nu(\vec{k}) .$$ (29)

This is a very compact expression indeed. It shows that no explicit variation of $\underline{C}_\nu$ needs to be considered; only variation of matrix elements matters, once the HF equations are satisfied.

IV. HF DENSITY OF STATES

The density of states (DOS), $\rho(E)$ can be obtained using a variety of mathematically equivalent, but computationally distinct formulas. For our purposes the expression

$$\rho(E) = \frac{v_0}{4\pi^3} \sum_\nu \int_S \frac{\vec{n}_s \cdot d\vec{S}}{|\vec{\nabla}E_\nu(\vec{k}_s)|}$$ (30)

is convenient. The integral is over equienergetic surfaces S, with position vectors $\vec{k}_s$, so that

$$E_\nu(\vec{k}_s) = E$$ (31)

for at least one ν value. $\vec{n}_s$ is the unit vector normal to S in $\vec{k}_s$. $\rho(E)$ is normalized so that

$$\int_0^{E_F} \rho(E)dE = \sum_{m=1}^{A} Z_m ,$$ (32)

with E_F the Fermi energy.

It is well known that in the electron-gas model $\rho(E_F) = 0$, i.e., the DOS vanishes at the Fermi surface S_F. This is caused by a logarithmic singularity in $\vec{\nabla}E(\vec{k})$ at the (spherical) S_F (see, for example, Ref. 26):

$$|\vec{\nabla}E(\vec{k}_s)| \sim \ln|k_s - k_F| \text{ as } S \to S_F .$$ (33)

We now wish to show that a similar singularity occurs in any crystal with partially filled bands.

Our starting point is Eq. (29). Going over Eqs. (14) and (17)–(25) we notice that the $\vec{k}$ dependence appears either in the basis orbital Fourier transforms or in the kernels of the sums for the $\hat{T}$ and $\hat{X}$ matrix elements. Typically Gaussian or Slater-type basis orbitals have been used; neither have Fourier transforms with singular gradients. In fact, quantum-mechanical continuity conditions mandate the $\vec{k}$ dependence of Bloch functions to be "smooth" analytically. Therefore, basis functions with discontinuous $\vec{k}$ behavior are to be excluded. Moreover, the factor $(\vec{K} + \vec{k})^2$ in Eq. (18) is obviously analytic in $\vec{k}$. We thus conclude that the only possible source for a singularity in $\vec{\nabla}E_\nu(\vec{k})$ is the "exchange kernel" of Eq. (25).

Let us look at this quantity more closely. Whenever

$$\vec{K}'' + \vec{Q} = \vec{K},$$

the $\vec{k}'$ integrals are of the form

$$\int d^3k' \frac{f(\vec{k}')}{|\vec{k} - \vec{k}'|^2},$$

with $f(\vec{k}')$ analytic, and $\vec{k}$ and $\vec{k}'$ both within the BZ. But now we have identified a possible singularity, since the integrand diverges whenever $\vec{k}' = \vec{k}$; the analyticity in $\vec{k}$ after $\vec{k}'$ integration need not be maintained. Therefore, we can restrict our attention to $\underline{X}(\vec{k})$, and write

$$E_\nu^x(\vec{k}) = \underline{C}_\nu^\dagger(\vec{k}) \underline{X}(\vec{k}) \underline{C}_\nu(\vec{k}).\tag{34}$$

In order to more clearly exhibit the underlying analytic structure of E_ν^x, we recognize that, in general, the density matrix contains a sum over both filled and partially filled bands. Therefore, with regard to the $\vec{k}'$ integration domains, we can write

$$E_\nu^x(\vec{k}) = \int_{BZ} d^3k' \sum_{\vec{K}} \frac{Y_\nu^1(\vec{K}, \vec{k}', \vec{K})}{|\vec{K} + \vec{k} - \vec{k}'|^2}$$
$$+ \int_{V_F} d^3k' \sum_{\vec{K}} \frac{Y_\nu^2(\vec{K}, \vec{k}', \vec{K})}{|\vec{K} + \vec{k} - \vec{k}'|^2}.\tag{35}$$

The details of Y_ν^1 and Y_ν^2 are irrelevant for our discussion except that these quantities (i) are analytic in $\vec{k}$ and $\vec{k}'$, and (ii) cause periodicity in $\vec{k}, \vec{k}'$ space to the integrands. V_F is the volume within S_F. Both $\vec{k}'$ integrations are to be confined to (at most) the first BZ. The first integral (the filled band contribution) is over this BZ, *including* its boundary. The second integral (the partially filled-band contribution) is over a fraction thereof, V_F, *including* the boundary, the Fermi surface S_F.

As we indicated, nonanalyticity in $\vec{k}$ can occur from $\vec{K} = 0$ in Eq. (35). We therefore single out those terms and Taylor-expand Y_ν^i,

$$Y_\nu^i(\vec{k}, \vec{k}', 0) = Y_\nu^i(\vec{k}, \vec{k}, 0) + (\vec{k}' - \vec{k})$$
$$\cdot \{\vec{\nabla}' Y_\nu^i(\vec{k}, \vec{k}', 0)\}_{\vec{k}'=\vec{k}} + \dots, \quad (i = 1, 2).\tag{36}$$

Substituting these expressions in (35) we generate $\vec{k}'$ integrals of the form

$$I_0(V, \vec{k}) = \int_V \frac{d^3k'}{|\vec{k} - \vec{k}'|^2},\tag{37}$$

$$\vec{I}_1(V, \vec{k}) = \int_V \frac{(\vec{k}' - \vec{k}) d^3k'}{|\vec{k} - \vec{k}'|^2},\tag{38}$$

where V is either BZ or V_F. We have now isolated the quantities that might be responsible for singularities.

V. INTEGRALS I_0 AND $\vec{I}_1$

Let us first consider I_0. We wish to apply Gauss's theorem. If $\vec{k}$ is within V we must exclude a small sphere, with volume v, radius ϵ,

and surface σ, around $\vec{k}$ so as to have continuity over $(V - v)$. Writing

$$\frac{1}{|\vec{k} - \vec{k}'|^2} = \vec{\nabla}' \cdot \frac{(\vec{k}' - \vec{k})}{|\vec{k} - \vec{k}'|^2},\tag{39}$$

we express I_0 in the form

$$I_0(V, \vec{k}) = I_0(V - v, \vec{k}) + I_0(v, \vec{k}),\tag{40}$$

or, using Gauss's theorem for the first term,

$$I_0(V - v, \vec{k}) = \int_\Sigma \frac{(\vec{k}_s - \vec{k}) \cdot d\vec{S}}{|\vec{k}_s - \vec{k}|^2} - \int_\sigma \frac{(\vec{k}_\sigma - \vec{k}) \cdot d\vec{\sigma}}{|\vec{k}_\sigma - \vec{k}|^2}.\tag{41}$$

Σ is the boundary to V (being either the BZ boundary or S_F). $\vec{k}_\sigma$ are the σ surface position vectors. Evaluating the integrals associated with v and σ:

$$I_0(v, \vec{k}) = \int_v \frac{d^3q}{q^2} = 4\pi\epsilon,\tag{42}$$

$$\int_\sigma \frac{(\vec{k}_\sigma - \vec{k}) \cdot d\vec{\sigma}}{|\vec{k}_\sigma - \vec{k}|^2} = -\frac{1}{\epsilon} \int_\sigma d\sigma = -4\pi\epsilon.\tag{43}$$

Combining (40)-(43) we thus conclude

$$I_0(V, \vec{k}) = \int_\Sigma \frac{(\vec{k}_s - \vec{k}) \cdot d\vec{S}}{|\vec{k}_s - \vec{k}|^2}.\tag{44}$$

As ϵ can be made arbitrarily small, this result also holds for $\vec{k}$ on Σ.

For $\vec{I}_1$, we can carry through a similar analysis. The result is

$$\vec{I}_1(V, \vec{k}) = \int_\Sigma \ln|\vec{k}_s - \vec{k}| d\vec{S};\tag{45}$$

as before, this holds for all $\vec{k}$.

We are now ready to discuss the gradient of I_0 and I_1. Whenever $\vec{k}$ is not on Σ, i.e., $\vec{k}$ is either within or outside V, the integrands are finite and continuous in $\vec{k}$. We therefore can bring the gradient operation under the integration. For example,

$$\vec{\nabla} I_0(V, \vec{k}) = \int_\Sigma \vec{\nabla} \frac{(\vec{k}_s - \vec{k}) \cdot d\vec{S}}{|\vec{k}_s - \vec{k}|^2};$$

or, using

$$\vec{q} = \vec{k}_s - \vec{k},\tag{46}$$

we can write

$$\vec{\nabla} I_0(V, \vec{k}) = 2 \int_\Sigma \frac{\vec{q} \cdot (\vec{q} \cdot d\vec{S})}{q^4} - \int_\Sigma \frac{d\vec{S}}{q^2}.\tag{47}$$

Clearly q never vanishes in this case, and we find

$$|\vec{\nabla} I_0(V, \vec{k})| < \infty, \quad \forall \vec{k} \notin \Sigma.\tag{48}$$

Similarly, it is easily found

$$|\vec{\nabla} I_1(V, \vec{k})| < \infty, \quad \forall \vec{k} \notin \Sigma.\tag{49}$$

We thus reach our first conclusion: (i) The band-

energy gradient $\vec{\nabla} E_\nu(\vec{k})$ will have finite values for all $\vec{k}$ *not* on either the BZ boundary or on the Fermi surface S_F.

Now we will consider the case that $\vec{k}$ approaches a vector $\vec{k}_s$ on Σ. Because of a lack of continuity of the integrands in the surface integrals (44), (45) we cannot bring the gradient operation under the integral signs. Therefore we must proceed as follows:

We can assume, without loss of generality, that $\vec{k}$ approaches $\vec{k}_s$ so that

$$\vec{\delta} = \vec{k} - \vec{k}_s \tag{50}$$

is an infinitesimal vector parallel to $\vec{n}_s$, the unit vector normal to Σ in $\vec{k}_s$,

$$\vec{\delta}/\delta = \mp \vec{n}_s . \tag{51}$$

δ is the distance of $\vec{k}$ to Σ. The minus (plus) sign applies when $\vec{k}$ approaches $\vec{k}_s$ from within (outside). We next cast a small circle denoted by c, around $\vec{k}_s$ on Σ. Its radius ϵ is taken small enough so that Σ can be considered locally flat. We then can express I_0, I_1 as

$$I_m(V,\vec{k}) = I_m^c(V,\vec{k}) + [I_m(V,\vec{k}) - I_m^c(V,\vec{k})] \quad (m = 0,1),$$
$$\tag{52}$$

where

$$I_0^c(V,\vec{k}) = \int_c \frac{(\vec{k}_\sigma - \vec{k}) \cdot d\vec{\sigma}}{|\vec{k}_\sigma - \vec{k}|^2} , \tag{53}$$

$$\vec{I}_1^c(V,\vec{k}) = \int_c \ln|\vec{k}_\sigma - \vec{k}| d\vec{\sigma} . \tag{54}$$

Obviously, the term in square brackets in Eq. (52) excludes $\vec{k}_s$ from the surface integral. Therefore, its gradient with respect to $\vec{k}$, as $\vec{k} \to \vec{k}_s$, will remain finite. However, this is not the case for the *other* term when $m = 0$, as we will now show. We introduce the variable $\vec{q}$,

$$\vec{q} = \vec{k}_\sigma - \vec{k} . \tag{55}$$

If we describe the integral over c with the radial variable r, then we have

$$\vec{q} \cdot d\vec{\sigma} = \delta \, r \, dr \, d\phi , \tag{56}$$

$$q^2 = r^2 + \delta^2 . \tag{57}$$

We thus are led to

$$I_0^c(V,\vec{k}) = \delta \int_0^{2\pi} d\phi \int_0^\epsilon \frac{r \, dr}{r^2 + \delta^2} ,$$

or

$$I_0^c(V,\vec{k}) = \pi [\delta \ln(\delta^2 + \epsilon^2) - 2\delta \ln\delta] . \tag{58}$$

Since $\delta = |\vec{k} - \vec{k}_s|$, we readily derive

$$\vec{\nabla} I_0^c(V,\vec{k}) = \pm 2\pi \vec{n}_s \left[\ln\delta + \frac{\epsilon^2}{\delta^2 + \epsilon^2} - \frac{1}{2} \ln(\delta^2 + \epsilon^2) \right] . \tag{59}$$

Finally, we are prepared to take the limit $\vec{k} \to \vec{k}_s$. Doing so, Eqs. (58) and (59) immediately give (with $\epsilon > 0$),

$$\lim_{\vec{k} \to \vec{k}_s} I_0^c(V,\vec{k}) = 0 , \tag{60}$$

$$\lim_{\vec{k} \to \vec{k}_s} \vec{\nabla} I_0^c(V,\vec{k}) = \pm \lim_{\vec{k} \to \vec{k}_s} 2\pi \vec{n}_s \ln|\vec{k} - \vec{k}_s| . \tag{61}$$

Now, considering $\vec{I}_1^c$, we quickly get

$$I_1^c(V,\vec{k}) \leq \left| \int \ln|\vec{k}_\sigma - \vec{k}| d\sigma \right| ,$$

or, with Eqs. (35)–(57) ,

$$I_1^c(V,\vec{k}) \leq \pi |(\epsilon^2 + \delta^2) \ln(\epsilon^2 + \delta^2) - \epsilon^2 - 2\delta^2 \ln\delta| . \tag{62}$$

Furthermore,

$$|\vec{\nabla} I_1^c| = \left| \frac{dI_1^c}{d\delta} \right| ,$$

or, using (62),

$$|\vec{\nabla} I_1^c(V,\vec{k})| \leq 2\pi |2\delta \ln\delta - \delta \ln(\epsilon^2 + \delta^2)| . \tag{63}$$

Again, we take the limit $\vec{k} \to \vec{k}_s$, and we obtain

$$\lim_{\vec{k} \to \vec{k}_s} I_1^c(V,\vec{k}) \leq \pi \epsilon^2 |2 \ln\epsilon - 1| < \infty , \tag{64}$$

$$\lim_{\vec{k} \to \vec{k}_s} |\vec{\nabla} I_1^c(V,\vec{k})| = 0 . \tag{65}$$

Looking at Eqs. (61), (65), and remembering the role I_m^c plays in I_m [Eq. (52)] we conclude

$$\lim_{\vec{k} \to \vec{k}_s} I_0(V,\vec{k}) < \infty ; \tag{66}$$

$$\lim_{\vec{k} \to \vec{k}_s} \vec{I}_1(V,\vec{k}) < \infty ; \tag{67}$$

$$\lim_{\vec{k} \to \vec{k}_s} |\vec{\nabla} I_0(V,\vec{k})| = \lim_{\delta \to 0} |2\pi \ln\delta| ; \tag{68}$$

$$\lim_{\vec{k} \to \vec{k}_s} |\vec{\nabla} I_1(V,\vec{k})| < \infty . \tag{69}$$

A. Singularity in $\vec{\nabla} E_\nu(\vec{k})$

Returning to the Taylor expansion (36), which gave rise to I_0 and I_1, it is clear that higher-order forms will not generate any divergences in $\vec{\nabla} E_\nu^a(\vec{k})$; the $\vec{k}'$ integrands will not be singular. Therefore, we have precisely pinpointed the singularity in $\vec{\nabla} E_\nu(\vec{k})$, and we will argue that it only occurs in partially filled band systems, with $\vec{k}$ any point $\vec{k}_F$ on the Fermi surface.

In order to see this, we first remind ourselves that the singularity in $\vec{\nabla} I_0$ emerges as a three-dimensional version of an endpoint singularity to an integral representation with singular kernel. We saw that no singular behavior was found for $\vec{k}$ away from the "endpoint", i.e., not on Σ.

Now, using the symmetry

$$D_{rs}(\vec{k}') = D_{rs}(\vec{k}' + \vec{K}'') \tag{70}$$

in Eq. (25), it is not hard to see that the first term in Eq. (35) is of the form

$$\sum_{\vec{K}''} \int_{BZ} d^3k' \frac{g(\vec{K}'' + \vec{k}')}{|\vec{K}'' + \vec{k}' - \vec{k}|^2} = \int^{\infty} d^3\kappa \frac{g(\vec{\kappa})}{|\vec{\kappa} - \vec{k}|^2}.$$

There is no endpoint singularity, as this integral covers the entire reciprocal lattice. But that means that the *full* BZ integration in $E_\nu(\vec{k})$ does *not* give a singular contribution to $\vec{\nabla}E_\nu(\vec{k})$, whatever $\vec{k}$ is.

Indeed, we are now in a position to make a precise statement concerning $\vec{\nabla}E_\nu(\vec{k})$:

$$\lim_{\vec{k} \to \vec{k}_F} |\vec{\nabla}E_\nu(\vec{k})| = \lim_{\vec{k} \to \vec{k}_F} 2\pi |Y_0^2(\vec{k}_F, \vec{k}_F, 0) \ln|\vec{k} - \vec{k}_F||. \tag{71}$$

We have now arrived at the second and main result of this section: (ii) In partially filled band systems the gradients of *all* band energies $E_\nu(\vec{k})$ diverge logarithmically whenever $\vec{k}$ is on the Fermi surface S_F.

In filled-band systems these gradients never diverge.

B. DOS at Fermi level

It is now immediately obvious that, indeed, the DOS vanishes at the Fermi energy E_F: the surface S becomes S_F for E_F. The integral in Eq. (30) is over a zero integrand, thus giving no contribution to $\rho(E_F)$. Obviously this result holds whether S_F is either multiply connected or entirely within the BZ; the cause of the singularity is the termination of the $\vec{k}'$ integration short of the full BZ.

Our result of Sec. IV A has an interesting implication. If, for a particular $E \ne E_F$, the equienergetic surface S coincides with S_F, then the associated $\rho(E)$ will vanish as well. We are unaware of a general principle that precludes this to happen. Although it seems highly unprobable, we have to be concerned about this possibility. We will return to this point in Sec. VI.

VI. DOS FOR SYSTEMS EXTENDED IN FEWER DIMENSIONS

Polymers and thin films are extended systems (usually) periodic in one or two dimensions, respectively. HF calculations at the same rigorous level as bulk crystal work are being performed,[19] or are underway.[20] In view of our finding that the HF DOS in crystals vanishes at the Fermi level the question can be raised whether this also ap-

plies to these lower-dimensional, extended systems. After all, one can imagine these systems to physically appear if one allows one or two unit cell dimensions of a bulk crystal to increase beyond limits, keeping all relative position vectors $\vec{s}_m$ finite in length. Periodicity in these (infinite) dimensions then becomes immaterial, and we have effectively a collection of noninteracting extended systems of lower dimensionality.

Theoretically we can answer this question in two different ways. Using the MS approach, we can formulate the HF problem for polymers[19] and thin films[21] as isolated systems, exploiting the one- and two-dimensional periodicities. The Fermi surfaces are two points in polymers, and a planar curve in thin films. Instead of the three-dimensional reciprocal lattice sums, double reciprocal-space integrals and one summation appear for polymers (two summations and one integral for thin films). An analysis similar to the one given here can then be carried through.

However, a physically more appealing, albeit mathematically somewhat less rigorous approach is to start from the crystal HF formalism of Secs. II–IV, and take certain limits so as to describe the reduction of dimensionality of the system. These limits should be associated with the stretching of unit cell sizes in one (two) directions to obtain the formulas for thin films (polymers) in the HF description.

First, let us consider the transition to thin-film systems. Thereto, without loss of generality, we assume a monoclinic, three-dimensional unit cell with a parallelogram basis with area a_0 and height h. It then follows that

$$v_0 = a_0 h. \tag{72}$$

The lattice and reciprocal lattice vectors are expressible as

$$\vec{R} = \vec{R}_{||} + \vec{R}_\perp ; \tag{73}$$

$$\vec{K} = \vec{K}_{||} + \vec{K}_\perp , \tag{74}$$

or as a sum of vectors parallel and perpendicular to the plane of the unit cell base. The perpendicular vectors are given by

$$\vec{R}_\perp = mh\hat{z}, \quad m = 0, \pm 1, \pm 2, \ldots . \tag{75}$$

$$\vec{K}_\perp = n(2\pi/h)\hat{z}, \quad n = 0, \pm 1, \pm 2, \ldots, \tag{76}$$

if it is assumed that the unit cell base is parallel to the x-y plane.

The obvious next step is to take the limit $h \to \infty$, keeping the $\vec{s}_m$ finite. In our formulas (17)–(27) this limit has two consequences. Noticing that a factor $(1/v_0)$ is associated with each $\vec{K}$ sum, the first effect is that the $\vec{K}$ sum becomes very dense,

i.e., in the limit $h \to \infty$ this becomes an integral. Indeed, we can write

$$\frac{1}{v_0} \sum_{\vec{K}} = \lim_{h \to \infty} \frac{1}{a_0 h} \sum_{\vec{K}_{\shortparallel}} \sum_{K_{\perp}}$$

$$= \lim_{h \to \infty} \left(\frac{1}{a_0 h} \right) \sum_{\vec{K}_{\shortparallel}} \left(\frac{h}{2\pi} \right) \int_{-\infty}^{\infty} dK_{\perp} ,$$

or

$$\lim_{h \to \infty} \frac{1}{v_0} \sum_{\vec{K}} = \frac{1}{2\pi a_0} \sum_{\vec{K}_{\shortparallel}} \int_{-\infty}^{\infty} dK_{\perp} . \qquad (77)$$

Formulas generated in this manner are identical to those obtained by a direct application of the MS approach to thin films.

The other consequence is that $\vec{k}'$ integrations reduce to integrals in the two-dimensional BZ, with $\vec{k}' \to \vec{k}'_{\shortparallel}$. More specifically

$$\lim_{h \to \infty} \frac{v_0}{(2\pi)^3} \int d^3 k' = \lim_{h \to \infty} \frac{a_0 h}{(2\pi)^3} \int d^2 k'_{\shortparallel} \int dk'_{\perp} .$$

The $k'_{\perp}$ integral will scale like $2\pi/h$. The occupation numbers $n_{\nu}(\vec{k})$ (contained in the integrands of the $\vec{k}$ integrations) will become independent of $\vec{k}_{\perp}$ in the limit $h \to \infty$ since its length vanishes. Therefore, we can say that in this limit, the $k'_{\perp}$ integral "fills up" the entire BZ width $(2\pi/h)$ in the perpendicular direction. We thus conclude that

$$\lim_{h \to \infty} \frac{v_0}{(2\pi)^3} \int d^3 k' = \frac{a_0}{(2\pi)^2} \int d^2 k'_{\shortparallel} . \qquad (78)$$

Again, the $k'_{\shortparallel}$ integrals generated are those obtained in a "direct" slab approach; as $h \to \infty$, all $\vec{k}'$ vectors approach a vector $\vec{k}'_{\shortparallel}$ in the two-dimensional BZ.

But now we can immediately state that the results of the previous section regarding the density of states apply to thin films as well. Volume integrals become surface integrals, and surface integrals become line integrals. In particular, the divergence in $|\vec{\nabla} E_{\nu}(\vec{k})|$ for partially filled bands [Eq. (68)] will hold as well in the limit $h \to \infty$. Since the divergence found is related to the *distance* of $\vec{k}$ to the Fermi surface, this result should be no surprise.

By subsequently taking the limit that a two-dimensional unit cell dimension approaches infinity, we generate the formulas for polymers. *Mutatis mutandis*, we arrive at the same conclusion, namely, that in a partially filled band polymer the HF DOS vanishes at the Fermi level. No vanishing $\rho(E)$ occurs in filled band polymers. In this case the Fermi surface consists of two points.

Lest the reader is worried whether the outlined treatment concerning the DOS is sufficiently rigorous, he can convince himself by carrying out the analysis directly on isolated thin films (polymers). For the exchange terms the integrals

over $K_{\perp}$ resulting from (77) have to be treated carefully around $K_{\perp} = 0$. Exclusion of a small region $[-\epsilon, \epsilon]$, with $\epsilon > 0$, will "extract" a small, pancake-shaped volume in reciprocal space around the origin, which captures the singularity. To that volume the same analysis as before can be applied, giving the same results.

To sum up then, we have arrived at the following conclusions:

(i) The HF band-energy gradients $\vec{\nabla} E_{\nu}(\vec{k})$ associated with systems, extended periodically in one or more dimensions and possessing partially filled bands, diverges logarithmically as $\vec{k}$ approaches a Fermi surface vector $\vec{k}_F$. No such divergence occurs for filled band systems.

(ii) The HF density of states $\rho(E)$ for such extended systems with partially filled bands vanishes at the Fermi level E_F. At any energy $E \neq E_F$ for which the equienergetic surface S [Eq. (31)] coincides with the Fermi surface S_F, $\rho(E)$ will also vanish.

In general, $\rho(E)$ will not vanish for filled band systems with E not in band gaps.

VII. DISCUSSION

The results of this paper concerning the HF DOS have a number of interesting and, in some cases, somewhat disturbing consequences for calculations already published or contemplated.

With regard to crystal HF work, in a number of cases HF DOS are presented that ought to show a vanishing $\rho(E_F)$. For example, the DOS for calcium,[22] lithium,[9] and TiO,[10] show a conspicuous absence of a zero HF DOS at E_F. In view of the computational methods used (polynomial interpolation, with or without Gaussian broadening, or a Gauss-Chebyshev method, formulated by Monkhorst and Pack[23]) it is impossible to see this behavior. Moreover, the above calculations have been performed in the CS approach. The truncation of the direct lattice sums (forced upon for practical reasons) causes the $\rho(E_F)$ to not even vanish rigorously. Yet, the intrinsic extensiveness of the systems considered *requires*, as we saw, the HF DOS to vanish. We therefore conclude that these DOS are qualitatively in error, at least near E_F, and cannot possibly be representative of the HF DOS near the Fermi level.

We also found that for an energy whose equienergetic surface S is identical to the Fermi surface S_F, the HF DOS should vanish. The occurrence of this seems highly improbable and might even be impossible. Certainly, viewing the band structure as to arise from a perturbed, nearly-free-electron (NFE) model one seems to have to rule out such coincidence. However, two remarks

are in order in this connection. First, the NFE model is inappropriate for crystals with strong Bragg scattering, such as highly localized orbitals of d and f character. Fermi surfaces in transition element compounds are notoriously complicated, and the same can be expected of above surfaces S. Second, even though the coalescence of surfaces S and S_F seems improbable, they could be close. If that happens chances are that unphysical shoulders, peaks, or near gaps could appear in $\rho(E)$. The reason for this can be found in FBB [Ref. 14]. In Fig. 3 of their second paper the authors present the HF DOS for the NFE gas, both the exact curve and numerical values. Apart from the inability of the numerical method to accurately reproduce $\rho(E)$ near E_F, another unsettling observation can be made: $\rho(E)$ peaks at an energy about ($\frac{2}{3}$) the band width. This is to be contrasted with the steadily increasing Hartree $\rho(E)$, which on many counts is closer to the "correct" DOS. The kinetic energy decreases faster with decreasing electron density than the exchange energy. Therefore, we expect this prepeaking to be even more pronounced at lower electron densities. But now we have to conclude that unphysical features to the $\rho(E)$ curve can already occur for energies E with equienergetic surfaces S quite different from S_F. We saw a pre-peaking in the NFE gas model. We thus can expect shoulders, peaks, or even near gaps to occur, depending on how closely S approaches S_F and what the electron density is.

All correlation corrections have concentrated on the Fermi level DOS or the band width or band gaps. Our results indicate that with complicated band structures such as for transition element compounds, considerable attention has to be paid to the correlation problem at *all* energies. The fact that numerical inaccuracies tend to wash out these HF-caused singularities (or near singularities) is irrelevant, although expedient in practice. The point is that the theory allows for them,

and therefore they should be either shown faithfully or corrected for. Unfortunately, so far no scheme has been formulated that is practical and theoretically sound.

It is even more likely that thin films and polymer HF DOS exhibit such unphysical features. In the case of thin films it is quite possible that two Fermi curves come close in shape and area. Since in polymers the Fermi surface consists of two points, there is an infinite number of energies (lying within bands) for which "S coincides with S_F." In practice, however, this is not very relevant; stable, partially filled band polymers do not occur, although a filamentary structure of equally spaced polymers of hydrogen atoms has been proposed and studied for metallic hydrogen.[19]

Summing up then, one has to be quite cautious when interpreting detailed features to $\rho(E)$ at the HF level, particularly for complicated crystals on thin films with partially filled bands.[9,10] By analogy with the widening of the HF NFE gas band width, we expect considerable exaggeration of bands and gaps near E_F. No vanishing $\rho(E)$ within bands of filled-band systems is expected.

Notwithstanding these fundamental failures to the crystal HF results we do not advocate a local approximation to exchange and correlation corrections. The work of Overhauser and others[24] has suggested that a considerable nonlocality has still to be associated with these corrections, although not as strong as "bare" exchange. The use of HF as a first approximation has many virtues: it is well defined, yields variational total energies, and gives good charge densities. Beyond that, the correlation problem for extended systems is still with us, and progress has been slow.[25]

ACKNOWLEDGMENT

*Present address: Dept. of Physics and Astronomy, Univ. of Florida, Gainesville, Fla. 32611.

[1]W. H. Adams, J. Chem. Phys. 34, 89 (1961); *ibid.* 37, 2009 (1962); T. L. Gilbert, in *Molecular Orbitals in Chemistry, Physics and Biology*, edited by P. O. Löwdin and B. Pullmann (Academic, New York, 1964), p. 409.

[2]A. B. Kunz, Phys. Status Solidi 36, 301 (1969); J. Phys. C 3, 1542 (1970).

[3]A. B. Kunz and D. J. Mickish, Phys. Rev. B 9, 779 (1973), and references cited therein.

[4]N. O. Lipari and A. B. Kunz, Phys. Rev. B 4, 4649 (1971), and references cited therein.

[5]A. B. Kunz and D. J. Mickish, J. Phys. C 6, L83

(1973).

[6]R. N. Euwema, D. L. Wilhite, and G. T. Surratt, Phys. Rev. B 7, 918 (1973); G. T. Surratt, R. N. Euwema, and D. L. Wilhite, Phys. Rev. B 8, 4019 (1973).

[7]R. N. Euwema, G. G. Wepfer, G. T. Surratt, and D. L. Wilhite, Phys. Rev. B 9, 2670, 5249 (1974).

[8]S. T. Pantelides, D. J. Mickish, and A. B. Kunz, Phys. Rev. B 10, 5203 (1974).

[9]J. L. Calais and G. Sperber, Int. J. Quantum Chem. 7, 501, 521 (1973); D. R. Jennison, Phys. Rev. B 16, 5147 (1977).

[10]D. R. Jennison and A. B. Kunz, Phys. Rev. Lett. 39, 418 (1977).

[11]F. E. Harris and H. J. Monkhorst, Phys. Rev. Lett.

23, 1026 (1969); Phys. Rev. B 2, 4400 (1970); *ibid.* 7, 2850 (1973); see also Ref. 17 for more references.

[12]A. Mauger and M. Lannoo, Phys. Rev. B 15, 2324 (1977).

[13]S. B. Cox and J. L. Fry, J. Comp. Phys. 23, 42 (1977).

[14]J. L. Fry, N. E. Brener, and R. K. Bruyere, Phys. Rev. B 16, 5225 (1977); N. E. Brener and J. L. Fry, *ibid.* 17, 506 (1978).

[15]J. D. Pack, Ph.D. Thesis (University of Utah, 1978); H. J. Monkhorst and J. D. Pack, Solid State Commun. 29, 675 (1979).

[16]N. E. Brener, Int. J. Quantum Chem. Symp. 9, 555 (1975), and references cited therein.

[17]F. E. Harris, *Theoretical Chemistry*, edited by H. Eyring and D. Henderson (Academic, New York, 1975), Vol. 1, p. 147.

[18]R. N. Euwema and G. T. Surratt, J. Phys. Chem. Solids 36, 67 (1975).

[19]F. E. Harris, J. Chem. Phys. 56, 4422 (1972);

M. Kertesz, J. Koller and A. Azman, Theor. Chim. Acta 41, 89 (1976); F. E. Harris and J. Delhalle, Phys. Rev. Lett. 39, 1340 (1977); see also, *Electronic Structure of Polymers and Molecular Crystals*, edited by J. Andre, J. Ladik, and J. Delhalle (Plenum, New York, 1975).

[20]H. J. Monkhorst and W. A. Schwalm (unpublished).

[21]H. J. Monkhorst (unpublished); see also Ref. 17.

[22]D. J. Mickish, A. B. Kunz, and S. T. Pantelides, Phys. Rev. B 10, 1369 (1974).

[23]H. J. Monkhorst and J. D. Pack, Phys. Rev. B 13, 5188 (1976); J. D. Pack and H. J. Monkhorst, *ibid.* 16, 1748 (1977).

[24]A. W. Overhauser, Phys. Rev. B 10, 4918 (1974), and references therein.

[25]H. J. Monkhorst and J. Oddershede, Phys. Rev. Lett. 30, 797 (1973).

[26]F. Seitz, *The Modern Theory of Solids* (McGraw-Hill, New York, 1940), pp. 339–342 and 421–423.

EXACT LCAO METHOD FOR TWO-DIMENSIONAL CRYSTALS, USING FOURIER TRANSFORM
TECHNIQUES[*]

Hendrik J. Monkhorst
Department of Physics
University of Utah
Salt Lake City, Utah 84112

Abstract

Integrals for LCAO calculations on thin films, with or without
overlayers, have been rigorously reduced to two-dimensional reciprocal
lattice sums and an infinite integration. Convergence properties
and computational effort are as favorable as in earlier bulk calcu-
lations. Hartree and Hartree-Fock calculations can be performed
with Slater orbital basis, without pseudo-potentials, surface clusters
or matching planes. The method should be ideal to study surface
states, reconstruction and adsorption.

During the past few years we have formulated[1] and implemented[2,3] a method to perform ab initio Hartree-Fock (HF) calculations on three-dimensional (3D) crystals. The essence of the method is the reduction of all crystal integrals over Bloch functions to 3D reciprocal lattice summations involving Fourier transforms of basic atomic orbitals only. Madelung-type conditional convergence is no problem, as the method is inherently based on an infinitely sized sample. Exchange was treated exactly, and various basis functions were used, such as Slater-type orbitals and plane waves. Simple metals[2,3] and molecular hydrogen crystal[4] were considered so far. Application to other crystals, such as diamond and beryllium, with a double-zeta Slater basis including 3d orbitals is underway.

I wish to show how the same technique can be used to obtain workable expressions for the exact evaluation of integrals in the LCAO method when applied to 2D crystals. These systems comprise thin films, without or with one (or more) overlayers of foreign material, and with long-range 2D periodicity. First I will explain the essential features by treating a single layer of atoms.

Consider N hydrogen atoms occupying the lattice sites of a planar 2D lattice that is characterized by the lattice vectors

$$(1) \quad \vec{R}_{m2} = m_1\vec{h}_1 + m_2\vec{h}_2.$$

$\vec{h}_1$ and $\vec{h}_2$ are primitive vectors in the 2D lattice with unit area $a_0 = \vec{h}_1 \cdot \vec{h}_2$. In the same spirit as our 3D crystal work I express the Schrödinger hamiltonian H as follows in atomic units ($\hbar = m = e = 1$):

$$(2) \quad H = \sum_{i=1}^{N} (-\tfrac{1}{2}\nabla_i^2) + \sum_{i>j=1}^{N} h(\vec{r}_i, \vec{r}_j),$$

where, as N approaches infinity,

$$(3) \quad h(\vec{r}_1,\vec{r}_2) = r_{12}^{-1} - \frac{1}{N}\sum_m (|\vec{r}_1 - \vec{R}_{m2}|^{-1} + |\vec{r}_2 - \vec{R}_{m2}|^{-1}) + \frac{1}{N^2}\sum_{m\neq n} |\vec{R}_{m2} - \vec{R}_{n2}|^{-1}$$

A 2D Bloch function based on a single orbital at each lattice site
can be expressed as

$$(4) \quad |\vec{k}_2\rangle = \sum_m e^{i\vec{k}_2 \cdot \vec{R}_{m2}} \varphi(\vec{r} - \vec{R}_{m2})$$

$\vec{k}_2$ is the Bloch vector in the 2D Brillouin zone associated with the
2D direct lattice. The HF expectation value of the Schrödinger
hamiltonian of Eq.(3) now involves one- and two-electron integrals
over 2D Bloch orbitals $|\vec{k}_2\rangle$ that I will reduce to computationally
more convenient forms. I follow the same procedure as in our earlier
3D work. All integrals will be expressed in a Fourier representation.
Then, after having interchanged lattice summations and Fourier argu-
ment integrations, I make use of the relation

$$(5) \quad \sum_m e^{-i\vec{q} \cdot \vec{R}_{m2}} = \frac{(2\pi)^2}{a_0} \sum_\ell \delta(\vec{q}_2 - \vec{K}_{\ell 2})$$

$\vec{q}_2$ is the projection of $\vec{q}$ onto the 2D reciprocal lattice with vectors
$\vec{K}_{\ell 2}$. Eq.(5) holds in the limit of N approaching infinity. Let me
give some examples. An overlap integral is reduced as follows

$$(6) \quad \langle \vec{k}_2 | \vec{k}_2 \rangle = N \sum_m e^{i\vec{k}_2 \cdot \vec{R}_{m2}} \langle \varphi(\vec{r}) | \varphi(\vec{r} - \vec{R}_{m2}) \rangle = \frac{N}{(2\pi)^3} \int d\vec{q} \, \varphi^{*T}(\vec{q}) \, \varphi^T(-\vec{q})$$

$$\times \sum_m e^{i(\vec{k}_2 - \vec{q}) \cdot \vec{R}_{m2}}$$

Application of Eq.(5) leads to

$$(7) \quad \langle \vec{k}_2 | \vec{k}_2 \rangle = \frac{N}{2\pi a_0} \int_{-\infty}^{+\infty} dq_\perp \sum_\ell \varphi^{*T}(\vec{q}_\perp + \vec{k}_2 + \vec{K}_{\ell 2}) \, \varphi^T(-\vec{q}_\perp - \vec{k}_2 - \vec{K}_{\ell 2})$$

$\vec{q}_{\perp}$ is the $\vec{q}$ component perpendicular to the 2D reciprocal lattice characterized by $\vec{K}_{\ell 2}$. If φ is a Slater-type orbital the $q_{\perp}$ integration can be performed analytically. Depending on the 2D crystal structure the 2D sum can probably be performed analytically. The kinetic energy integrals reduce to very similar expressions.

Before going to the electrostatic integrals I would like to make some remarks. Notice that, due to a lack of lattice periodicity in the direction perpendicular to the layer plane, we obtain in Eq.(7) an infinite integral in lieu of a sum encountered in the 3D crystal case [1,2,3]. In fact, one can derive all 2D formulas in this paper by starting from the earlier 3D formulas and allowing one 3D cell dimension (say parallel to $\vec{q}_{\perp}$) to become infinitely large. Physically this generates non-interacting layers of atoms, each of which is described by a hamiltonian like Eq.(3). Furthermore, from a numerical standpoint Eq.(7) is not harder to evaluate than the earlier 3D version. Instead of evaluating φ^T at 3D reciprocal lattice points and then forming the 3D sum, we have to compute these functions at a 3D grid $(q_{\perp}, \vec{K}_{\ell 2})$ with $q_{\perp}$ values dictated by the numerical quadrature used. Clearly the convergence properties will be essentially the same for similar types of atoms. I want to stress that convergence for all 3D core-valence and valence-valence integrals is invariably found to be very favorable.

I will now turn to the expressions for Coulomb and exchange matrix elements. For those integrals the power of the Fourier transform method shows again most impressively. In reducing the one- and two-electron integrals I made use of the following formuals.

$$(8)\ \frac{1}{R} = \frac{1}{2\pi^2} \int \frac{d\vec{q}}{q^2} e^{-i\vec{q}\cdot\vec{R}}$$

$$(9)\ \int d\vec{r} f(\vec{r})|\vec{r} - \vec{R}|^{-1} = \frac{1}{2\pi^2} \int \frac{d\vec{q}}{q^2} f^T(\vec{q}) e^{-i\vec{q}\cdot\vec{R}}$$

(10) $\int d\vec{r}_1 d\vec{r}_2 f(\vec{r}_1)(\frac{1}{r_{12}})g(\vec{r}_2 - \vec{R}) = \frac{1}{2\pi^2}\int \frac{d\vec{q}}{q^2} f^T(\vec{q})g^T(-\vec{q})e^{-i\vec{q}\cdot\vec{R}}$

f and g represent lattice sums of two-center overlap distributions.
Skipping details it should now be easy for the reader to verify the
following expressions.

(11) $\langle \vec{K}_2\vec{K}_2'|h|\vec{K}_2\vec{K}'_2\rangle = \frac{N}{2\pi^2} C_2 \Phi(\vec{K}_2,0)\Phi(\vec{K}_2',0) + \frac{2N}{a_0}\int_{-\infty}^{+\infty}dq_\perp \sum_\ell (K_{\ell 2}^2 + q_\perp^2)^{-1}$

$[\Phi(\vec{K}_2,\vec{q}_\perp + \vec{K}_{\ell 2})\Phi(\vec{K}_2',-\vec{q}_\perp - \vec{K}_{\ell 2}) - \Phi(\vec{K}_2,\vec{q}_\perp + \vec{K}_{\ell 2})\Phi(\vec{K}_2',0)$

$- \Phi(\vec{K}_2,0)\Phi(\vec{K}_2',-\vec{q}_\perp - \vec{K}_{\ell 2}) + \delta_{\ell 0}\Phi(\vec{K}_2,0)\Phi(\vec{K}_2',0)]$

(12) $C_2 = \frac{4\pi^3}{a_0} \sum_{\substack{\vec{K}_{\ell 2}\neq 0}} \frac{1}{K_{\ell 2}} - \int \frac{d\vec{q}_2}{q_2}$

(13) $\Phi(\vec{K}_2,\vec{q}) = \frac{1}{2\pi a_0}\int_{-\infty}^{+\infty}dp_\perp \sum_m \varphi^{*T}(\vec{p}_\perp + \vec{K}_{m2} + \vec{K}_2) \varphi^T(\vec{q} - \vec{p}_\perp - \vec{K}_{m2} - \vec{K}_2)$

(14) $\langle \vec{K}_2\vec{K}_2'|r_{12}^{-1}|\vec{K}_2'\vec{K}_2\rangle = \frac{2N}{a_0}\int_{-\infty}^{+\infty}dq_\perp \sum_\ell \frac{\Phi(\vec{K}_2,-\vec{Q})\Phi(\vec{K}_2',\vec{Q})}{Q^2}$

where

(15) $\vec{Q} = \vec{q}_\perp + \vec{K}_{\ell 2} + \vec{K}_2 - \vec{K}_2'$

By comparing Eqs.(11) to (15) with earlier expressions for 3D crystals[1,2]
one will notice striking similarities. Just as I indicated for the
overlap integrals the numerical efforts will be essentially the same.
The lattice constant C_2 is the 2D analog of our earlier constant in
Ref.2(a); it is the potential of the 2D lattice of unit charges at
the lattice points balanced by a uniform 2D sheet of compensating
charge in the plane of the lattice. We already encountered this

quantity in the 3D work[2], where we developed reliable computational methods for its evaluation.

Eqs.(7) and (12) thru (15) exemplify the types of integrals that will occur in Hartree or HF calculations for a single layer of hydrogen atoms. One can formulate a self-consistent calculation by describing the 2D Bloch function as a linear combination of basis Bloch functions like Eq.(3) with appropriately chosen φ's (the LCAO method). Clearly the crystal integrals over the different basis orbitals can be expressed in a similar fashion. As we have done in the 3D case, the expansion coefficients are then computed self-consistently.

Let me now indicate how easily, both formally and practically, above technique can be applied to realistic thin films. Consider a 2D basis-Bloch orbital $|\vec{K}_2 p\rangle$ given by

$$(16) \quad |\vec{K}_2 p\rangle = \sum_m e^{i\vec{K}_2 \vec{R}_{m2}} \varphi_p(\vec{r} - \vec{R}_{m2} - \vec{s}_p)$$

associated with the p-th atomic orbital at relative positions $\vec{s}_p$ within each 2D unit cell. In general $\vec{s}_p$ is given by

$$(17) \quad \vec{s}_p = \vec{s}_{p\perp} + \vec{s}_{p2}$$

$\vec{s}_{p\perp}$ and $\vec{s}_{p2}$ are the components orthogonal and parallel to the plane of 2D periodicity, respectively. As before actual 2D Bloch functions are then expressed as linear combinations of $|\vec{K}_2 p\rangle$. Integrals over these functions are now very simply related to those obtained above. For example, an overlap integral is given as

$$(18) \quad \langle k_2 p | k_2 t \rangle = \frac{N}{2\pi a_0} e^{i\vec{K}_2 \cdot (\vec{s}_{t2} - \vec{s}_{p2})} \int_{-\infty}^{+\infty} dq_\perp e^{iq_\perp (s_{t\perp} - s_{p\perp})}$$

$$\times \sum_\ell e^{i\vec{K}_{\ell2} \cdot (\vec{s}_{t2} - \vec{s}_{p2})} \varphi_p^{*T}(\vec{q}_\perp + \vec{K}_2 + \vec{K}_{\ell2}) \varphi_t^T(-\vec{q}_\perp - \vec{K}_2 - \vec{K}_{\ell2})$$

-6-

When Slater orbitals are used, the $q_\perp$ integration can be performed analytically, if so desired. The remaining 2D reciprocal lattice sum is then found to be exponentially convergent. The most remarkable aspect is the great similarity between Eqs.(7) and (18), particularly from a numerical point of view. The reader should be able to convince himself that the same holds for all other integrals above when evaluated for general 2D Bloch orbitals. The convergence properties will clearly be very similar as well. The oscillatory character of the summand (and integrand) will not cause numerical troubles, because typically their magnitudes fall off rapidly.

This formalism obviously allows one to perform calculations on a large number of thin-film like systems. By increasing the number of layers of a material, and using an appropriate basis, one can monitor the emergence of surface states in a self-consistent calculation. Surface contraction and rearrangement can be studied since the energy can be reliably optimized. One or more overlayers, with different coverages, can be brought onto the surfaces. As we will obtain Hartree or HF 2D band energies and charge densities many surface-related properties can be computed. By considering low coverages adsorption can be studied. All types of orbitals, including 3d functions, can be used. As found earlier, it will be advantageous to use direct lattice sums for core-core matrix elements[3].

When comparing with other methods one will recognize that our method will not be plagued by finite-cluster problems[5], matching planes[6], or pseudo-potential choices[7] in the surface region. Possible disadvantages are associated with the use of thin films to mimic the behavior of surfaces on half-infinite samples. The identification of surface states (or bands) from 2D band structure calculations will be non-trivial. However, it is reassuring that typical "healing" is only over a few atomic layers[5,6]. This suggests that it is physically realistic to use thin films with only a few layers to calculate surface properties[6]. Also it is not clear how low a coverage of adsorbate we can numerically handle to describe single-adsorbate/substrate interaction. More theoretical and numerical results will be published elsewhere.

-7-

References

1. F.E. Harris and H.J. Monkhorst, Phys. Rev. Letters $\underline{23}$, 1026 (1969).

2. F.E. Harris and H.J. Monkhorst, Phys. Rev. $\underline{B2}$, 4400 (1970); F.E. Harris, L. Kumar and H.J. Monkhorst, Phys, Rev. $\underline{B7}$, 2850 (1973).

3. L. Kumar, H.J. Monkhorst and F.E. Harris, Phys. Rev. $\underline{B9}$, 4084 (1974); L. Kumar and H. J. Monkhorst, J. Phys. $\underline{F4}$, 1135 (1974).

4. D.E. Ramaker, L. Kumar and F.E. Harris, Phys. Rev. Letters, $\underline{34}$, 812 (1975).

5. K.H. Johnson and R.P. Messmer, J. Vac. Sci. Techn. $\underline{11}$, 236 (1974); H. Deuss and A. Van Der Avoird, Phys. Rev. $\underline{B8}$, 2441 (1973).

6. J.A. Appelbaum and D.R. Hamann, Phys. Rev. $\underline{B6}$, 2166 (1972); Bull. Am. Phys. Soc. $\underline{20}$ (3), 304, 325 (1975).

7. L. Kleinman, E. Caruthers and G.P. Alldredge, Phys, Rev. $\underline{B9}$, 3325, 3330 (1974); G.P. Alldredge and L. Kleinman, Phys. Rev. $\underline{B10}$, 559 (1974); Phys. Letters $\underline{48A}$, 337 (1974).

Hartree–Fock formalism for the calculation of total energies and charge densities of thin films

Frank E. Harris, Hendrik J. Monkhorst, and William A. Schwalm

Department of Physics, University of Utah, Salt Lake City, Utah 84115

(Received 19 March 1979; accepted 16 April 1979)

A formalism has been developed by which the Hartree–Fock self-consistent equations for thin films and surfaces are solved in an essentially exact way from first principles. The Fourier transform method, which was developed and used very successfully for the calculation of bulk properties, has now been extended to permit the study of the surfaces of crystals of a wide variety of materials. The development is sufficiently general to permit the treatment of any surface of any crystal geometry together with relaxations and reconstructions. A basis set of Slater-type, layer orbitals is used to compute a self-consistent density matrix for electrons in the field of bare nuclei in a slab geometry. The basis functions are handled in the Fourier representation which reduced many of the integrals to sums of one-dimensional ones which are computed in closed form. The use of the Fourier integral representation also permits an analytical treatment of the cancellation of the Coulomb singularities in the classical potential.

I. INTRODUCTION

The basis and the starting point for most one-electron calculations for extended systems, including tight-binding methods and pseudopotential methods, lies in the Hartree–Fock self-consistent equations. It has been traditionally accepted that the Hartree–Fock equations for extended systems are not to be solved exactly, "even by machines."[1] Although this is no longer the case,[2-7] these solutions have not been carried out for systems with surfaces. The thought that such a thing might be possible or even that it might be enlightening is seldom evident in the literature. Beside the fact that the Hartree–Fock equations are difficult to solve, it is quite well known that the solutions have certain unphysical properties, such as the vanishing of the density of states near the Fermi level.[8] Since we are often interested in understanding details of some spectroscopic data, these unphysical properties make the method seem unattractive. For correlating and extrapolating spectroscopic data, pseudopotential or tight-binding methods which do not suffer from any of these difficulties and offer some simple insight are often more appropriate. These methods have been developed extensively and applied repeatedly to many different kinds of interface problems with great success.

However, a number of things can be learned from the Hartree–Fock solution. In order to assess the plausibility of various surface reconstruction models it would be very helpful to have a reliable estimate of the relative total energy of closely related structures. There are a few methods which seem to be able to produce such estimates from rather simple force-constant models.[9] Neither the microscopic foundation for these models nor the reason for their apparent success is especially clear, although it is felt that much of the force-constant energy results from core–core and core–valence interactions. This ability to determine relative total energies is vitally important, because together with low energy electron diffraction and angle resolved photoemission it provides a means of discriminating between surface geometries. It is known from the large body of experience with molecules that the important part of the relative energy which determines the geometric structure (to within structures related by small displacements) is given by the Hartree–Fock solution.[10] By using the density matrix, one can partition the energy into various contributions and in this way get a more detailed understanding of the mechanisms which determine geometry. At the same time, one might hope to understand the simpler methods in a more fundamental way. Since the converged Fock matrix for a particular problem contains the Coulomb and exchange potentials as a function of the translation quantum number, it is interesting to compare this matrix with various model potentials. Also, since the one-electron charge densities are quite realistic, one can find the difference in electrostatic potential between infinity and some point inside the bulk, and this defines the work function. Finally, the Hartree–Fock solution is a solution of a well defined problem which is related to the true solution of the many-electron problem in quite a specific way. The nature of this relation is such as to make the Hartree–Fock solutions a convenient starting point for any more ambitious project which would take correlation effects into account.

The use of Fourier representation is the key to the treatment of extended systems. There are at least three reasons for using momentum representation. First, on account of the conv-

tion properties, various one and two-electron integrals over the Coulombic interactions will naturally decompose into products of simpler integrals. Secondly, due to translation symmetry in the layer, each of the remaining integrals further decomposes into a two-dimensional sum over one-dimensional integrals in the dimension perpendicular to the layer. These are done in closed form. After doing the integrals, the convergence of the sum is quite satisfactory. Another good reason for doing the calculation this way is that singularities in the classical Coulomb terms arising from the lattice-plus-Hartree part of the potential may be treated explicitly.

This paper is devoted to a description of the formalism being used to investigate thin films composed of light element atoms and molecules. Eventually this method will be extended with treatment of semiconductor surfaces and interfaces.

II. OUTLINE OF THE METHOD

The method is a generalization of the Fourier transform method which has been used in the bulk with notable success.[2-5] We have used a basis set expansion. Layer orbitals are constructed from Slater-type orbitals in the usual way. However, these are then projected onto plane waves and the entire computation is carried out in momentum representation. It should be noted that this is completely different from any attempt to expand the potentially localized electronic structure of these types of systems in plane waves. By using all of the infinite numbers of Fourier components in the Slater-type basis set, the convergence properties are preserved in the case of localization.

Complete definition of the Hamiltonian requires only the identification of the chemical species and the specification of the geometry, that is, of the positions of each of the atoms

in the infinite system. The fundamental unit of the basis set is a layer orbital corresponding to a translation symmetry index p'' in the plane of the layer:

$$|p'',n,\alpha\rangle = \sum_m \exp(ip'' \cdot R_m)|m,n,\alpha\rangle, \qquad (1)$$

where the symbol $|m,n,\alpha\rangle$ is a Slater orbital of type α centered at a position specified by m,n, and α in a way illustrated in Fig. 1. The index n denotes the layer, m is a vector index within each layer, and α which denotes the basis function type is also used as an index which may indicate a nonprimitive displacement within the unit cell. The sum in Eq. (1) is thus over all lattice positions in a layer, but not over nonprimitive positions and not over the different layers.

Since atomic positions may differ in the selvedge region as compared to the bulk or inner layers of the film, the position vector may be broken up into two parts, only one of which is determined by the bulk basis vectors. Figure 1 illustrates the simple case with the selvedge region the same as the inner layers. Actually, any specific number of layers may be set aside as having orbitals different in both position and form from those of the bulk. Notice that Fig. 1 has been simplified in order to reduce the number of lines and make it more comprehendable. There would be atomic sites along the dotted edge in the rear as well as other nonprimitive sites within each cell congruent to the one pictured on layer 4.

Matrix elements of the Fock matrix are calculated explicitly with respect to this basis set. We have chosen to use Slater-type functions rather than Gaussians in our calculations because these represent the solutions well in the regions of the nuclei and because there is no advantage to using Gaussians in the Fourier representation.

Evaluation of integrals is facilitated by using plane-wave components $\langle k|p'',n,\alpha\rangle$ defined with respect to normalized plane waves.

$$\langle k|p'',n,\alpha\rangle = \frac{1}{(2\pi)^{3/2}} \int e^{-ik \cdot r} \langle r|p'',n,\alpha\rangle \, d^3r. \quad (2)$$

Clearly this is zero unless the parallel component k'' of the transform variable is congruent by reciprocal layer vector to p''. It is this property which reduces inner products to sums of one dimensional integrals. In fact

$$\langle k|p'',n,\alpha\rangle = \Delta(k'' - p'')\langle k|p'',n,\alpha\rangle, \qquad (3)$$

where the capital delta symbol is defined to be a sum over Kronecker symbols at each point K'' on the reciprocal layer lattice.

$$\Delta(k'' - p'') = \sum_{K''} \delta_{K'',k''-p''} \qquad (4)$$

The basic problem is to solve the self-consistent equations which arise in matrix form for each value of the translation quantum number p''. These p'' values are taken to be quadrature points which will be used to sum over the continuum of filled states. At each one of these points, the 'th eigenvector is expanded in layer orbitals

$$|p'',v\rangle = \sum_{n,\alpha} c_{v,n\alpha}(p'')|p'',n,\alpha\rangle, \qquad (5)$$

$$\vec{R}_{mn\alpha} = \vec{R}_m + \vec{R}_{n\alpha}$$
$$n: \text{layer}$$
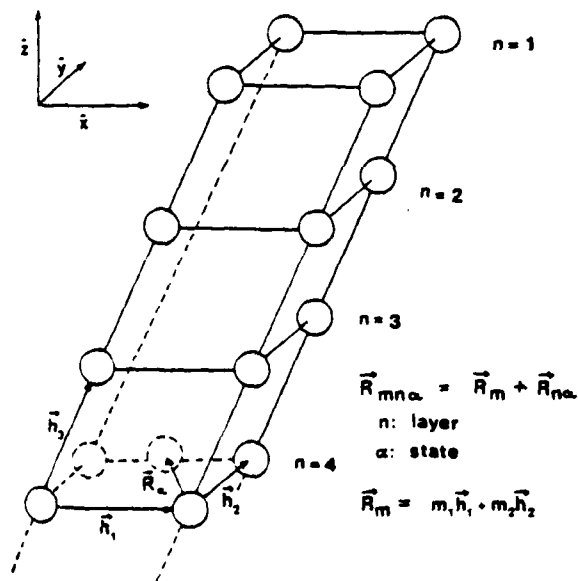$$\alpha: \text{state}$$
$$\vec{R}_m = m_1\vec{h}_1 + m_2\vec{h}_2$$

FIG. 1 Definition of geometry showing the bulk lattice vectors, layer numbers, and a nonprimitive displacement. Note that atoms on the left, rear edge have been omitted for clarity as have those in the other nonprimitive sites.

and the coefficients must satisfy (in matrix form)

$$F(p'')c_v(p'') = E_v(p'')S(p'')c_v(p''). \quad (6)$$

The first set of questions to be asked concerns the way in which each term of the Fock matrix is defined.

$$F(p'') = T(p'') + V(p'') + C(p'') + X(p''). \quad (7)$$

The overlap matrix is simply given by

$$S_{n\alpha,n'\beta}(p'') = \langle p'',n,\alpha \mid p'',n',\beta \rangle. \quad (8)$$

The kinetic energy T has the form (in atomic units)

$$T_{n\alpha,n'\beta}(p'') = \int \langle p'',n,\alpha \mid k \rangle (\tfrac{1}{2})k^2 \langle k \mid p'',n',\beta \rangle \, d^3k. \quad (9)$$

The terms which provide for the interaction between an electron and the lattice or between an electron and the other electrons can be written most easily as convolutions involving the distribution matrices. The matrix elements of these are the transforms of the products of layer orbitals, or equivalently, convolutions of the transforms of layer orbitals.

$$Q_{n\alpha,n'\beta}(p'',q'',k) = \int \langle p'',n,\alpha \mid t \rangle \langle t + k \mid q'',n'\beta \rangle \, d^3t. \quad (10)$$

In Eq. (10), the product in real space has become a convolution in k space. As a result of this convolution and of translation symmetry, a rather pleasant decoupling of terms results which is easily comprehended. The lattice-plus-Hartree terms are of the form

$$V(p'') + C(p'') = \int W(k)Q(p'',p'',k)[\Delta(k) - 2\varrho(k)]d^3k, \quad (11)$$

$$W(k) = \frac{1}{2\pi^2}\frac{1}{k^2}, \quad (12)$$

$$\Delta(k) = \sum_{n,\alpha} z_\alpha e^{ik \cdot R_{n\alpha}}; \quad (13)$$

where $W(k)$ is the transform of the Coulomb kernel, $\Delta(k)$ is the structure factor for the bare nuclei with charges z_α, and $\varrho(k)$ is a similar structure factor defined in terms of the self-consistent electronic charge density. The factor of 2 comes about due to double occupancy of the levels, one electron per spin state.

In order to define the electronic structure factor $\varrho(k)$ or any other expression depending upon the solution, the density matrix $D(p'')$ must first be defined. The matrix elements of $D(p'')$ are expressed in terms of the coefficients appearing in Eq. (5) as

$$D_{n\alpha,n'\beta}(p'') = \sum_v c^*_{v,n\alpha}(p'')c_{v,n'\beta}(p'')\Theta_v(p''), \quad (14)$$

the sums being over all eigenstates and the $\Theta_v = 1$ if the eigenstate energy is below the Fermi level and zero otherwise. Then $\varrho(k)$ becomes

$$\varrho(k) = \frac{a}{(2\pi)^2} \int_{zone} \text{trace}[D(q'')Q(q'',q'',-k)] \, d^2q''. \quad (15)$$

The integral being over the two-dimensional Brillouin zone. A similar expression holds for the exchange matrix, except that here the translation quantum numbers are coupled in a more complicated way.

$$X(p'') = \frac{a}{(2\pi)^2} \int W(k) \int_{zone} Q(p'',q'',k)D(q'')$$
$$\times Q(q'',p'', -k) \, d^2q''d^3k. \quad (16)$$

The reason for this difference between the Coulomb and exchange parts is quite clear, as illustrated in Fig. 2. Because the desired solutions have translation symmetry, at each stage in the iteration the density matrix will preserve q''. Likewise, the entire Fock matrix conserves p'' so that, in analogy with the electron gas, the interaction either preserves or exchanges the translation quantum numbers p'' and q''. In the case of the classical term C, the fact that only a single translation variable p'' occurs in either distribution means that far fewer Q terms need be computed.

A very important cancellation takes place in Eq. (11) for the classical potential. The integration over either $\Delta(k)$ or $2\varrho(k)$ by itself would clearly diverge in view of the fact that these are the contributions due to the separate positive and negative charge distributions, which are infinite in extent. This Madelung-like cancellation will be discussed below.

III. EVALUATION OF INTEGRALS

Consider first the integrals [Eq. (10)] which form the elements of the distribution matrix for a given p'', q'', and k. Due to the translation selection rule, the integrand of one of these integrals is zero, unless $p'' + k'' - q''$ is a reciprocal layer vector. Here, k'' is the component of the Fourier transform variable k parallel to the layer. Moreover, even with this condition satisfied, the only contribution to the integral comes from t'' close to $p'' + K''$, where K'' is some reciprocal layer vector. There are peaks in the integrand resulting from the sum over phase factors within the layer orbitals, and these are centered near $p'' + K''$ for each K'' and have a width of the order of the reciprocal of the linear size of the film, which we will finally take to infinity. Taking this limit transforms the distributions into sums over one-dimensional integrals in the direction perpendicular to the film.

Now we note the form of these one-dimensional integrals. Since the layer orbitals are composed of Slater-type functions whose Fourier transforms are simple combinations of rational functions, these integrals may be done in closed form. In fact,
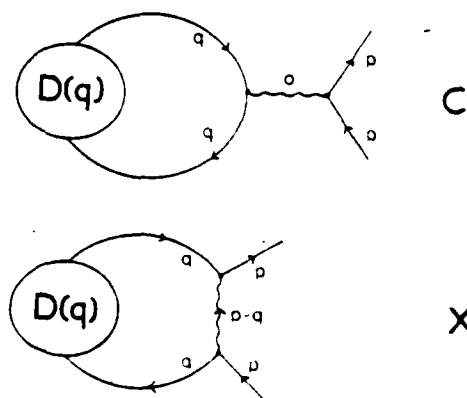

FIG. 2. Translation symmetry and by the Coulomb and exchange matrix elements. The density matrix preserves the q'' quantum number.

a typical integral is a sum of a small number (two or three) of functions of the type

$$J_{\ell mn}(a,b,k,\mu) = \int_{-\infty}^{\infty} \frac{t^{\ell} e^{i\mu t}\, dt}{(t^2 + a^2)^m[(t-k)^2 + b^2]^n},$$

(17)

where the integration variable t is the z component of $\mathbf{t}$ and the k parameter is minus the z component of $\mathbf{k}$. The parameter a is the square root of the sum of the square of the Slater exponent of α and the square of the length of $\mathbf{p}'' + \mathbf{t}''$, b is a similar expression with α replaced by β and $\mathbf{p}'' + \mathbf{t}''$ replaced by $\mathbf{q}'' + \mathbf{t}'' + \mathbf{k}''$. The μ of this expression is the perpendicular distance between the two layers n and n' which appear in the definition of the Q matrix elements [Eq. (10)]. The J's may be integrated by residues in the standard way and a result for the general case is obtained.

The one-dimensional integrals may be summed over t'' to produce Q, as is convenient when $\mathbf{p}'' = \mathbf{q}''$, or sometimes it will be wise not to do this summation. The reason why one may not wish to sum here is that the integral over k in Eq. (16) may also be done in closed form. This is due to the fact that the values of the integrals over t resulting from the residues of Eq. (17) are in fact rational functions of k. When two of them are multiplied with $W(k)$, the result is a rational function with only a few poles which are due to explicit factors of the denominator.

In the case when the summation to form Q is done first, it must be performed numerically. Although these sums converge quite well, the k integrals must then also be done numerically.

Another difference between the Coulomb and exchange terms becomes evident with consideration of the integrations over the two-dimensional Brillouin zone of the translation quantum number q''. Integrals of this type appear in Eqs. (15) and (16). It is clear that these integrations must be done numerically, since the value of the integrand at each point results from the solution of the secular Eq. (6). The fact that all of the functions appearing in these integrands must be periodic with respect to q'' provides a natural technique for this numerical integration. Each integrand may be expanded in a Fourier series. The coefficient of the constant term is proportional to the value of the function over the Brillouin zone. The coefficients of any fixed number of terms in the expansion may be found by summation over a grid of quadrature points spaced equally over the zone. The quadrature is thus exact up to a fixed number of Fourier coefficients. This method is closely related to Gauss–Tchebychev quadrature extended to two dimensions. This method may be applied to both the integrals of the type appearing in $e(k)$ and the type appearing in $X(p'')$.

There is an extra simplification which reduces the two-dimensional integrals of the Coulomb type still further. It has been pointed out by Monkhorst and Pack that in the special but very important case when the integrand transforms according to the identity representation of the point group of the surface, then the integration may be performed using only the small subset of the quadrature points which lie within the irreducible wedge of the zone.[11] Integrals of the $V(p'')$ + $C(p'')$ terms are of this form, and this can be demonstrated as

follows:

Consider the integrand of Eq. (15). It is not obvious that the integration variable q'' may be rotated through a symmetry operation g in the plane of the layer without affecting the value of the integral. First of all, the matrix Q will undergo a similarity transformation with respect to a representation matrix of g. However, D will transform the same way, and the rotation matrices will multiply to unity because of the trace operation. This will produce an expression exactly like Eq. (15), except that $\mathbf{k}$ will be transformed by g. The integral is thus invariant with respect to symmetry operations on $\mathbf{k}$. This shows that in the integrand of the integral of Eq. (11) $e(k)$ is symmetric in $\mathbf{k}$. Thus it may be replaced by the average of itself over all $\mathbf{k}$ related by operations of the group. When this is done, the integrand in Eq. (15) now becomes symmetric in q'' as required.

It is unfortunate that the $\mathbf{p}''$ in the integrand of Eq. (16) makes a similar simplification impossible for the exchange terms. These terms must be treated separately.

The final set of integrals to be considered are those over the three components of $\mathbf{k}$ in Eqs. (11) and (16). The selection rule [Eq. (3)] for $\langle \mathbf{k} | \mathbf{p}'', n, \alpha \rangle$ is written in terms of Kronecker's delta symbols. Under certain conditions, these deltas also have Dirac delta function properties with respect to integration, but one must use caution since there is an interesting size effect which turns out to have a physical meaning. As noted above, these delta functions have a width when considered as a function of k'' which depends inversely upon the linear size of the layer.

The details of the reduction of the Coulomb-plus-lattice matrix elements to the form presented in (11) have been treated quite carefully.[2,12] The delta functions in Eq. (3) come about because of a sum over phase factors embedded in the definition of the layer orbitals in Eq. (1). If these deltas can be thought of as being proportional to Dirac deltas, then the integral over the sum will become a sum of integrals. However the sums, which were originally sums of phase factors do not converge uniformly for an infinite layer near the point where $\mathbf{k} = 0$. Near this point, the terms in the sum are all going to one. This lack of uniform convergence near $\mathbf{k} = 0$ prevents the exchange of summation and integration, and thus some small ball around this point must be removed from the region of integration and treated separately. The contribution from this ball must be treated in the limit that the size of the ball goes to zero.

The result of the analysis outlined above is that when the symmetry is such that the self-consistent solution does not produce a net dipole moment per unit volume with a component in the plane of the layer, then Eq. (11) reduces to a sum of one-dimensional integrals with only minor qualifications.[ ] The integrand of the one-dimensional integral with $k'' = 0$ is singular at zero. The Cauchy principal value is to be understood in this case.

The expression for the total energy of the film is not simply the sum over filled states of the band energies, as this would count the electron–electron interaction energy twice, but is given by

$$E = \frac{a}{(2\pi)^2} \sum \int \Theta_v(\mathbf{p}'') E_v(\mathbf{p}'')\, d^2p''$$

$$+ \frac{1}{2} \langle T \rangle + \frac{1}{2} \langle V \rangle + R, \quad (18)$$

where a is the area of the unit cell in the layer and the term denoted by R is the lattice–lattice interaction. A similar careful analysis of these terms shows that except for the T term, each one leads to sums of integrals plus residual parts due to the exclusion of the origin in k. The singularities cancel in such a way that there may be a contribution to the energy due to the explicit treatment of this excluded part. This contribution is the multipole expansion of the classical electrostatic potential due to the edge of the film. In the case when there is no dipole moment per unit volume in the plane of the layer, these terms do not contribute in the limit of an infinite layer.

The details of the reduction of the total energy expression will be presented elsewhere.[8,12] There are terms arising from the electrostatic energy of the lattice of positive nuclei balanced by a uniform negative background charge. These Madelung-like terms do not depend upon the density matrix, and so they may be computed once and for all for a given crystal geometry. Then, there are other terms which describe the change in the potential energy due to the nonzero Fourier components of the electronic charge density. These do depend upon the solution through the density matrix.

IV. SUMMARY

The formalism presented above is flexible enough to permit the investigation of a large number of interesting systems. The lattice size may be expanded in order to investigate the isolated molecular limit, or the selvedge region may be reconstructed almost arbitrarily. Calculations are in progress on hydrogen and will proceed to other light elements. The next major formal development to be undertaken is the introduction of an *ab initio* pseudopotential in order to treat the case of atoms with cores in a way which avoids computing a large number of integrals.

ACKNOWLEDGMENT

[1]P. W. Anderson, *Concepts in Solids* (Benjamin, New York, 1964), p. 28.
[2]F. E. Harris, *Electronic Structure of Polymers and Molecular Crystals*, edited by J. Andre, J. Ladik, and J. Delhalle (Plenum, New York, 1975).
[3]F. E. Harris, Theor. Chem. 1, 147 (1975).
[4]F. E. Harris, L. Kumar, and H. J. Monkhorst, Phys. Rev. B 7, 2850 (1973).
[5]H. J. Monkhorst and J. D. Pack, Phys. Rev. B 13, 5188 (1976).
[6]A. Mauger and M. Lannoo, Phys. Rev. B 15, 2324 (1977).
[7]N. E. Brener and J. L. Fry, Phys. Rev. B 17, 506 (1978).
[8]H. J. Monkhorst (accepted for publication, Phys. Rev. B).
[9]D. J. Chadi and R. M. Martin, Solid State Commun. 19, 643 (1976).
[10]W. G. Richards, T. E. Walker, R. K. Hinkley, *Biography of Ab Initio Molecular Wave Functions* (Clarendon Press, Oxford, 1970).
[11]H. J. Monkhorst and J. D. Pack, (unpublished).
[12]H. J. Monkhorst (unpublished).

Analytic continuation in exchange perturbation theory

Bogumił Jeziorski

*Department of Physics, University of Utah, Salt Lake City, Utah 84112
and Quantum Chemistry Laboratory, University of Warsaw, Pasteural, 02-093 Warsaw, Poland[a]*

William A. Schwalm

Department of Physics, University of Utah, Salt Lake City, Utah 84112

Krzysztof Szalewicz

Quantum Chemistry Laboratory, University of Warsaw, Pasteura 1, 02-093 Warsaw, Poland

It has been shown that the divergence or pathologically slow convergence of perturbation expansions involving a weak or none symmetry forcing (Murrell–Show–Musher–Amos, symmetrized polarization or polarization expansions) can be circumvented by using a simple analytic continuation procedure. When applied to the interaction of a hydrogen atom with a proton this procedure provides accurate values of the exchange energy from the knowledge of the polarization series alone. When the *ungerade* symmetry is forced the symmetrized polarization series is shown to converge to a spurious, unphysical interaction energy. The true interaction energy can only be recovered by the analytic continuation procedure. This procedure provides us also with the information about location of singularities of the analytic functions defined by the perturbation series. Such information turns out to be sufficient for an understanding of peculiar convergence properties of the perturbation expansions and their Padé approximants.

I. INTRODUCTION

It is well known that there exist very many different perturbation expansions for molecular interaction energies, usually referred to as exchange perturbation theories.[1] It is less known, however, that in practice the majority of them cannot be applied to study interactions of many-electron systems. This majority includes all theories which require solving perturbation equations involving the full N-electron antisymmetrizer $\mathcal{A}$. The presence of this operator prohibits any separation of variables in perturbation equations and even for separable H_0 the first-order wave function would have to contain all many-electron clusters up to an N-electron cluster.[2] Very recently Adams[3] showed that the Eisenschitz–London–Hirschfelder–van der Avoird (EL–HAV) theory can be modified in such a way that only a partial antisymmetrization including only single interchanges appears in perturbation equations. This is an essential simplification since the first-order wave function then involves only up to four-electron clusters.[3] Nevertheless such a method would be less practical than the methods in which $\mathcal{A}$ does not appear in perturbation equations at all, i.e., in which the nth-order wave function can be expressed in terms of at most $(n+1)$-electron clusters.[2] It turns out that this condition can be satisfied only by perturbation formalisms involving a weak or no symmetry forcing.[4,5] These are the standard Rayleigh–Schrödinger (RS) perturbation expansion, referred to as the polarization expansion after Hirschfelder, the symmetrized Rayleigh–Schrödinger (SRS) expansion, usually referred to as the symmetrized polarization expansion, and the Murrell–Show–Musher–Amos (MSMA) expansion. The symmetry forcing peculiar to these expansions is characterized in more detail in Ref. 5. The

fact that the interaction energy in the MSMA theory can be calculated without solving perturbation equations involving a projection operator is a direct consequence of the interchange theorem proved in Ref. 4.

The results of the numerical calculations for the interaction of a hydrogen atom and a proton, reported in Refs. 5 and 6, show that the convergence properties of the three expansions mentioned above are far from desirable. The convergence of the polarization expansion is pathologically slow (especially at large distances R), and, moreover, the series can provide us only with the energy of a physically uninteresting fully symmetric state. The symmetrized polarization expansion also converges pathologically slowly, and, when the ungerade symmetry is forced the series does not seem to converge to any eigenvalue of the Hamiltonian. The MSMA series, on the other hand, clearly diverges to infinity in this case. To find a way out of this highly unsatisfactory situation the usual (rational) Padé approximants have been calculated for these expansions.[7] It turned out that the Padé approximants for the MSMA series converged very quickly to the exact energy, thereby providing effective analytic continuation of the series beyond its convergence radius. On the other hand, the Padé approximation was a complete failure in the case of the RS and SRS series.

In the present paper we want to show that these two series can be very effectively summed using a different kind of analytic continuation, based upon employing a simple algebraic function having only square root type singularities. This procedure, being a particular case of the so-called quadratic Padé approximation introduced by Shafer,[8] also works very well in the case of the MSMA method and can be used to locate singularities of all three perturbation series. The knowledge of the positions and the character of these singularities turns out to be sufficient to explain the peculiar convergence properties of

---

[a] Permanent address.

the RS, SRS, and MSMA expansions as well as of the corresponding Padé approximants.

The plan of this paper is as follows. In Sec. II we formulate the problem in a rigorous mathematical way by defining interpolation functions, i.e., analytic functions which after expanding them in a power series around $\lambda = 0$ produce the perturbation series considered by us. In Sec. III these interpolation functions and their singularities are investigated for an exactly soluble model. The information obtained from this model is used in Sec. IV to set up an analytic continuation procedure, which is subsequently tested for the realistic system consisting of a hydrogen atom interacting with a proton. Section V contains a discussion and conclusions.

II. INTERPOLATION FUNCTIONS

When the interaction between two subsystems, denoted below by A and B, is completely neglected, the Hamiltonian H_0, the wave function ψ_0, and the energy ϵ_0 of the system AB are simply expressed via the Hamiltonians, the wave functions, and the energies of isolated subsystems: $H_0 = H_0^A + H_0^B$, $\psi_0 = \varphi_0^A \varphi_0^B$, and $\epsilon_0 = \epsilon_0^A + \epsilon_0^B$. To find the interaction energy ϵ we have to add the interaction operator V to H_0, accounting for the Coulombic interactions between elementary particles of A and B, and subsequently, to find the appropriate eigenvalue of $H = H_0 + V$. To solve this problem by the RS perturbation theory we introduce a complex variable λ, the perturbed Hamiltonian $H(\lambda) = H_0 + \lambda V$, and the function $\epsilon^{RS}(\lambda)$ defined by the eigenvalue equation

$$H(\lambda)\psi^{RS}(\lambda) = [\epsilon_0 + \epsilon^{RS}(\lambda)]\psi^{RS}(\lambda) . \tag{1}$$

The function $\epsilon^{RS}(\lambda)$ will be referred to as the RS interpolation function. We know from the Kato theory[9] that $\epsilon^{RS}(\lambda)$ exists and is analytic in some neighborhood of $\lambda = 0$. The RS expansion is then defined as the power series expansion of $\epsilon^{RS}(\lambda)$:

$$\epsilon^{RS}(\lambda) = \sum_{n=1}^{\infty} \epsilon_n^{RS} \lambda^n , \tag{2}$$

and the interaction energy ϵ can be calculated from

$$\epsilon = \epsilon^{RS}(1) = \sum_{n=1}^{\infty} \epsilon_n^{RS} . \tag{3}$$

Obviously, in practice the perturbation corrections ϵ_n^{RS} are calculated directly from perturbation equations[10] without the knowledge of $\epsilon^{RS}(\lambda)$. The importance of $\epsilon^{RS}(\lambda)$ lies in the fact that its singularities determine the convergence radius of (2), the rate of convergence of the series (3), and the convergence properties of the Padé approximants to the power series (2). The expansion (3) would be particularly useful if the convergence radius of (2) were greater than unity, i.e., if the singularities of $\epsilon^{RS}(\lambda)$ lay far outside the unit circle. Unfortunately, it is known[11,12] that the polarization expansion cannot satisfy this condition. Moreover, as shown by Claverie,[13] in the case of more than two-electron systems, the series (3) can converge only to the energy of states which are incompatible with the Pauli exclusion principle. It is interesting that in spite of the above drawbacks the series (3) generates the correct large R asymptotic expansion for ϵ,

$$\epsilon \sim \sum_{k=1}^{\infty} C_k R^{-k} , \tag{4}$$

where R is a measure of the distance between A and B. This means that each term in (4) can be obtained from (3) in finite order treatment.[14] Particularly, if A and B are neutral systems we have

$$\epsilon - \sum_{n=1}^{m} \epsilon_n^{RS} = O(R^{-3m-3}) , \tag{5}$$

i.e., the mth order treatment gives all C_k constants from $k = 1$ through $k = 3m + 2$. It should be stressed, however, that practical usefulness of the asymptotic expansion (4) is very limited since the exponentially decreasing components of the interaction energy are obviously neglected by this expansion. Moreover, although this fact has not been rigorously proven, it is generally assumed that the expansion (4) is divergent for each value of R.[14,15]

The exchange perturbation theories designed to obviate the difficulties mentioned above provide us with many other interpolation functions $\epsilon(\lambda)$, having different singularities and leading to different power series expansions:

$$\epsilon(\lambda) = \sum_{n=1}^{\infty} \epsilon_n \lambda^n . \tag{6}$$

As a matter of fact these interpolation functions are constrained only by two conditions:

(i) $\epsilon(0) = 0$,

(ii) $\epsilon(1) = \epsilon$,

and can be defined in many possible ways (see Refs. 1, 4, and 16 for a review of recent literature). For practical reasons it is also sensible to require that

(iii) $\lim_{R \to \infty} R^k(\epsilon_n - \epsilon_n^{RS}) = 0$ for each $k > 0$

and

(iv) for separable H_0, ϵ_n can be calculated in practice for many-electron systems. Condition (iii) guarantees that the exchange contributions ϵ_n vanish exponentially with R, i.e., that the perturbation expansion for ϵ does not produce any long-range exchange terms.[4] It is tempting to also require that

(v) singular points of $\epsilon(\lambda)$ lie far outside the unit circle.

Unfortunately this condition seems to be incompatible with (iv) and none of the proposed perturbation formalisms satisfy both (iv) and (v). As a matter of fact, it is the purpose of this article to show that condition (v) may be relaxed in practice.

A convenient way to construct interpolation functions is to use the idea of symmetry forcing[4,5] and to define $\epsilon(\lambda)$ by the system of equations

$$\epsilon(\lambda) = \lambda \frac{\langle \psi_0 | V F_1 \psi(\lambda) \rangle}{\langle \psi_0 | F_1 \psi(\lambda) \rangle} , \tag{7}$$

$$\psi(\lambda) = \psi_0 + R_0(\epsilon(\lambda) - \lambda V) F_2 \psi(\lambda) , \tag{8}$$

where R_0 is the reduced resolvent of H_0, and F_1 and F_2 are symmetry forcing operators which can be equal to

the identity operator, the idempotent antisymmetrizer $\mathcal{A}$, or some other more complicated operator.[4] It can be shown that for $\lambda = 1$, Eqs. (7) and (8) are equivalent to the Schrödinger equation (1) constrained to the symmetry subspace determined by F_1 and F_2. Therefore, $\epsilon(1) = \epsilon$.

If $F_1 = F_2 = 1$ (no symmetry forcing) Eqs. (7) and (8) are equivalent to (1) for each λ and in this case $\epsilon(\lambda) = \epsilon^{RS}(\lambda)$. The choice $F_1 = \mathcal{A}$, $F_2 = 1$, classified as a weak symmetry forcing, leads to the perturbation expansion of the MSMA theory.[4] The interpolation function $\epsilon(\lambda) = \epsilon^{MSMA}(\lambda)$ is then defined by the equation

$$\langle \psi_0 | (\epsilon^{MSMA}(\lambda) - \lambda V)\mathcal{A}[1 - R_0(\epsilon^{MSMA}(\lambda) - \lambda V)]^{-1} \psi_0 \rangle = 0 \ , \quad (9)$$

resulting after eliminating $\psi(\lambda)$ from Eqs. (7) and (8). Note, that if we skipped $\mathcal{A}$ in (9) this equation would define the RS interpolation function $\epsilon^{RS}(\lambda)$. We see that $\epsilon^{RS}(\lambda)$ and $\epsilon^{MSMA}(\lambda)$ are implicitly defined multivalued functions of the complex variable λ. Their values lie on many branches which may be obtained by analytic continuation of the series (2) or (6).

The choice $F_2 \neq 1$ gives a stronger symmetry forcing employed, for example, in the EL–HAV ($F_1 = F_2 = \mathcal{A}$) or the Hirschfelder–Silbey (F_1 and F_2 are given in Ref. 4) theories. Although the strong symmetry forcing seems to guarantee very fast convergence of the perturbation expansion,[4,5] it is incompatible with condition (iv) and cannot be applied to studying physically interesting systems. Therefore, strong symmetry forcing expansions will not be discussed in this paper.

The interpolation function of the symmetrized polarization expansion[5] is defined explicitly as

$$\epsilon^{SRS}(\lambda) = \lambda \frac{\langle \psi_0 | V \mathcal{A} \psi^{RS}(\lambda) \rangle}{\langle \psi_0 | \mathcal{A} \psi^{RS}(\lambda) \rangle} \ , \quad (10)$$

where $\psi^{RS}(\lambda)$ is defined by Eq. (1) or by Eqs. (7) and (8) with $F_1 = F_2 = 1$. It may be argued that the SRS method cannot be useful for physically interesting states for with $\mathcal{A}\psi^{RS}(1) = 0$ and $\epsilon^{SRS}(\lambda)$ has a singularity at the physical value of the expansion parameter.[5,18] In fact, this singularity is removable, at least for sufficiently large R, since, as can easily be shown by expressing $\partial/\partial\lambda$ $\langle\psi^{RS}(\lambda)\rangle_{\lambda=1}$ in terms of eigenfunctions of $H(1)$,

$$\lim_{R \to \infty} R^{-k} \frac{\partial}{\partial\lambda} \langle \psi_0 | \mathcal{A}\psi^{RS}(\lambda) \rangle |_{\lambda=1} = \infty \quad \text{for each } k > 0 \ . \quad (11)$$

It must be stressed, however, that $\epsilon^{SRS}(1)$ defined as a limit of $\epsilon^{SRS}(\lambda)$ for $\lambda \to 1$ cannot be shown to be an eigenvalue of $H(1) = H_0 + V$. Thus, even if the power series for $\epsilon^{SRS}(\lambda)$ converges at $\lambda = 1$, its sum need not have a physical meaning (although it must have the same large R asymptotic expansion as ϵ). However, as can be seen from Eq. (10), $\epsilon^{SRS}(\lambda)$ has a second branch arising from that branch of $\psi^{RS}(\lambda)$ which satisfies $\psi^{RS}(1) = \mathcal{A}\psi^{RS}(1)$. This branch of $\epsilon^{SRS}(\lambda)$ is regular at $\lambda = 1$, and $\epsilon^{SRS}(1) = \epsilon$ on it.

Two questions concerning the interpolation functions now appear to be relevant:

(1) How are the eigenvalues of $H(1)$ connected with those of $H(0)$ through the complex curves $\epsilon(\lambda)$, where ν distinguishes between different branches of $\epsilon(\lambda)$.

(2) What are the singular points of the chosen branches of $\epsilon(\lambda)$.

The answer to the first question determines the possible sums of perturbation expansions. The answer to the second question determines the convergence properties of the series. It seems to be impossible now to calculate interpolation functions exactly, even for very simple systems like H_2^+. Therefore, we shall try to answer the above questions studying an exactly soluble model possessing all essential features of the H_2^+ system.

III. AN EXACTLY SOLUBLE MODEL

In 1972 Schulman[17] considered a two-state model for which he was able to prove the convergence of the polarization expansion at small values of the internuclear distance R. This model consists in the perturbative expansion of the H_2^+ secular equation in the minimal $\{1s_A, 1s_B\}$ basis set, the Hamiltonian matrix being partitioned as $H_0 + \lambda V$, where H_0 and V are the matrices of the operators H_0 and V defined at the beginning of Sec. II. From our point of view this model has two essential drawbacks. Firstly, as plainly stated by Schulman, it is inadequate at large R, and secondly, it is trivially solved by any symmetry forcing perturbation procedure. To obtain a nontrivial model, valid at large R, we extended the minimal basis by the polarization functions $2p_A = \varphi(r - R_A)$ and $2p_B = -\varphi(r - R_B)$, where

$$\varphi(r) = \pi^{-1/2} z(1 + \tfrac{1}{2} r)e^{-r} \ . \quad (12)$$

We have assumed here that the vectors R_A and R_B, specifying the nuclear positions, lie on the z axis. It will be shown later that due to this particular choice of $\varphi(r)$ the model gives asymptotically 100% of the total energy and 98% of the exchange energy for the H_2^+ system. At small R this model is also quite adequate. At $R = 3$ bohr the energy of the $2p\sigma_u$ state is given with only 0.3% error.

The exact Schrödinger equation for H_2^+ is now replaced by the four-dimensional secular equation

$$(H_0 + V)c = (\epsilon_0 + \bar{\epsilon})Sc \ , \quad (13)$$

where the matrices H_0, V, and S are now calculated with $\{1s_A, 1s_B, 2p_A, 2p_B\}$ as the basis set. In complete analogy with the infinite-dimensional case, this equation can be solved using the Rayleigh–Schrödinger or symmetry forcing perturbation techniques. In the latter case the symmetry projector is defined as[5]

$$A = \frac{1}{2}\begin{pmatrix} 1 & -1 & 0 & 0 \\ -1 & 1 & 0 & 0 \\ 0 & 0 & 1 & -1 \\ 0 & 0 & -1 & 1 \end{pmatrix} \ . \quad (14)$$

Assuming A in the above form we force the ungerade symmetry of c, i.e., we consider the $2p\sigma_u$ state of H_2^+.

The interpolation function yielding the polarization expansion for $\bar{\epsilon}$ is an implicit function defined by $F(\bar{\epsilon}^{RS}, \lambda) = 0$, where

$$F(\omega, \lambda) = \det(H_0 - \epsilon_0 S + \lambda V - \omega S) . \tag{15}$$

The MSMA expansion for $\bar{\epsilon}$ is obtained by expanding the interpolation function $\bar{\epsilon}^{MSMA}(\lambda)$, defined implicitly by the system of equations

$$\bar{\epsilon}^{MSMA} = \lambda \frac{c_0^* V A c}{c_0^* S A c} , \tag{16}$$

$$c = c_0 + R_0 (\bar{\epsilon}^{MSMA} S - \lambda V) c , \tag{17}$$

where c_0 is the unperturbed vector satisfying $(H_0 - \epsilon_0 S) c_0 = 0$, i.e., $c_0^* = (1, 0, 0, 0)$, and R_0 is a matrix counterpart of the reduced resolvent, normalized so that $c_0^* S R_0 = 0$,[6]

$$R_0 = (1 - c_0 c_0^* S)(H_0 - \epsilon_0 S + c_0 c_0^*)^{-1} . \tag{18}$$

Eliminating c from (17) we find that $\bar{\epsilon}^{MSMA}(\lambda)$ is an implicit function defined by $G(\bar{\epsilon}^{MSMA}, \lambda) = 0$, where

$$G(\omega, \lambda) = c_0^* (\omega S - \lambda V) A [1 - R_0(\omega S - \lambda V)]^{-1} c_0 . \tag{19}$$

The interpolation function $\bar{\epsilon}^{SRS}(\lambda)$ of the symmetrized polarization function is defined explicitly as

$$\bar{\epsilon}^{SRS}(\lambda) = \lambda \frac{c_0^* V A c^{RS}(\lambda)}{c_0^* S A c^{RS}(\lambda)} , \tag{20}$$

where $c^{RS}(\lambda)$ is a solution of Eq. (13) in which V has been replaced by λV.

Since $F(\omega, \lambda)$ and the numerator of $G(\omega, \lambda)$ are fourth-order polynomials in ω with λ independent coefficients at ω^4, the functions $\bar{\epsilon}^{RS}(\lambda)$ and $\bar{\epsilon}^{MSMA}(\lambda)$ are four-valued algebraic functions having only branch point singularities. The SRS interpolation function $\bar{\epsilon}^{SRS}(\lambda)$ must have the same branch point singularities as $\bar{\epsilon}^{RS}(\lambda)$ plus some polar singularities due to the presence of the denominator in Eq. (20). After some algebraic manipulations with the rhs of Eq. (19), it is possible to show that $F(\omega, 1)$ has the same roots as $G(\omega, 1)$, i.e., $\bar{\epsilon}^{RS}(1) = \bar{\epsilon}^{MSMA}(1)$

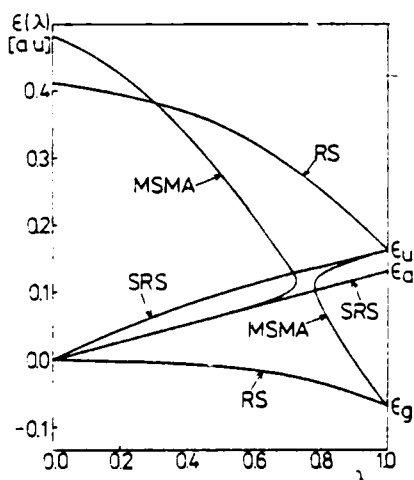FIG. 1. Schematic plot of the two lowest branches of $\epsilon^{RS}(\lambda)$, $\epsilon^{SRS}(\lambda)$, and $\epsilon^{MSMA}(\lambda)$ calculated at $R = 3.0$ bohr within the four-state model of Sec. III. The ungerade symmetry was forced in defining $\epsilon^{SRS}(\lambda)$ and $\epsilon^{MSMA}(\lambda)$. The separation between two branches of $\epsilon^{SRS}(\lambda)$ is highly exaggerated. ϵ_g and ϵ_u denote the interaction energies in the gerade and ungerade states, respectively, and ϵ_a is the "apparent interaction energy."

TABLE I. Branch points determining the convergence properties of the polarization, symmetrized polarization, and MSMA expansions in the case of the exactly soluble four-state model of H_2^+. The MSMA branch points correspond to the ungerade symmetry forcing.

R	λ_b^{RS}	λ_b^{MSMA}
3	$1.05157834 \pm 0.27924566i$	$0.70574669 \pm 0.02558853$
4	$1.01538451 \pm 0.12900230i$	$0.85643594 \pm 0.02067580$
6	$1.00096729 \pm 0.02537625i$	$0.97345544 \pm 0.00228434$
8	$1.00004189 \pm 0.00447076i$	$0.99545067 \pm 0.00017819$
10	$1.00000147 \pm 0.00074047i$	$0.99925786 \pm 0.00001358$
12.5	$1.00000002 \pm 0.00007446i$	$0.99992552 \pm 0.00000062$

for all four values of these functions. On the other hand, among the four values of $\bar{\epsilon}^{SRS}(1)$ only two are common with $\bar{\epsilon}^{RS}(1)$. This is due to the removable singularity appearing at $\lambda = 1$ on those Riemann sheets of $\bar{\epsilon}^{SRS}(\lambda)$ for which $c^{RS}(1)$ has gerade symmetry. On these Riemann sheets $\bar{\epsilon}^{SRS}(1)$ does not satisfy Eq. (13).

Since the matrices H_0, V, and S are known functions of R and the quartic equations can be solved via roots, the interpolation functions can in principle be expressed analytically in closed form. However, the resulting formulas would be enormously complicated and in practice it is much easier to calculate the roots of $F(\omega, \lambda)$ and $G(\omega, \lambda)$ numerically for interesting values of λ and R. Figure 1 shows the RS, SRS, and MSMA interpolation functions obtained in this way for $R = 3.0$ bohr. We present only the two lowest branches of these functions since only these branches of the exact interpolation functions can be reasonably well approximated by our model.

Finding branch points of $\bar{\epsilon}^{RS}(\lambda)$ and $\bar{\epsilon}^{MSMA}(\lambda)$ is more difficult since eliminating ω from the system of equations

$$F(\omega, \lambda) = 0 ,$$
$$\frac{\partial F}{\partial \omega}(\omega, \lambda) = 0 , \tag{21}$$

and similarly for $G(\omega, \lambda)$, leads to a twelfth-degree resultant polynomial,[18] the roots of which are numerically unstable at large R and, obviously, cannot be expressed in closed form. Nevertheless, using the double precision arithmetic of the DEC 20/40 computer we were able to find these roots numerically up to $R = 12.5$ bohr. The branch points calculated in such a way are shown in Table I. We list only those branch points which are directly related to the convergence properties of the perturbation expansions. These are the branch points which are closest to the origin and lie on the Riemann sheet of $\bar{\epsilon}^{RS}(\lambda)$ or $\bar{\epsilon}^{MSMA}(\lambda)$ for which $\bar{\epsilon}(0) = 0$.

To complete the description of our model we report the large R asymptotic expansions for two lowest energies and for the relevant branch points λ_b of $\bar{\epsilon}^{RS}(\lambda)$ and $\bar{\epsilon}^{MSMA}(\lambda)$:

$$\bar{\epsilon} = -\tfrac{9}{4} R^{-4} - 24 R^{-7} - \tfrac{147}{32} R^{-8} + O(R^{-10})$$
$$\pm R e^{-R} [\tfrac{101}{140} + \tfrac{12}{35} R^{-1} - \tfrac{141}{280} R^{-2} + O(R^{-3})] , \tag{22}$$

$$\operatorname{Re} \lambda_b^{RS} = 1 + R^3 e^{-2R} [\tfrac{1718683}{5536800} + O(R^{-1})] . \tag{23}$$
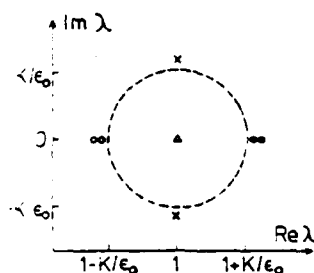
FIG. 2. The location of the branch points determining the convergence properties of the RS, SRS, and MSMA expansions at the internuclear distance $R = 12.5$ bohr. The crosses denote λ_b^{RS}, the empty dots λ_b^{MSMA}, corresponding to the ungerade symmetry forcing, and the black dots λ_b^{MSMA} corresponding to the gerade symmetry forcing. The empty triangle denotes the physical value of the expansion parameter $\lambda = 1$. The dashed circle has a radius K/ϵ_0, where K is the exchange energy, and has been drawn around the point $\lambda = 1$.

$$\text{Im}\lambda_b^{RS} = \pm Re^{-R}\left[\tfrac{101}{70} + \tfrac{149}{70}R^{-1} - \tfrac{243}{140}R^{-2} + O(R^{-3})\right], \quad (24)$$

$$\lambda_b^{MSMA} = 1 - Re^{-R}\left[\tfrac{101}{70} + \tfrac{149}{70}R^{-1} - \tfrac{243}{140}R^{-2} + \tfrac{1613}{240}R^{-3}\right.$$

$$\left. = \left(\tfrac{101}{140}R^{-2} - \tfrac{2371}{140}R^{-3}\right) + O(R^{-4})\right]. \quad (25)$$

The MSMA branch points given above correspond to the interpolation function obtained by forcing the ungerade symmetry of the wave function. The branch points corresponding to gerade symmetry forcing can be obtained from Eq. (25) by inverting the sign of the exponential part. The asymptotic location of the RS and MSMA branch points is shown in Fig. 2.

The formulas (22)–(25) have been obtained perturbatively by setting $e^{-R} = \mu$ and expanding F, G, $\bar{\epsilon}$, λ_b, and ω_b as power series in μ. Coefficients in these series are regular or have at most polar singularities at $R = \infty$. After expanding them in powers of R^{-1} we obtain double power series (in μ and R^{-1}) for $\bar{\epsilon}$, λ_b^{RS}, and λ_b^{MSMA}, the leading terms of which are just presented in Eqs. (22)–(25). Since the analytical dependence of the functions F and G upon ω, λ, R, and μ is extremely complicated, the formulas (22)–(25) have to be derived automatically by a computer. In fact all derivations leading to Eqs. (22)–(25), including integrations in evaluating matrix elements, matrix operations in Eqs. (15)–(19), and differentiation in Eq. (21), were performed automatically by the REDUCE program for algebraic manipulations and took about 1 h of CPU time of the DEC 20/40 computer.

To appraise the accuracy of our model, Eq. (22) may be compared with the exact asymptotic expansion for the interaction energy[19]:

$$\epsilon = -\tfrac{8}{4}R^{-4} - \tfrac{15}{2}R^{-6} - \tfrac{213}{4}R^{-7} + O(R^{-8})$$

$$\pm Re^{-R}\left(\tfrac{2}{e} + \tfrac{1}{e}R^{-1} - \tfrac{25}{4e}R^{-2} + O(R^{-3})\right). \quad (26)$$

It is seen that the leading R^{-4} term in the asymptotic expansion of the interaction energy is given exactly in our model and the first term in the asymptotic expansion of the exchange splitting is in error by less than 2%. The adequacy of our four-state model is also confirmed

by the fact that the leading term in our asymptotic expansion for $\text{Im}\lambda_b^{RS}$ represents 98.1% of the exact value obtained by Whitton and Byers Brown.[12]

We have also calculated individual corrections in the RS, SRS, and MSMA perturbation expansions for $\bar{\epsilon}$. Since the convergence pattern we found was completely analogous to that obtained in high accuracy calculations of Ref. 5, these corrections are not reported here.

Now let us summarize the main implications of the exact solution presented above. First, we note that for all distances considered, and asymptotically at large R, the convergence radius of the polarization expansion $\rho^{RS} = |\lambda_b^{RS}|$ is greater than unity, hence this expansion is convergent for our model. It is interesting, however, that at large R we have $\rho^{RS} = \text{Re}\lambda_b^{RS} + O(R^2 e^{-2R})$, i.e., the convergence radius is determined by the real part of λ_b^{RS}. Thus, the estimation of $\text{Im}\lambda_b^{RS}$ alone[12] is not sufficient to prove the convergence of the polarization expansion.[20] Since at large R the convergence radius is almost equal to unity, the polarization series must converge extremely slowly, which is really observed in numerical calculations.[5] Moreover, as can be seen in Fig. 2, the physical value of the expansion parameter $\lambda = 1$ lies at large R almost exactly on the line joining the branch points. According to Nuttall's results,[21] in such a situation the Padé approximants cannot be expected to improve the convergence of a perturbation series.

Now let us consider the symmetrized polarization expansion. Since the poles of $\bar{\epsilon}^{SRS}(\lambda)$ are far outside the unit circle and the branch points of $\bar{\epsilon}^{SRS}(\lambda)$ and $\bar{\epsilon}^{RS}(\lambda)$ are the same, we have $\rho^{SRS} = \rho^{RS}$, i.e., the SRS expansion is convergent, independently of the symmetry forced by A. However, cf. Fig. 1, if A forces the ungerade symmetry, the symmetrized polarization converges to some unphysical, "apparent interaction energy" resulting from removing the singularity at $\lambda = 1$. The actual value of the interaction energy lies on the second branch of $\bar{\epsilon}^{SRS}(\lambda)$ resulting from that branch of $c(\lambda)$ which has ungerade symmetry at $\lambda = 1$. Although this second branch also passes through zero, its power series at $\lambda = 0$ can be obtained only from an excited-state perturbation treatment. As will be shown in the next section a proper analytical continuation procedure enables us to calculate the true value of the interaction energy from the perturbation series converging to a spurious one.

The exact solution of our model shows that the "apparent" and true interaction energies are very close, even at small R. At large R, as a consequence of Ahlrichs' theory[14] both these energies must have the same R^{-1} expansion. What is more, the difference of these energies appears to vanish faster than the exchange energy itself. It must be noted, however, that between $\lambda = 0$ and $\lambda = 1$ the two lowest branches of $\bar{\epsilon}^{SRS}(\lambda)$ are generally very well separated and their difference does not vanish at large R.

The most striking feature of the MSMA interpolation function is the presence of real branch points in the vicinity of $\lambda = 1$. If A forces ungerade symmetry, these branch points lie to the left of the point $\lambda = 1$ and produce

a characteristic gap in the real values of $\bar{\epsilon}^{MSMA}(\lambda)$. Obviously, between the branch points the function $\bar{\epsilon}^{MSMA}(\lambda)$ takes on complex values, which are not shown in Fig. 1. The MSMA series cannot be convergent in this case and, indeed, it diverges quickly to infinity at small R. At large R, the branch points lie very close to $\lambda = 1$ and this divergence is extremely slow. Note that the point $\lambda = 1$ always lies outside the line joining the branch points, see Fig. 2. One can expect, then, that the Padé approximants to $\bar{\epsilon}^{MSMA}(\lambda)$ will converge at $\lambda = 1$.[21] This is really observed in practical calculations.[7] One may wonder how a Padé approximant, which is a single-valued function, selects the right value of the multivalued function $\bar{\epsilon}^{MSMA}(\lambda)$. In fact, the Padé approximants converge to a single-valued function obtained from $\bar{\epsilon}^{MSMA}(\lambda)$ by introducing a cut between the branch points.[22] Along the cut this single-valued function is discontinuous and the Padé approximants are divergent.[22]

In Ref. 7 it was noted that the divergent MSMA series can be summed using the geometric approximation or, in other words, a sequence of $[N/1]$ Padé approximants. We see now that this can be done only approximately and the conjecture[7] that $\epsilon^{MSMA}(\lambda)$ has a simple pole close to $\lambda = 1$ is not confirmed. The high accuracy of the geometric approximation is simple to understand in this case since a pair of closely lying branch points, when viewed from a distance, looks very much like a simple pole. This fact is well illustrated by the formula

$$\sqrt{(a-\lambda)^2 \pm \eta^2} = (a-\lambda) \pm \tfrac{1}{2}\eta^2 \frac{1}{a-\lambda} - \tfrac{1}{8}\eta^4 \frac{1}{(a-\lambda)^3} + \cdots ,$$

(27)

where the branch points are at $a \pm \eta$ or $a \pm i\eta$ and η is a small parameter.

IV. ANALYTIC CONTINUATION OF INTERPOLATION FUNCTIONS

The exact solution of our four-state model presented in the preceding section shows that the interpolation functions connect eigenvalues of $H(0)$ and $H(1)$ in a quite nontrivial way. Moreover the singularities of these functions lie in the immediate neighborhood of the physical value of the expansion parameter, affecting unfavorably the convergence of the perturbation expansions. In practice what we can calculate for real systems are only some low-order perturbation corrections, i.e., some low-order derivatives of $\epsilon(\lambda)$ at $\lambda = 0$. In this section we shall show that this information is sufficient for a practical reconstruction of $\epsilon(\lambda)$ at $\lambda = 1$. Such a reconstruction can be carried out only if we have qualitative information about singularities of $\epsilon(\lambda)$. Therefore, we assume, in full accord with the exact solution for the four-state model, that within the unit circle and its closest vicinity the interpolation functions may have only first-order branch points. The power series for $\epsilon(\lambda)$ can then be continued analytically in this region using the algebraic function of the form

$$\{N, M\}(\lambda) = p_N(\lambda) + [p_N^2(\lambda) + q_M(\lambda)]^{1/2} ,$$

(28)

where $p_N(\lambda) = p_0 + p_1\lambda + \cdots + p_N\lambda^N$ and $q_M(\lambda) = q_0 + q_1\lambda + \cdots + q_M\lambda^M$. The polynomials $p_N(\lambda)$ and $q_M(\lambda)$ can be uniquely determined, requiring that the derivatives of

$\{N, M\}(\lambda)$ taken at $\lambda = 0$ are the same through the $(N+M+1)$th order as the known derivatives of $\epsilon(\lambda)$. This condition and the identity $\{N, M\}^2(\lambda) = 2\{N, M\}(\lambda)p_N(\lambda) + q_M(\lambda)$ immediately gives the following system of linear equations for $p_0, p_1, \ldots, p_N$ and $q_0, q_1, \ldots, q_M$:

$$2\sum_{i=0}^{\min(n, M)} p_i \epsilon_{n-i} - q_n = \sum_{i=0}^{n} \epsilon_i \epsilon_{n-i} \quad \text{for } 0 \le n \le M ,$$

$$2\sum_{i=0}^{N} p_i \epsilon_{n-i} = \sum_{i=0}^{n} \epsilon_i \epsilon_{n-i} \quad \text{for } M+1 \le n \le N+M+1 .$$

(29)

For simplicity we assume here that $M \ge N$. Since $\{N, M\}(\lambda)$ is a double-valued function we obtain two values of $\{N, M\}(1)$ from one series of perturbation corrections ϵ_n. We denote the larger value by $\{N, M\}_+$ and the smaller one by $\{N, M\}_-$. For the RS and MSMA theories both values are expected to correspond to the eigenvalues of $H(1)$, whereas in the case of the SRS method one of them should correspond to a spurious interaction energy.

The analytic continuation procedure described above is a particular case of a generalization of the Padé approximation proposed by Shafer[8] and referred to as "quadratic Padé approximation." The Shafer approximants $[K, L, M](\lambda)$ are defined as roots of the general quadratic equation with polynomial coefficients:

$$p_K(\lambda)[K, L, M]^2(\lambda) + q_L(\lambda)[K, L, M](\lambda) + r_M(\lambda) = 0 ,$$

(30)

the polynomials $p_K(\lambda)$, $q_L(\lambda)$, and $r_M(\lambda)$ being chosen such that $\epsilon(\lambda) - [K, L, M](\lambda) = O(\lambda^{K+L+M+3})$. It is easy to see that $\{N, M\}(\lambda) = [0, N, M](\lambda)$. Besides first-order branch points the Shafer approximants may have poles and inverse square root singularities. These singularities are not expected to be important in our case, except possibly for the SRS method.

To test the effectiveness of the $\{N, M\}$ approximation, we calculate the $\{N, N+1\}$ approximants for the RS, SRS, and MSMA series using highly accurate values of the perturbation corrections obtained recently for the interaction of a hydrogen atom and a proton.[5,8] In Tables II–VII the accuracy of this procedure is compared with the accuracy of corresponding sums of perturbation expansions, and in the case of the MSMA method, with the accuracy of the rational Padé approximation. The tabulated numbers show the percent error resulting from the approximate procedure indicated in the first row:

$$\text{percent error} = 100(\epsilon_{approximate} - \epsilon_{accurate})/\epsilon_{accurate} , \quad (31)$$

where by $\epsilon_{accurate}$ we mean the variational energy obtained with the basis set used to calculate perturbation corrections. This variational energy is practically equal to the exact energy of Table VI of Ref. 5.

The branch points reported in Tables II–VII have been obtained by solving equations $p_N^2(\lambda_b) + q_{N+1}(\lambda_b) = 0$ and estimating the limit $N \to \infty$. The effectiveness of this procedure was checked previously for the four-state model where the branch points could be calculated directly from Eq. (21).

It is worthwhile to note that if we knew the coefficients of the power series expansion of $\epsilon(\lambda)$ on the second

Riemann sheet, they could be used in calculating the poly nomials $p_N(\lambda)$ and $q_M(\lambda)$. More specifically, $p_N(\lambda)$ and $q_M(\lambda)$ could then be found directly by performing the power series expansion of

$$p(\lambda) = \tfrac{1}{2}\left[{}^1\epsilon(\lambda) + {}^2\epsilon(\lambda)\right] \tag{32}$$

and

$$q(\lambda) = -{}^1\epsilon(\lambda)\,{}^2\epsilon(\lambda) , \tag{33}$$

respectively, where ${}^1\epsilon(\lambda)$ and ${}^2\epsilon(\lambda)$ represent the two branches of $\epsilon(\lambda)$ which branch in the neighborhood of $\lambda = 1$. Such a method of calculating $p_N(\lambda)$ and $q_M(\lambda)$ has been recently suggested by Whitton.[18] In our opinion the above method is not particularly useful in calculating interaction energy since the method requires an excited state perturbation treatment[23] for studying ground state interactions.

V. DISCUSSION AND CONCLUSIONS

The results presented in Tables II and III clearly show that, contrary to a generally accepted belief, the standard RS polarization series can provide us with the information about the accurate value of the exchange part of the interaction energy. Moreover, this exchange part of the interaction energy can be calculated not only for the state to which the series eventually converges, but also for the other state having the same $1/R$ asymptotic expansion of the interaction energy. It should be stressed here, however, that to extract the exchange energies from the polarization series, full knowledge of the charge-overlap effects[24] is necessary. This means that the perturbation corrections must be calculated accurately without using the multipole expansion.

The usual rational Padé approximants are not reported

TABLE II. Convergence of the polarization series and the $\{N, N+1\}$ approximants thereto for the interaction of a hydrogen atom and a proton at the distance of $R = 3.0$ bohr. The listed values show the percent error as defined in Eq. (31). The error of $\epsilon_1 + \cdots + \epsilon_{2N+2}$ and $\{N, N+1\}_-$ is calculated relative to the energy of the $1s\sigma_g$ state and the error of $\{N, N+1\}_+$ relative to the energy of the $2p\sigma_u$ state. For $N = 1$ and $N = 2$ the approximants do not exist since $p_N^2(1) + q_{N+1}(1)$ is negative. The empty places mean that the error is smaller than 0.00001%.

N	$\epsilon_1 + \cdots + \epsilon_{2N+2}$ [a]	$\{N, N+1\}_-$	$\{N, N+1\}_+$	K [b]
3	−12.035	0.98247	36.75500	23.50960
4	−4.339	−0.37492	14.30340	5.36850
5	0.407	−0.06958	2.62515	1.62738
6	2.180	−0.00418	−0.84357	−0.53277
7	2.398	−0.00254	−0.59975	−0.37862
8	1.848	−0.00080	−0.09743	−0.06165
9	1.070	0.00004	−0.10517	−0.06621
10	0.375	0.00005	−0.07919	−0.04985
12	−0.333		−0.00797	−0.00502
14	−0.304		−0.00168	−0.00106
16	−0.065		−0.00004	−0.00003
18	0.067			

[a] The convergence radius of the series equals 1.09300776 and is determined by the branch points $\lambda_b^{RS} = 1.05616161 \pm 0.28140474i$.
[b] This column shows the percent error resulting when the exchange energy $K = (\epsilon_f - \epsilon_u)/2$ is approximated by $(\{N, N+1\}_- - \{N, N+1\}_+)/2$.

TABLE III. Convergence of the polarization series and the $\{N, N+1\}$ approximants thereto for the interaction of a hydrogen atom and a proton at the distance of $R = 12.5$ bohr. The listed values show the percent error as defined in Eq. (31). The error of $\epsilon_1 + \cdots + \epsilon_{2N+2}$ and $\{N, N+1\}_-$ is calculated relative to the energy of the $1s\sigma_g$ state and the error of $\{N, N+1\}_+$ relative to the energy of the $2p\sigma_u$ state. The dashes mean that the approximants do not exist since $p_N^2(1) + q_{N+1}(1)$ is negative. The $\{1, 2\}$ and $\{2, 3\}$ approximants are very poor and are not shown.

N	$\epsilon_1 + \cdots + \epsilon_{2N+2}$ [a]	$\{N, N+1\}_-$	$\{N, N+1\}_+$	K [b]
3	−26.706 [c]	−26.0959489	−2.4254808	−47.3333651
4−8	−26.70	—	—	—
9	−26.694	0.1435192	−0.3140393	0.5420119
10	−26.691	−0.0020539	−0.0004052	−0.0034696
12	−26.687	−0.0024142	−0.0052102	0.0000209
14	−26.683	−0.0004474	−0.0009656	0.0000039
16	−26.679	0.0000006	0.0000020	−0.0000006
18	−26.675	−0.0000001	0.0000002	−0.0000004

[a] The convergence radius of the series equals 1.00000003 and is determined by the branch points $\lambda_b^{RS} = 1.00000003 \pm 0.00007590i$.
[b] See footnote b of Table II.
[c] The exchange energy represents 26.725% of the interaction energy in the gerade state.

in Tables II and III since they are not able to improve the convergence of the polarization series. For small R the improvement is marginal and for large R none. This is due to the fact that at large R the physical value of the expansion parameter $\lambda = 1$ lies almost exactly on the cut chosen by the Padé approximants to make $\epsilon^{RS}(\lambda)$ single valued, cf. Fig. 2. Along this cut the Padé approximants cluster their poles and are not expected to converge.[22] In fact, one of these poles is located exactly in the middle of the cut very close to $\lambda = 1$. This makes the Padé approximants numerically unstable.

The results obtained for the symmetrized polarization series are shown in Tables IV and V. Unfortunately, for the internuclear distance 12.5 bohr we were not able to

TABLE IV. Convergence of the symmetrized polarization series and the $\{N, N+1\}$ approximants thereto for the interaction of a hydrogen atom and a proton at the distance 3.0 bohr. The ungerade symmetry is forced. The listed values show the percent error relative to the accurate energy of the $2p\sigma_u$ state, see Eq. (31).

N	$\epsilon_1 + \cdots + \epsilon_{2N+2}$ [a]	$\{N, N+1\}_+$	$\{N, N+1\}_-$
1	0.51196	0.06388	0.28121
2	0.62205	8.27935	0.69223
3	0.68335	0.74671	0.03984
4	0.72382	0.67561	0.26414
5	0.74887	0.75109	−0.74943
6	0.76233	1.08485	0.73836
7	0.76778	0.75872	0.06621
8	0.76839	0.76036	0.07705
9	0.76659	0.76058	−0.00569
10	0.76407	0.76057	0.00925
12	0.76028	0.76057	0.00021
14	0.75935	0.76057	0.00075
16	0.75996	0.76057	0.00010
18	0.76063	0.76057	0.00001

[a] The convergence radius of the series equals 1.09300776 and is determined by the branch points $\lambda_b^{SRS} = 1.05616161 \pm 0.28140474i$.

TABLE V. Convergence of the symmetrized polarization series and of the $[N,N,N]$ Shafer approximants thereto for the interaction of a hydrogen atom and a proton of the distance of 12.5 bohr. The ungerade symmetry is forced. The listed values show the percent error relative to the accurate energy of the $2p\sigma_u$ state, see Eq. (31). The empty places indicate that the error is smaller than 0.000001%. The approximants $[1,1,1]$ and $[2,2,2]$ are very poor and are not shown.

N	$\epsilon_1 + \cdots + \epsilon_{3N+2}$ [a]	$[N,N,N]_+$	$[N,N,N]_-$
3	−0.01571	−386.86818	−0.016457
4	−0.01638	−1223.36532	−0.016453
5	−0.01645	−0.02580	0.146426
6	−0.01645	−0.04186	0.020906
7	−0.01646	−0.03270	−0.000175
8	−0.01646	−0.03291	0.000036
9	−0.01646	−0.03287	−0.000004
10	−0.01646	−0.03287	
11	−0.01647	−0.03287	
12	−0.01647	−0.03287	

[a] The convergence radius of the series equals 1.00000003 and is determined by the branch points $\lambda_5^{SRS} = 1.00000003 \pm 0.00007590i$.

attain a good convergence with the $\{N, M\}$ approximants. For this reason we calculated the full Shafer $[N, N, N]$ approximants. These turned out to converge very well and are shown in Table V instead of simpler $\{N, N+1\}$ approximants. The success of the Shafer approximants might suggest that the poor convergence of $\{N, N+1\}$ is caused by some polar singularities of $\epsilon^{SRS}(\lambda)$. Unfortunately, in the case of the four-state model of H_2^+ we did not find such singularities in the vicinity of $\lambda = 1$.

The results presented in Tables IV and V convincingly show that the SRS series converges to the "apparent interaction energy" resulting from the removable singularity at $\lambda = 1$. In spite of that, the actual value of the interaction energy, corresponding to a different Riemann sheet of $\epsilon^{SRS}(\lambda)$, can be very accurately calculated by continuing the SRS series analytically using a proper algebraic function.

It is worthwhile to note that at large R the symmetrized polarization series converges to the "apparent interaction energy" in a very nonuniform way. As can be seen in Table V the series converges quickly only to the arithmetic mean of the true and "apparent" interaction energies. Afterwards, the convergence becomes extremely slow and the remaining part of the "apparent interaction energy" is practically not recovered. This convergence pattern is quite similar to that observed in the RS theory. Particularly, the residual exchange energy in the SRS theory, noted in Ref. 5, is an analog of the exchange energy in the RS theory and can be rigorously defined as one-half of the difference between the true and "apparent" interaction energies.

Note that the peculiar convergence properties of the RS and SRS expansions are due to the fact that the physical value of the expansion parameter $\lambda = 1$ lies almost exactly between the branch points. This can be seen in the following way. Since at large R the relevant branch points of $\epsilon(\lambda)$ [$\epsilon(\lambda)$ stands here for $\epsilon^{RS}(\lambda)$ and $\epsilon^{SRS}(\lambda)$] behave as $1 \pm i\eta$, where $\eta > 0$ decreases exponentially with

increasing R, the sum of series (6) can be represented as

$$\sum_{n=1}^{\infty} \epsilon_n \lambda^n = f(\lambda) + g(\lambda)\sqrt{(1-\lambda)^2 + \eta^2} \; . \tag{34}$$

The functions $f(\lambda)$ and $g(\lambda)$ are assumed to be analytic within a circle of the radius much greater than ρ^{RS} and can be expanded as power series converging quickly for $\lambda = 1$. Assuming that $g(1) < 0$ the two values of $\epsilon(1)$ can now be written as $\epsilon(1) = f(1) \pm \eta g(1)$, where the minus sign corresponds to the sum of the series in (34).

Applying Eq. (27) and expanding the rhs of Eq. (34) as a power series in λ we easily find that

$$\epsilon_n = f_n + g_n - g_{n-1} + \tfrac{1}{2}\eta^2 \sum_{k=0}^{n} g_k + O(\eta^4) \; , \tag{35}$$

where f_n and g_n are the coefficients in the power series expansions of $f(\lambda)$ and $g(\lambda)$, respectively. Formula (35) shows that both the polarization and symmetrized polarization expansion can be thought of as a sum of two series. The first, summing only $f_n + g_n - g_{n-1}$, converges quickly to $f(1)$, i.e., to the arithmetic mean of the two lowest values of $\epsilon(1)$. The second one, converging to the exchange energy $K = \eta g(1)$ is built up of terms which for large n and R behave as $\eta^2 g(1)/2$, i.e., which are practically constant. The number of such terms necessary to recover K would have to be greater than $2\eta^{-1}$, i.e., would have to increase exponentially with R.

If n is large enough that the series $f_n + g_n - g_{n-1}$ has already converged to its limit, then $\epsilon_n = \eta^2 g(1)/2$, and, consequently $\epsilon_n = \eta K/2$. We found numerically that at $R = 12.5$ bohr, $\epsilon_n = -0.132408 \times 10^{-8}$ hartree for $22 \le n \le 38$ (see also Ref. 6). Using the exact value of $K = -0.34891 \times 10^{-4}$ hartree we find that $\eta = 0.75898 \times 10^{-4}$, which agrees very well with the value given in Table III. It may also be shown that $g(1) = -2 + O(R^{-1})$, independently of the dimension of the model used. Therefore, at large R we have $\epsilon_n = -K^2$. This is a remarkable result. It shows that the exchange energy, and consequently the frequency of the resonance tunneling between two Coulomb wells, can be estimated if we know the large n behavior of the nth-order energy in the polarization series.

As we have already mentioned, the usual Padé approximants are not effective in coping with the convergence defects of the polarization expansion. The contrary is a case in the MSMA theory, where the point $\lambda = 1$ lies well outside the line joining the branch points, cf. Fig. 2, and the divergence of the series is very effectively circumvented by the usual Padé approximation, see Tables VI and VII. It may be checked that the $[N, N-1]$ approximants converge to that value of $\epsilon^{MSMA}(1)$ which can be reached from $\lambda = 0$ without passing between branch points, i.e., without crossing the cut that the Padé approximation introduces to make $\epsilon^{MSMA}(\lambda)$ single valued. Since the $\{N, N+1\}$ approximants are double-valued functions they can converge to both values of $\epsilon(1)$. It turns out, however, that, whereas the convergence to the energy of the ungerade state is excellent, the convergence to the energy of the gerade state is very poor and the corresponding approximants are not shown in the

les. This asymmetry is perhaps not very surprising since in the very definition of $\epsilon^{MSMA}(\lambda)$ the ungerade symmetry forcing was employed.

At large R the divergence of the MSMA expansion is extremely slow and very accurate values of the interaction energy can be obtained in a low-order treatment. Particularly, at $R = 12.5$ bohr the interaction energy can be calculated in such a way with the error of only -0.00409%. This can easily be understand when we know the relevant branch points of $\epsilon^{MSMA}(\lambda)$. Since at large R these branch points are $1 - \eta \pm \delta$, where η is the same as in the RS theory and $\delta \ll \eta$, the sum of the MSMA series can be represented as

$$\sum_{n=1}^{\infty} \epsilon_n^{MSMA} \lambda^n = s(\lambda) + t(\lambda) \sqrt{(1-\eta-\lambda)^2 - \delta^2} \ , \qquad (36)$$

here $|\lambda| < \rho^{MSMA} = 1 - \eta - \delta$ and we assume that the singularities of $s(\lambda)$ and $t(\lambda)$ are far outside the unit circle. Continuing the rhs of Eqs. (36) analytically to the point $\lambda = 1$, we find that the interaction energy in the ungerade state can now be written as

$$\epsilon = s(1) - t(1) \sqrt{\eta^2 - \delta^2} \cong s(1) - t(1) \eta + \frac{\delta^2}{2\eta} t(1) \ . \qquad (37)$$

Note, that we had to take a minus sign for the square root in Eq. (36) because $t(\lambda)$ is assumed to be negative for $0 \leq \lambda \leq 1$. Since δ is very small we can employ Eq. (27) and write

TABLE VI. Convergence of the MSMA series and of the Padé and $\{N,N+1\}$ approximants thereto for the interaction of a hydrogen atom and a proton at the distance 3.0 bohr. The ungerade symmetry is forced. The listed values show the percent error relative to the accurate energy of the $2p\sigma_u$ state, see Eq. (31). The dashes mean that the approximants do not exist since $p_N^2(1) + q_{N+1}(1)$ is negative.

N	$\epsilon_1 + \cdots + \epsilon_{2N+2}$ [a]	$[N,N+1]$ [b]	$\{N,N+1\}$ [c]
1	0.40	0.2657364	0.2328721
2	0.73	−1.7685817	—
3	1.23	0.1848294	—
4	2.07	0.0032578	0.0058634
5	3.48	0.0027985	0.0000389
6	5.86	0.0004636	−0.0000056
7	9.37	0.0000085	−0.0000187
8	16.61	0.0000073	0.0000004
9	27.98	−0.0000020	0.0000001
10	47.13	0.0000006	

[a] The convergence radius of the series equals 0.75833870 and is determined by the smaller of the branch points λ_b^{MSMA} = 0.77154393 ± 0.01320523.

[b] The $[N,M](\lambda)$ Padé approximant to $\epsilon_0 + \epsilon(\lambda)$ is defined as a quotient of two polynomials $p_N(\lambda)/q_M(\lambda)$ chosen such that $[N,M](\lambda) - \epsilon_0 - \epsilon(\lambda) = O(\lambda^{N+M+1})$. The listed values of $[N,N+1]$ are slightly different from those published in Ref. 7. The reason for this is that in Ref. 7 a different value for ϵ_0 was assumed and $[N,N+1] - \epsilon_0$ is not invariant under the choice of

[c] For large N the energies of the $1s\sigma_g$ and $2p\sigma_u$ states are approximated by the $\{N,N+1\}_-$ and $\{N,N+1\}_+$, respectively. When N is small, however, $\{N,N+1\}_-$ may jump to the upper branch of $\epsilon^{MSMA}(\lambda)$ and $\{N,N+1\}_-$ may be meaningless. The numbers listed for $N = 1$ and $N = 4$ are just $\{N,N+1\}_-$ approximants.

TABLE VII. Convergence of the MSMA series and of the Padé and $\{N,N+1\}$ approximants thereto for the interaction of a hydrogen atom and a proton at the distance 12.5 bohr. The ungerade symmetry is forced. The listed values show the percent error relative to the exact energy of the $2p\sigma_u$ state, see Eq. (31).

N	$\epsilon_1 + \cdots + \epsilon_{2N+2}$ [a]	$[N,N+1]$ [b]	$\{N,N+1\}$ [c]
1	0.187200	0.3214601	0.1854056
2	0.033580	−0.3032929	0.0081292
3	0.003557	−0.0033884	−0.0036580
4	−0.002485	−0.0041473	−0.0040344
5	−0.003747	−0.0040897	−0.0040902
6	−0.004016	−0.0040884	−0.0040923
7	−0.004074	−0.0042096	−0.0037224
8	−0.004088	−0.0017780	−0.0110923
9	−0.004091	−0.0003365	0.0000047
10	−0.004092	−0.0000031	−0.0000002

[a] The convergence radius of the series equals 0.99992316 and is determined by the smaller of the branch points λ_b^{MSMA} = 0.9999240914 ± 0.0000009055.

[b] See footnote b to Table VI.

[c] For large N the energies of the $1s\sigma_g$ and $2p\sigma_u$ states are approximated by $\{N,N+1\}_-$ and $\{N,N+1\}_+$, respectively. This is the case here only for $N \geq 12$. When N is smaller than 12, $\{N,N+1\}_-$ jumps to the upper branch of $\epsilon^{MSMA}(\lambda)$ and $\{N,N+1\}_+$ becomes meaningless. As a matter of fact, all numbers listed here are $\{N,N+1\}_-$ approximants, except those calculated for $N = 3$ and $N = 4$.

$$\sum_{n=1}^{\infty} \epsilon_n^{MSMA} \lambda^n = s(\lambda) + t(\lambda)(1 - \eta - \lambda) - \frac{1}{2} \delta^2 \frac{t(\lambda)}{1-\eta-\lambda}$$
$$- \frac{1}{8} \delta^4 \frac{t(\lambda)}{(1-\eta-\lambda)^3} + \cdots \ , \qquad (38)$$

where we have chosen the plus sign for the square root in Eq. (27) to stay at $\lambda = 0$ on the proper Riemann sheet of $\epsilon^{MSMA}(\lambda)$. Expanding the rhs of Eq. (38) about $\lambda = 0$ we get

$$\epsilon_n^{MSMA} = s_n + t_n - t_{n-1} - \eta t_n - \frac{1}{2} \delta^2 \sum_{k=0}^{n} \frac{t_k}{(1-\eta)^{n-k+1}} + O(\delta^4) \ , \qquad (39)$$

where s_n and t_n are the coefficients in the power series expansion of $s(\lambda)$ and $t(\lambda)$, respectively. We now see that the MSMA expansion is a sum of two series. The first, summing $s_n + t_n - t_{n-1} - \eta t_n$, converges quickly to $s(1) - \eta t(1)$ and the second, consisting of almost constant terms of the order δ^2, diverges very slowly to infinity. Comparing this with Eq. (37), we see that the sum of the first series differs from the exact energy by $\delta^2 t(1)/(2\eta)$. Thus, the fraction of the interaction energy not recovered is $-\delta^2 K/(2\epsilon\eta^2)$, where K is the exchange energy $K \cong \eta t(1)$. Using the values of η and δ from the footnote of Table VII we find that this fraction is -0.00408%, in very good agreement with the numerically observed values.

In view of expression (36)'s success in explaining the convergence properties of perturbation expansions, one may wonder why this expression was not used in the numerical analytic continuation instead of an apparently more complicated formula (28). The reason for this is that the system of algebraic equations determining s_n,

t_n, η, and δ is highly nonlinear and cannot be solved in an easy way.

The above discussion plainly shows how important a precise information about positions of singularities of the interpolation functions is for an understanding of the convergence properties of a perturbation theory. The large R convergence problems of all perturbation expansions considered in this paper are due to the presence of branch points in the closest vicinity of the physical value of the expansion parameter. The specific convergence pattern, however, depends critically on the orientation of the branch points relative to the point $\lambda = 1$. On the other hand, our results clearly demonstrate how useful any qualitative information about singularities of the interpolation functions may be. Having such information we can apply a proper analytic continuation technique and thus effectively cope with the divergence or pathologically slow convergence of perturbation expansions.

ACKNOWLEDGMENTS

[1] D. M. Chipman, J. D. Bowman, and J. O. Hirschfelder, J. Chem. Phys. 59, 2838 (1973).
[2] K. Szalewicz and B. Jeziorski, Mol. Phys. 38, 191 (1979).
[3] W. H. Adams, Chem. Phys. Lett. 68, 511 (1979).
[4] B. Jeziorski and W. Kołos, Int. J. Quant. Chem. 12, Suppl. 1, 91 (1977).
[5] B. Jeziorski, K. Szalewicz, and G. Chałasiński, Int. J. Quant. Chem. 14, 271 (1978).
[6] G. Chałasiński, B. Jeziorski, and K. Szalewicz, Int. J. Quant. Chem. 11, 247 (1977).
[7] B. Jeziorski, K. Szalewicz, and M. Jaszuński, Chem. Phys. Lett. 61, 391 (1979).
[8] R. E. Shafer, S.I.A.M. J. Numer. Anal. 11, 447 (1974).
[9] T. Kato, Perturbation Theory for Linear Operators (Springer-Verlag, Berlin, 1966).
[10] J. O. Hirschfelder, W. Byers Brown, and S. T. Epstein, Adv. Quant. Chem. 1, 256 (1964).
[11] P. R. Certain and W. Byers Brown, Int. J. Quant. Chem. 6, 131 (1972); R. Ahlrichs and P. Claverie, Int. J. Quant. Chem. 6, 1001 (1972).
[12] W. N. Whitton and W. Byers Brown, Int. J. Quant. Chem. 10, 71 (1976).
[13] P. Claverie, Int. J. Quant. Chem. 5, 273 (1971).
[14] R. Ahlrichs, Theor. Chem. Acta (Berlin) 41, 7 (1976).
[15] E. Brezin and J. Zinn-Justin, J. Phys. (Paris) 40, L-511 (1979); J. Morgan III and B. Simon, Int. J. Quant. Chem. 17, 1143 (1980); J. Cizek, M. R. Clay, and J. Paldus, Phys. Rev. A 22, 793 (1980).
[16] W. Kutzelnigg, J. Chem. Phys. 73, 343 (1980).
[17] J. M. Schulman, J. Chem. Phys. 57, 4413 (1972).
[18] W. N. Whitton, Mol. Phys. 36, 941 (1978).
[19] R. J. Damburg and R. K. Propin, J. Phys. B 1, 681 (1968).
[20] W. Kutzelnigg, Int. J. Quant. Chem. 14, 101 (1978).
[21] J. Nuttal, in E. B. Saff and R. S. Varga, Eds., Padé and Rational Approximation, Theory and Applications (Academic, New York, 1977), p. 101.
[22] G. A. Baker, Essentials of Padé Approximation (Academic, New York, 1975).
[23] G. Chałasiński and K. Szalewicz, Int. J. Quant. Chem. (in press).
[24] T. R. Singh, H. Kreek, and W. J. Meath, J. Chem. Phys. 52, 5565 (1970).

Electrostatics for periodic films of atoms

Hendrik J. Monkhorst* and William A. Schwalm

Department of Physics, University of Utah, Salt Lake City, Utah 84112

(Received 18 August 1980)

The total electrostatic energy of a charge distribution, periodic in two dimensions, which may consist of both point charges and a continuous distribution, is analyzed in detail. From the long-range nature of the Coulombic force, singularities arise which must be treated with considerable care. The Fourier-transform method developed by Harris and Monkhorst is carried forward, and the way in which these singularities cancel is clearly demonstrated. A convenient procedure for computing total energies is given, and various applications to periodic arrays of point charges are presented.

I. INTRODUCTION

In a review article Harris[1] has outlined the Fourier-transform method for computing classical Madelung sums, and for performing Hartree-Fock calculations on periodic, extended systems such as crystals. In particular, a connection has been made between the internal structure of the Coulombic singularities in such calculations, which cancel at the origin of the transform domain, and the multipole-moment densities of the repeating units which can lead to surface terms in the real-space continuum limit. Here we wish to present the details of an application of the method to the electrostatics of a system with two-dimensional periodicity.

The types of charge configurations we have in mind consist of film arrays of nuclear point charges and continuous charge distributions arising from delocalized valence and/or conduction electrons. As a special case we will consider Dirac δ-function localized electrons which results in the classical Madelung-type problem of point ions localized as an array periodic in two dimensions. No limitations are imposed on the charge distributions in the perpendicular dimension in any way. As we will show, this application can be effectively formulated for fully general symmetries, compositions, and structure in the perpendicular direction. Most significantly, the expressions are numerically well behaved, in the sense that reciprocal-lattice summations converge rapidly or can sometimes be summed analytically. This is particularly true for the point-ion lattice.

The paper starts with a definition of all the quantities in the problem. Subsequently the nuclear-nuclear repulsion energy is partitioned into terms that are treated analytically in different ways. Then follows the Fourier representation of the electron-nuclear and electron-electron energies. We show how singularities cancel and what the role is of any dipole moment of the repeating unit. Next we present a brief outline of the significance of the results in performing self-consistent calculations. This is followed by the special case of a δ-function localization of the electron distribution (leading to point-ionic films) and numerical examples demonstrating the efficacy and flexibility of the method. Finally we present in the Appendix a summary of the working formulas as derived in the main text.

II. LATTICE AND RECIPROCAL-LATTICE VECTORS

Consider a two-dimensional lattice spanned by the vectors $\vec{h}_1$ and $\vec{h}_2$. An arbitrary lattice vector is

$$\vec{R}_m = m_1\vec{h}_1 + m_2\vec{h}_2 . \tag{1}$$

The index m stands for the pair of integers m_1, m_2. The systems to be treated below must have the translation symmetry of this lattice, but will not be required to have any particular symmetry in the other spatial direction. Assume, however, that these systems can be divided into layers in some meaningful way, and let n be an integer index identifying the layer. Fixing m_1, m_2, and n will not in general be enough to address a particular atomic site, since on a particular layer and within a given period there may be several atoms, each at a different, nonprimitive displacement. Let τ specify the particular atomic site; then the complete position of an atomic site is given by

$$\vec{R}_{mn\tau} = \vec{R}_m + \vec{R}_{n\tau} . \tag{2}$$

The nuclear charge associated with this particular site will be denoted by $Z_{n\tau}$.

It is convenient to define also the reciprocal lattice at this time. The three-dimensional basis is chosen to be $\vec{h}_1, \vec{h}_2, \hat{z}$, where $\hat{z}$ is the unit vector perpendicular to the layer. The period area is thus

$$A_0 = \hat{z} \cdot (\vec{h}_1 \times \vec{h}_2) . \tag{3}$$

Reciprocal basis vectors are, as usual,

$$\bar{k}_1 = \frac{2\pi}{A_0}(\bar{h}_2 \times \hat{z}) \ . \tag{4a}$$

$$\bar{k}_2 = \frac{2\pi}{A_0}(\hat{z} \times \bar{h}_1) \ . \tag{4b}$$

A basis in reciprocal space is thus provided by $\bar{k}_1, \bar{k}_2, \hat{z}$.

III. PARTITIONING OF THE LATTICE REPULSIVE ENERGY U

Assuming a Coulombic interaction among a collection of bare nuclei, we see that the energy required to assemble this lattice of positive point charges is

$$U = \frac{1}{2} \sum_{\substack{mn\tau \\ m'n'\tau'}}{}' \frac{Z_{n\tau} Z_{n'\tau'}}{|\bar{R}_{mn\tau} - \bar{R}_{m'n'\tau'}|} \ . \tag{5}$$

The prime on the summation sign means that the term $(mn\tau) = (m'n'\tau')$ is to be omitted. Even with the self-energy term omitted, it is clear that the infin-

ite, formal summation of Eq. (5) cannot converge. The lattice energy of a bare, positive lattice would in fact diverge if it were not dressed in a negative electronic charge distribution. We must isolate exactly this divergent part of the summation and cancel it together with the divergent, repulsive part of the electron-electron interaction, against the divergent, attractive electron-lattice interaction. Part of the purpose of the current paper is to isolate these divergences and arrange for their cancellation in an analytical way. Thus the remaining energy contributions will be well behaved and may conveniently be dealt with numerically.

Following the development of Harris,[1] we introduce the Fourier repesentation

$$\frac{1}{r} = \frac{1}{2\pi^2} \int \frac{e^{-i\bar{k}\cdot\bar{r}}}{k^2} d^3k \ , \tag{6}$$

where the angle integration is to be performed first. We should like to insert this expression into Eq. (5) and interchange summation and integration. If this is done carefully, we have

$$U = -\frac{1}{2(2\pi^2)} \int_{|\bar{k}|>\epsilon} \frac{1}{k^2} \left[\sum_{\substack{mn\tau \\ m'n'\tau'}}{}' Z_{n\tau} Z_{n'\tau'} \exp[-i\bar{k}\cdot(\bar{R}_{mn\tau} - \bar{R}_{m'n'\tau'})] \right] d^3k + U_\epsilon \ . \tag{7}$$

where the extra term which has been plucked from the region around the origin at $\bar{k} = 0$ is

$$U_\epsilon = -\frac{1}{2(2\pi^2)} \sum_{\substack{mn\tau \\ m'n'\tau'}}{}' Z_{n\tau} Z_{n'\tau'} \int_{|\bar{k}|<\epsilon} \frac{1}{k^2} \exp[-i\bar{k}\cdot(\bar{R}_{nm\tau} - \bar{R}_{m'n'\tau'})] d^3k \ . \tag{8}$$

The reason for this exclusion can be seen by examination of the nature of the summands in Eq. (7). The sum does not converge uniformly in $\bar{k}$ for $\bar{k}$ in the vicinity of $\bar{0}$. Thus, had we not excluded a ball of radius ϵ around $\bar{k} = \bar{0}$, the interchange of summation and integration would not have been possible.

It will be useful for the sake of normalization to temporarily suppose that the range of summation of m_1 and m_2 in Eqs. (7) and (8) is finite, and that the total number of periods is M^2 where M is a very large integer. It is then possible to take advantage of periodicity and write

$$U = U_\epsilon + \frac{M^2}{4\pi^2} \int_{|\bar{k}|>\epsilon} \frac{1}{k^2} \left[\left(\sum_{n\tau} Z_{n\tau}^2 \right)\left(\sum_m \exp(-i\bar{k}\cdot\bar{R}_m) - 1 \right) \right.$$

$$\left. + \left(\sum_m \exp(-i\bar{k}\cdot\bar{R}_m) \right)\left(\sum_{\substack{n\tau \\ n'\tau'}}{}' Z_{n\tau} Z_{n'\tau'} \exp[i\bar{k}\cdot(\bar{R}_{n\tau} - R_{n'\tau'})] \right) \right] d^3k \ . \tag{9}$$

The first term in the integrand of Eq. (9) accounts for the repulsive energy between sites on the same sublattice, i.e., sites with the same n, τ values. The second term is the intersublattice repulsion.

With the introduction of the nuclear structure factor

$$s(\bar{k}) = \sum_{n\tau} Z_{n\tau} \exp(i\bar{k}\cdot\bar{R}_{n\tau}) \ . \tag{10}$$

we can write

$$U = U_\epsilon + \frac{M^2}{4\pi^2} \int_{|\bar{k}|>\epsilon} \frac{1}{k^2} \left[|s(\bar{k})|^2 \sum_m \exp(-i\bar{k}\cdot\bar{R}_m) - \sum_{n\tau} Z_{n\tau}^2 \right] d^3k \ . \tag{11}$$

between the harmonic series and the logarithm.

$$U_1 = \frac{\pi M^2}{A_0 k_2} \left(\sum_{n,\tau} Z_{n,\tau}^2 \right) F_2 \left(\frac{k_1}{k_2}, \cos\gamma \right) . \tag{25}$$

where F_2 depends on the geometry of the reciprocal lattice through the ratio of the lengths of the vectors $\vec{k}_1$ and $\vec{k}_2$, and through the cosine of the angle γ between them

$$F_2 \left(\frac{k_1}{k_2}, \cos\gamma \right) = k_2 \left(\sum_{I = \infty} \frac{1}{K_I} - \frac{A_0}{4\pi^2} \int \frac{d^2 k_{\shortparallel}}{k_{\shortparallel}} \right) . \tag{26}$$

If we express $\vec{k}_{\shortparallel}$ according to

$$\vec{k}_{\shortparallel} = u\vec{k}_1 + v\vec{k}_2 . \tag{27}$$

$\vec{K}_I$ according to Eq. (14), and define

$$f(u,v) = k_2(k_1^2 u^2 + 2\vec{k}_1 \cdot \vec{k}_2 u v + k_2^2 v^2)^{-1/2}$$

$$= (\alpha^2 u^2 + 2\alpha t u v + v^2)^{-1/2} . \tag{28}$$

where α is the ratio k_1/k_2 and t is $\cos\gamma$, the form of F_2 then becomes

$$F_2(\alpha,t) = \left(\sum_{I \neq 0} f(l_1,l_2) - \int f(u,v) \, du \, dv \right) . \tag{29}$$

The difference between the sum and the integral of any function $f(u,v)$ over a simple region can be evaluated numerically via an Euler-Maclaurin formula[3]

$$\sum_{l_1=a}^{b} \sum_{l_2=c}^{d} f(l_1,l_2) - \int_a^b \int_c^d f(u,v) \, du \, dv = \sum_i g_i \int_a^b [f_{0,i}(u,d) - f_{0,i}(u,c)] \, du + \sum_i g_i \int_c^d [f_{i,0}(b,v) - f_{i,0}(a,v)] \, dv$$

$$+ \sum_{i,j} g_i g_j [f_{i,j}(b,d) - f_{i,j}(a,d) - f_{i,j}(b,c) + f_{i,j}(a,c)] . \tag{30}$$

where i,j range over all odd, positive integers,

$$f_{i,j}(u,v) = \frac{\partial^{i+j}}{\partial u^i \partial v^j} f(u,v) . \tag{31}$$

and the coefficients g_i is related to the Bernoulli number B_{i+1} via

$$g_i = B_{i+1}/(i+1)! . \tag{32}$$

In the double summation on the left-hand side of Eq. (30), boundary points are to be given half-weight. Thus, for example, the contribution $f(l_1,l_2)$ is to be mutliplied by $\frac{1}{4}$ if I is a corner of the region of sum-

mation by $\frac{1}{2}$ if I is an edge, and by 1 if it is an interior point.

To evaluate F_2, we divide the infinite region into nine subregions as shown in Fig. 1. Region I is defined by restricting the range of l_1 and l_2 to be from $-L$ to L for some fixed integer L. The integral of $f(u,v)$ over region I can be done in closed form using polar coordinates. Thus, the contribution to F_2 from the inner region I is evaluated explicitly, while the Euler-Maclaurin method is applied to the infinite regions. Taking symmetries of $f(u,v)$ into account we deduce an expression for $F_2(\alpha,t)$:

$$F_2(\alpha,t) = \sum_{I \in I}'' f(l_1,l_2) - 2L \left(\ln \left| \frac{\alpha t + 1 + (\alpha^2 + 2\alpha t + 1)^{1/2}}{\alpha t - 1 + (\alpha^2 - 2\alpha t + 1)^{1/2}} \right| + \frac{1}{\alpha} \ln \left| \frac{(\alpha^2 - 2\alpha t + 1)^{1/2} + \alpha - t}{(\alpha^2 + 2\alpha t + 1)^{1/2} - \alpha - t} \right| \right)$$

$$- \frac{2}{\alpha} \sum_i g_i \left(\frac{\partial}{\partial v} \right)^i \ln \left| \frac{(\alpha^2 L^2 + 2\alpha t L v + v^2)^{1/2} + \alpha L + t v}{(\alpha^2 L^2 - 2\alpha t L v + v^2)^{1/2} - \alpha L + t v} \right|_{v=L}$$

$$- 2 \sum_i g_i \left(\frac{\partial}{\partial u} \right)^i \ln \left| \frac{(\alpha^2 u^2 + 2\alpha t u L + L^2)^{1/2} + L + \alpha t u}{(\alpha^2 u^2 - 2\alpha t u L + L^2)^{1/2} - L + \alpha t u} \right|_{u=L} - 2 \sum_{i,j} g_i g_j [f_{i,j}(L,L) - f_{i,j}(L,-L)] . \tag{33}$$

The double prime on the summation on I over region I indicates that points on the edge are to be weighted by $\frac{1}{2}$, those on the corners by $\frac{1}{4}$ and the point $I = 0,0$ is to be skipped altogether.

Although it would certainly by possible to perform the differentiations appearing in Eq. (33) explicitly, this has not been done. Instead, forward tabular difference derivatives have been used and the size of L and the number of derivative terms included in the expansion adjusted to minimize the combined roundoff and truncation error. F_2 is thus computed as in Eq. (33) and U_1 results from substituting this into Eq. (25).

The *final partitioning of the* U *expression into* computationally convenient pieces depends upon the properties of the remaining m summation in Eq. (11). In order to avoid confusion later, we must proceed circumspectly. Basically we have

$$\sum_m \exp(-i\vec{k}\cdot\vec{R}_m) = \frac{4\pi^2}{A_0}\sum_l \delta(\vec{k}_\parallel - \vec{K}_l) \ , \qquad (12)$$

where

$$\vec{k}_\parallel = \hat{z}\times(\vec{k}\times\hat{z}) = \vec{k} - \hat{z}(\hat{z}\cdot\vec{k}) \qquad (13)$$

is the component of $\vec{k}$ parallel to the plane.

$$\vec{K}_l = l_1\vec{k}_1 + l_2\vec{k}_2 \ , \qquad (14)$$

with l_1 and l_2 integers, is an arbitrary, reciprocal-lattice vector. The δ symbol appearing in Eq. (12) is not Dirac's δ, but rather it is a peaked function of finite width which depends on M, the range of sum-

mation. In fact,

$$\delta(\vec{k}_\parallel) = \delta_M(\vec{h}_1\cdot\vec{k})\delta_M(\vec{h}_2\cdot\vec{k}) \ , \qquad (15)$$

with

$$\delta_M(x) = \frac{\sin[(M+\tfrac{1}{2})\tfrac{1}{2}x]}{\pi\sin\tfrac{1}{2}x} \ . \qquad (16)$$

The function $\delta(\vec{k}_\parallel)$ peaks at $\vec{k}_\parallel = \vec{0}$ and has its first zero on the perimeter parallelogram the reciprocal area of which is $4\pi^2/A_0$. From this point on, we suppose that the excluded region of radius ϵ is small compared to the reciprocal-lattice spacing, but that

$$\frac{4\pi^2}{M^2 A_0} \ll \pi\epsilon^2 \ll \frac{4\pi^2}{A_0} \ , \qquad (17)$$

so that the central peak remains tightly within the region of integration of U_ϵ.

Thus, we arrive at

$$U = U_\epsilon + \frac{M^2}{4\pi^2}\left\{\left[\frac{4\pi^2}{A_0}\int_{-\infty}^{\infty}\sum_{l\neq 00}\frac{|s(\vec{K}_l+k_z\hat{z})|^2}{K_l^2+k_z^2}dk_z - \left(\sum_{n\tau}Z_{n\tau}^2\right)\int\frac{d^3k}{k^2}\right] + \frac{4\pi^2}{A_0}\not\int_{-\infty}^{\infty}\frac{|s(k_z\hat{z})|^2}{k_z^2}dk_z\right\} \ . \qquad (18)$$

The slash through the final integral sign indicates that the range $-\epsilon$ to ϵ is to be excluded. The exclusion of the ball of radius ϵ has been omitted from the second integration in Eq. (18) since the integrand is continuous there. Regrouping terms yields

$$U = U_1 + U_2 + U_3 + U_\epsilon \ . \qquad (19)$$

with

$$U_1 = \frac{M^2}{4\pi^2}\left(\sum_{n\tau}Z_{n\tau}^2\right)\int_{-\infty}^{\infty}\left[\frac{4\pi^2}{A_0}\sum_{l\neq 00}\frac{1}{K_l^2+k_z^2} - \int\frac{d^2k_\parallel}{k_\parallel^2+k_z^2}\right]dk_z \ , \qquad (20)$$

$$U_2 = \frac{M^2}{A_0}\sum_{\substack{n\tau \\ n'\tau'}}' Z_{n\tau}Z_{n'\tau'}\sum_{l\neq 00}\int_{-\infty}^{\infty}\left[\frac{\exp[i(\vec{R}_{n\tau}-\vec{R}_{n'\tau'})\cdot(\vec{K}_l+k_z\hat{z})]}{K_l^2+k_z^2}\right]dk_z \ . \qquad (21)$$

$$U_3 = \frac{M^2}{A_0}\not\int_{-\infty}^{\infty}\frac{|s(k_z\hat{z})|^2}{k_z^2}dk_z \ . \qquad (22)$$

The k_z integration can easily be done in Eqs. (20) and (21) giving

$$U_1 = \frac{M^2}{4\pi^2}\left(\sum_{n\tau}Z_{n\tau}^2\right)\left[\frac{4\pi^3}{A_0}\sum_{l\neq 00}\frac{1}{K_l} - \pi\int\frac{d^2k_\parallel}{k_\parallel}\right] \qquad (23)$$

and

$$U_2 = \frac{\pi M^2}{A_0}\sum_{\substack{n\tau \\ n'\tau'}}' \sum_{l\neq 00}\frac{Z_{n\tau}Z_{n'\tau'}}{K_l}$$

$$\times \exp[i\vec{K}_l\cdot(\vec{R}_{n\tau}-\vec{R}_{n'\tau'})$$

$$- |\vec{K}_l||\hat{z}\cdot(\vec{R}_{n\tau}-\vec{R}_{n'\tau'})|] \ . \qquad (24)$$

It is quite clear that U_3 of Eq. (22) diverges as $\epsilon\to 0$. This is the divergent term which must be balanced against the divergent, electron-lattice attractive energy, as noted above.

We now evaluate the terms of Eq. (19) in detail.

IV. EVALUATION OF U_1

As presented in Eq. (23), U_1 is the difference between a divergent sum and a divergent integral. In this sense it is rather like a two-dimensional generalization[2] of Euler's constant, which is the difference
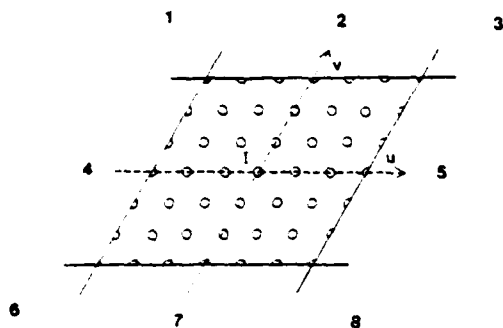
FIG. 1 Summation regions for Euler-McLaurin summations. I is the inner region over which sums and integrals are explicitly performed. In regions 2, 4, 5, and 7 the one-dimensional Euler-McLaurin formula, together with a finite summation is used. In regions 1, 3, 6 and 8 the two-dimensional Euler-McLaurin formula is applied. The case illustrated is that of $L = 3$.

V. EVALUATION OF U_2

Whenever in Eq. (24) it is the case that

$$(\vec{R}_{n\tau} - \vec{R}_{n'\tau'}) \cdot \hat{z} \neq 0 , \qquad (34)$$

then the I summation converges exponentially. As a result, there is no need for further reduction of the expression and Eq. (24) may be used directly. However, there will be cases when there is more than one inequivalent site in the same plane, and then Eq. (34) does not hold. Thus a more generally convergent expression is desirable.

Define

$$P(x_1, x_2, y; \alpha, t)$$
$$= \sum_{l \neq 00} e^{il_1 x_1} e^{il_2 x_2} \frac{\exp[-y(\alpha^2 l_1^2 + 2\alpha t l_1 l_2 + l_2^2)^{1/2}]}{(\alpha^2 l_1^2 + 2\alpha t l_1 l_2 + l_2^2)^{1/2}} \qquad (35)$$

with α and t again being k_1/k_2 and the cosine of the angle between $\vec{k}_1$ and $\vec{k}_2$, and with

$$x_1 = \vec{k}_1 \cdot (\vec{R}_{n\tau} - \vec{R}_{n'\tau'}) , \qquad (36a)$$

$$x_2 = \vec{k}_2 \cdot (\vec{R}_{n\tau} - \vec{R}_{n'\tau'}) , \qquad (36b)$$

and

$$y = k_2 |\hat{z} \cdot (\vec{R}_{n\tau} - \vec{R}_{n'\tau'})| . \qquad (37)$$

Thus P depends upon the atomic positions and shape of the period but not on the size. In terms of P

$$U_2 = \frac{\pi M^2}{A_0 k_2} \sum_{\substack{n\tau \\ n'\tau'}}{}' Z_{n\tau} Z_{n'\tau'} P(x_1, x_2, y; \alpha, t) . \qquad (38)$$

P must now be reduced. First,

$$P(x_1, x_2, y; \alpha, t) = P_1(x_2, y) + P_2(x_1, x_2, y; \alpha, t) . \qquad (39)$$

where

$$P_1(x_2, y) = \sum_{l_2 \neq 0} \frac{\exp(il_2 x_2)}{|l_2|} e^{-l_2 y} . \qquad (40)$$

and

$$P_2(x_1, x_2, y; \alpha, t) = \sum_{l_1 \neq 0} e^{il_1 x_1} \left[\sum_{l_2 = -\infty}^{\infty} \frac{e^{il_2 x_2} \exp[-y(\alpha^2 l_1^2 + 2\alpha t l_1 l_2 + l_2^2)^{1/2}]}{(\alpha^2 l_1^2 + 2\alpha t l_1 l_2 + l_2^2)^{1/2}} \right] . \qquad (41)$$

P_1 is closely related to a geometric series and can be summed exactly while P_2 may be transformed by means of the Poisson summation formula.[4] The results are

$$P_1(x_2, y) = -\ln(\cosh y - \cos x_2) + y - \ln 2 . \qquad (42)$$

$$P_2(x_1, x_2, y; \alpha, t) = 4 \sum_{n=1}^{\infty} \sum_{m=-\infty}^{\infty} (\cos[(x_1 - x_2 \alpha t - 2\pi m \alpha t)n] K_0\{\alpha(1 - t^2)^{1/2} n[(x_2 + 2\pi m)^2 + y^2]^{1/2}\}) . \qquad (43)$$

K_0 in Eq. (43) is a modified Bessel function. U_2 is evaluated by using Eqs. (42) and (43) for the P's of Eq. (38). Equation (43) is now exponentially convergent unless y and x_2 are both zero, in which case k_2 is interchanged with k_1.

VI. CANCELLATION OF SINGULARITIES

The two remaining terms in the expression for the lattice repulsive energy U, namely, U_1 and U_4, contain divergences which will now be shown to balance against one-half of the electron-lattice interaction energy U_4 may be rewritten without the exclusion of the finite number of terms for which $\vec{R}_m = \vec{0}$ and $\vec{R}_{n\tau} = \vec{R}_{n'\tau'}$. since each of these vanishes linearly with ϵ

$$U_e = \frac{M^2}{4\pi^2} \sum_m \sum_{\substack{n\tau \\ n'\tau'}} Z_{n\tau} Z_{n'\tau'} \int_{|\vec{k}| < \epsilon} \frac{1}{k^2} \exp[-i\vec{k}\cdot(\vec{R}_m + \vec{R}_{n\tau} - \vec{R}_{n'\tau'})] \, d^3k \quad . \tag{44}$$

Doing the angle integration yields

$$U_e = \frac{M^2}{\pi} \sum_m \sum_{\substack{n\tau \\ n'\tau'}} Z_{n\tau} Z_{n'\tau'} \int_0^\epsilon j_0(k|\vec{R}_m + \vec{R}_{n\tau n'\tau'}|) \, dk \quad . \tag{45}$$

where

$$j_0(x) = \sin x / x \tag{46}$$

and

$$\vec{R}_{n\tau n'\tau'} = \vec{R}_{n\tau} - \vec{R}_{n'\tau'} \quad . \tag{47}$$

Consider now the integral

$$I(a, \epsilon) = \int_0^\epsilon j_0(ax) \, dx \quad , \tag{48}$$

$$I(a, \epsilon) = \frac{1}{a} \int_0^\epsilon \frac{\sin a \epsilon x}{x} \, dx \quad . \tag{49}$$

If $a\epsilon$ is much larger than π, then I becomes approximately π/a, while if $a\epsilon$ is much less than π, I is ϵ. From this it is seen that one can estimate the size of the summands in Eq. (45). M is the limit of the magnitude of m_1 and m_2, thus the magnitude of $|\vec{R}_m - \vec{R}_{n\tau n'\tau'}|$ is bounded by a number in the order of

$$R_{max} = M\sqrt{A_0} \quad . \tag{50}$$

But, from the discussion resulting in the restriction Eq. (17), most of the contributions to the summation come from terms for which $|\vec{R}_m|$ is of the order of R_{max}. It is clear that for such summands

$$\epsilon|\vec{R}_m - \vec{R}_{n\tau n'\tau'}| \approx \epsilon R_{max} \gg 1 \quad . \tag{51}$$

the latter inequality following from Eq. (17). Thus, using the above results, each significantly contributing integral is very nearly π/R_{max}, and the number of such terms is clearly proportional to M^2. So, again using Eq. (17),

$$U_e \propto (M^2)(M^2)(\pi/R_{max}) \sim M^3 \quad . \tag{52}$$

Therefore this term also is divergent.

The divergence of U_e, which may be called an inner divergence, since it occurs near the origin in reciprocal space, will be balanced against an exactly similar term in the electron-lattice attraction. Likewise, another term will appear in the electron-lattice attraction which will have a divergence with exactly the form of that noted in Eq. (22). These two divergences must also be permitted to cancel.

The expression for the total electron-lattice energy is

$$\langle V \rangle = -\int \rho(\vec{r}) \sum_{mn\tau} \frac{Z_{n\tau}}{|\vec{r} - \vec{R}_{nm\tau}|} \, d^3r \quad . \tag{53}$$

Here, $\rho(\vec{r})$ is the total electronic number density, so that the minus sign is treated explicitly. Again using Eq. (6)

$$\langle V \rangle = -\int \rho(\vec{r}) \sum_{mn\tau} Z_{n\tau} \left[\frac{1}{2\pi^2} \int \frac{\exp[-i\vec{k}\cdot(\vec{r} - \vec{R}_{mn\tau})]}{k^2} \, d^3k \right] d^3r \quad ; \tag{54}$$

once more, cautiously interchanging the sum and the integral

$$\langle V \rangle = \langle V \rangle_e + \langle V \rangle_r \quad . \tag{55}$$

where

$$\langle V \rangle_e = -\frac{1}{2\pi^2} \int \rho(\vec{r}) \sum_{mn\tau} Z_{n\tau} \left[\int_{|\vec{k}| < \epsilon} \frac{\exp[-i\vec{k}\cdot(\vec{r} - \vec{R}_{mn\tau})]}{k^2} \, d^3k \right] d^3r \tag{56}$$

and

$$\langle V \rangle_r = -\frac{1}{2\pi^2} \int_{|\vec{k}| > \epsilon} \sum_{mn\tau} Z_{n\tau} \left[\int e^{-i\vec{k}\cdot\vec{r}} \rho(\vec{r}) \, d^3r \right] \frac{\exp(i\vec{k}\cdot\vec{R}_{mn\tau})}{k^2} \, d^3k \quad . \tag{57}$$

Equation (57) appears to contain the Fourier integral transform of the number density $\rho(\vec{r})$. Care is again required, since this integral does not exist. We require two properties of the electron density: (i) $\rho(\vec{r})$ is periodic over the lattice defined by Eq. (1); (ii) the integral of $\rho(\vec{r})$ over one period is exactly Q where

$$Q = \sum_{n\tau} Z_{n\tau} \quad . \tag{58}$$

Thus, if the size of the lattice is again temporarily restricted,

$$\int \rho(\vec{r})e^{-i\vec{k}\cdot\vec{r}}d^3r = M^2\hat{\rho}(\vec{k}) \ . \tag{59}$$

where $\hat{\rho}(\vec{k})$ is an electronic structure factor defined by

$$\hat{\rho}(\vec{k}) = \int_{-\infty}^{\infty}\left[\int_{period}\rho(\vec{r})e^{-i\vec{k}\cdot\vec{r}}dx\,dy\right]dz \ . \tag{60}$$

Then Eq. (57) for $\langle V\rangle$, divides again into two parts:

$$\langle V\rangle_r = \langle V\rangle_{12} + \langle V\rangle_3 \ . \tag{61}$$

with

$$\langle V\rangle_{12} = -\frac{2M^2}{A_0}\int_{-\infty}^{\infty} \\ \times \sum_{l\neq 00}\left\{\frac{s(K_l+k_z z)\hat{\rho}(\vec{K}_l+k_z\hat{z})}{K_l^2+k_z^2}\right\}dk_z \ . \tag{62}$$

The completeness relation Eq. (12) has been used to produce Eq. (62). Likewise

$$\langle V\rangle_3 = -\frac{2M^2}{A_0}\oint_{-\infty}^{\infty}\frac{1}{k_z^2}s(k_z\hat{z})\hat{\rho}(k_z\hat{z})\,dk_z \ . \tag{63}$$

Comparing Eq. (63) with the U_3 contribution for the lattice repulsive energy, one has

$$U_3 + \tfrac{1}{2}\langle V\rangle_3 = \frac{M^2}{A_0}\oint_{-\infty}^{\infty}\frac{s(k_z\hat{z})}{k_z^2} \\ \times [s(-k_z\hat{z}) - \hat{\rho}(k_z\hat{z})]\,dk_z \ . \tag{64}$$

The singularity as the excluded region from $-\epsilon$ to ϵ (denoted by the bar) tends to zero has now been canceled, for s and ρ are analytic for all real $\vec{k}$, and since they are each equal to Q of Eq. (58) as $\vec{k}\rightarrow\vec{0}$, their difference has at least a simple zero at $\vec{k}=\vec{0}$. Thus Eq. (64) has a finite, Cauchy principal value

$$\lim_{\epsilon\rightarrow 0}(U_3 + \tfrac{1}{2}\langle V\rangle_3) = (const)M^2 \ . \tag{65}$$

Expression (62) for $\langle V\rangle_{12}$, which is of a form similar to that of U_2, is perfectly well behaved and needs no further reduction. The method of producing the electronic structure factor will be presented subsequently.

The combination of U_4 and $\tfrac{1}{2}\langle V\rangle_4$ must now be examined. After performing the angle integration in Eq. (56) and taking periodicity into account

$$\langle V\rangle_4 = -\frac{2M^2}{\pi}\sum_{mn\tau}Z_{n\tau}\int_{-\infty}^{\infty}\int_{period}\rho(\vec{r})\int_0^{\epsilon}j_0(k|\vec{R}_m+\vec{R}_{n\tau}-\vec{r}|)\,dk\,dx\,dy\,dz \tag{66}$$

which is very similar in form to Eq. (45) for U_4. The important tool for evaluating both expressions is the Taylor-series expansion[1]

$$\int_0^{\epsilon}j_0(k|\vec{R}+\vec{a}|)\,dk = \frac{1}{R}\left[Si(\epsilon R) + \left\{\frac{\vec{R}\cdot\vec{a}}{R^2} - \frac{3(\vec{R}\cdot\vec{a})^2-R^2a^2}{2R^4}\right\}[\sin(\epsilon R)-Si(\epsilon R)] - \frac{(\vec{R}\cdot\vec{a})^2}{2R^3}\right. \\ \left. \times\left\{\frac{\sin(\epsilon R)}{R} - \epsilon\cos(\epsilon R)\right\} + O\left\{\frac{a^4}{R^4}\right\}\right] \ . \tag{67}$$

where $Si(x)$ is the sine integral function defined by

$$Si(x) = \int_0^x\frac{\sin t}{t}dt \ . \tag{68}$$

Applying this to Eq. (66) and keeping only the terms which can contribute at large R_m

$$\langle V\rangle_4 = -\frac{2M^2}{\pi}\sum_m\sum_{n\tau}Z_{n\tau}\left\{\frac{Q}{R_m}Si(\epsilon R_m) + \frac{\vec{R}_m\cdot(\vec{R}_{n\tau}Q-\vec{P}_-)}{R_m^3}[\sin(\epsilon R_m)-Si(\epsilon R_m)] + \cdots\right\} \ . \tag{69}$$

with Q given by Eq. (58) and $\vec{P}_-$ being the coordinate within a cell of the centroid of the electron distribution

$$\vec{P}_- = \int_{-\infty}^{\infty}\left[\int_{period}\rho(\vec{r})\vec{r}\,dx\,dy\right]dz \ . \tag{70}$$

Likewise, treating U_4 in a similar way, the result is

$$U_{\epsilon} = +\frac{M^2}{\pi} \sum_m \sum_{n\tau} Z_{n\tau} \left[\frac{Q}{R_m} \text{Si}(\epsilon R_m) + \frac{\vec{R}_m \cdot (\vec{R}_{n\tau} Q - \vec{P}_+)}{R_m^3} \left[\sin(\epsilon R_m) - \text{Si}(\epsilon R_m) \right] + \cdots \right] , \tag{71}$$

with $\vec{P}_+$ the centroid of the nuclear charge distribution,

$$\vec{P}_+ = \sum_{n'\tau'} Z_{n'\tau'} \vec{R}_{n'\tau'} . \tag{72}$$

Therefore, the sum for small ϵ

$$U_{\epsilon} + \tfrac{1}{2}\langle V \rangle_{\epsilon} = \frac{M^2}{\pi} \sum_m Q \left[\frac{\vec{R}_m \cdot (\vec{P}_- - \vec{P}_+)}{R_m^3} \right]$$

$$\times \left[\sin(\epsilon R_m) - \text{Si}(\epsilon R_m) \right] . \tag{73}$$

One sees that if the total dipole moment of the cell has no component in the plane of the lattice, then there is strict cancellation and the sum of these two terms is zero in the limit $\epsilon \to 0$. Under this condition, the exact cancellation of all singularities in U

against similar singularities in $\tfrac{1}{2}\langle V \rangle$ has thus been demonstrated. Without the vanishing of the parallel component of the total dipole moment, the long-range terms in Eq. (73) become difficult to handle.

Since it is very reasonable to ask what happens to the other half of the singularity in $\langle V \rangle$, the answer is provided here as follows: the other half of the $\langle V \rangle$ divergence cancels against a similar divergence in the electron-electron repulsive energy C

$$C = \tfrac{1}{2} \int \int \frac{\rho(\vec{r})\rho(\vec{r}')}{|\vec{r} - \vec{r}'|} d^3r \, d^3r' . \tag{74}$$

Proceeding as in the treatment of $\langle V \rangle$, translation symmetry produces

$$C = C_{\epsilon} + C_r . \tag{75}$$

where

$$C_{\epsilon} = +\frac{M^2}{\pi} \int_{-\infty}^{\infty} \int_{\text{period}} \rho(\vec{r}) \left[\int_{-\infty}^{\infty} \int_{\text{period}} \rho(\vec{r}') \left[\int_0^{\epsilon} j_0(k\,|\vec{r} - \vec{R}_m|)\,dk \right] dx' \, dy' \, dz' \right] dx \, dy \, dz , \tag{76}$$

$$C_r = C_{12} + C_3 . \tag{77}$$

with

$$C_{12} = \frac{M^2}{A_0} \int_{-\infty}^{\infty} \sum_{l \neq 00} \frac{|\hat{\rho}(k_z \hat{z} + \vec{K}_l)|^2}{k_z^2 + K_l^2} dk_z . \tag{78}$$

and

$$C_3 = \frac{M^2}{A_0} \oint_{-\infty}^{\infty} \frac{|\hat{\rho}(k_z \hat{z})|^2}{k_z^2} dk_z . \tag{79}$$

C_{12} is finite and needs no further reduction. Applying Eq. (67) to Eq. (76) for C_{ϵ} yields for the nonvanishing part

$$C_{\epsilon} = +\frac{M^2}{\pi} \sum_m \int_{-\infty}^{\infty} \int_{\text{period}} \rho(\vec{r}) \left[\frac{Q}{R_m} \text{Si}(\epsilon R_m) + \frac{\vec{R}_m \cdot (\vec{r}Q - \vec{P}_-)}{R_m^3} \left[\sin(\epsilon R_m) - \text{Si}(\epsilon R_m) \right] + \cdots \right] dx \, dy \, dz . \tag{80}$$

Whence, for small ϵ one has again as in Eq. (73)

$$C_{\epsilon} + \tfrac{1}{2}\langle V \rangle_{\epsilon} = \frac{M^2}{\pi} \sum_m Q \left[\frac{\vec{R}_m \cdot (\vec{P}_- - \vec{P}_+)}{R_m^3} \right] \left[\sin(\epsilon R_m) - \text{Si}(\epsilon R_m) \right] . \tag{81}$$

which vanishes, provided the net dipole moment is perpendicular to the plane of the lattice.

The cancellation of the singularity in C_3 against that of $\tfrac{1}{2}\langle V \rangle_3$ follows from a discussion entirely similar to that preceding Eq. (65). The conclusion in this case is that

$$\lim_{\epsilon \to 0} (C_3 + \tfrac{1}{2} + \langle V \rangle_3) = (\text{const})M^2 . \tag{82}$$

VII. TOTAL ENERGY

All of the essential ingredients are now at hand to express the total energy of quantized systems with translation symmetry on the two-dimensional lattice defined by Eq. (1). It will be assumeed that the results of a self-consistent electronic structure calculation are available in the form of band energies and

Bloch functions, and furthermore that, as a result of the self-consistent procedure, the Fermi energy E_F is also known.[4]

If there is no spin-orbit coupling, each single-particle eigenstate $|\mu, \vec{k}_\parallel\rangle$ for the μth band satisfying

$$H|\mu, \vec{k}_\parallel\rangle = E_\mu(\vec{k}_\parallel)|\mu, \vec{k}_\parallel\rangle \tag{83}$$

will be doubly occupied if the band energy $E_\mu(\vec{k}_\parallel)$ is less than E_F and unoccupied otherwise.

The one-electron operator H may generally be assumed to consist of kinetic energy T, electron-lattice interaction V, Hartree-like electron-electron energy J, and possibly an exchange operator K

$$H = T + V + J - K \ . \tag{84}$$

Define the ground-state expectation value of an arbitrary operator Ω by

$$\langle \Omega \rangle = \sum_\mu \frac{A_0}{4\pi^2} \int_{\text{zone}} 2\Theta(E_F - E_\mu(\vec{k}_\parallel))$$

$$\times \langle \mu, \vec{k}_\parallel | \Omega | \mu, \vec{k}_\parallel \rangle \ d^2k_\parallel \ , \tag{85}$$

with

$$\Theta(x) = \begin{cases} 0, & \text{if } x < 0 \\ 1, & \text{if } x > 0 \end{cases} \ , \tag{86}$$

and the integration being over any convenient period of the reciprocal lattice defined by the vectors $\vec{k}_1, \vec{k}_2$ of Eq. (4). The total energy of the system is not the sum of the single-particle energies, which would be the expectation value of H. This is because the operators J and $(-K)$, which depend in a nonlinear way on the solution, contain an averaged electron-electron interaction. The expectation value $\langle J - K \rangle$ would count this interaction twice, once from the point of view of each electron. On the one hand, the total energy per period is given by

$$E = \langle T \rangle + \langle V \rangle + C + X + U \ , \tag{87}$$

where U is the lattice-lattice repulsive energy as treated above, and where

$$C = \frac{1}{2}\langle J \rangle \tag{88}$$

and

$$X = \frac{1}{2}\langle -K \rangle \ . \tag{89}$$

the exchange energy. On the other hand, the sum of the single-particle energies is

$$\sum_\mu \frac{A_0}{4\pi^2} \int_{\text{zone}} 2E_\mu(\vec{k}_\parallel)\Theta(E_F - E_\mu(\vec{k}_\parallel)) \ d^2k_\parallel$$

$$= \langle H \rangle = \langle T \rangle + \langle V \rangle + \langle J \rangle + \langle -K \rangle \ . \tag{90}$$

A most convenient method of extracting the total energy from a self-consistent, energy-band calculation is to use half of Eq. (90) to evaluate the Coulomb and exchange contributions to E in Eq. (87).

$$E = \frac{1}{2} \sum_\mu \frac{A_0}{4\pi^2} \int_{\text{zone}} 2E_\mu(\vec{k}_\parallel)\Theta(E_F - E_\mu(\vec{k}_\parallel)) \ d^2k_\parallel$$

$$+ U + \frac{1}{2}\langle T \rangle + \frac{1}{2}\langle V \rangle \ . \tag{91}$$

The U and $\frac{1}{2}\langle V \rangle$ evaluations must be done together in a way similar to that presented above in order to ensure numerical cancellation of the singularity. Otherwise, these two parts will provide large numbers, computed in generally different ways, which then must almost cancel to give a finite result.

VIII. DISCUSSION

The present analysis of the classical electrostatic energy of two-dimensional periodic systems has led to a proliferation of many expressions, some of which are quite involved. Therefore, in order to aid the reader in implementing this formulation we have summarized the definitions and the working formulas in the Appendix. We have grouped terms in a manner convenient for computation.

It is worthwhile pointing out that the determination of $\rho(\vec{r})$ has to be made in some independent way, such as from Hartree-Fock-type calculations[4] or from some experiment.

It is also possible to obtain an expression for the electrostatic potential at an atomic lattice site.[1] One obtains this formally by the expression

$$\Phi(\vec{R}_{n\tau}) = \frac{\delta E_{\text{cl}}}{\delta Z_{n\tau}} \ , \tag{92}$$

thus leading to the potential at the atomic sites at position $\widetilde{R}_{n\tau}$ with respect to the origins of the unit periods. If one wishes to determine the potential at an arbitrary, nonlattice point $\vec{R}$ in the slab one simply adds this point to the lattice summations with "nuclear" charge $Z = 0$, and uses Eq. (92). This procedure is described in Harris and Monkhorst[5] for three-dimensionally periodic solids. We will present applications of this approach in a forthcoming paper.[6]

Finally, we can specialize our formulations for the case of point-charge distributions only. This can be achieved by introducing the expression for $\rho(\vec{r})$

$$\rho(\vec{r}) = \sum_{mn\tau} \nu_{n\tau}\delta(\vec{r} - \vec{R}_{mn\tau}) \ . \tag{93}$$

i.e., a distribution of discrete number densities $\nu_{n\tau}$ at nuclear sites $R_{mn\tau}$. But then $\langle V \rangle$ and C reduce to

$$\langle V \rangle = -\sum_{\substack{mn\tau \\ m'n'\tau'}}{}' \frac{\nu_{n\tau}Z_{n'\tau'}}{|\vec{R}_{mn\tau} - \vec{R}_{m'n'\tau'}|} \ . \tag{94}$$

$$C = \frac{1}{2}\sum_{\substack{mn\tau \\ m'n'\tau'}}{}' \frac{\nu_{n\tau}\nu_{n'\tau'}}{|\vec{R}_{mn\tau} - \vec{R}_{m'n'\tau'}|} \ . \tag{95}$$

The primes to above summations indicate that we have left out the (infinite) self-energy terms, just as in the expression for U. It is easily seen that E_{cl} assumes the form

$$E_{cl} = \frac{1}{2} \sum_{\substack{mn\tau \\ m'n'\tau'}}' \frac{q_{n\tau} q_{n'\tau'}}{|\vec{R}_{mn\tau} - \vec{R}_{m'n'\tau'}|} . \qquad (96)$$

where $q_{n\tau} = Z_{n\tau} - \nu_{n\tau}$ are the net charges at sites $\vec{R}_{n\tau}$. Indeed, we have obtained the expression for the Coulomb interaction between point charges $q_{n\tau}$ localized at sites $\vec{R}_{mn\tau}$. Comparing this results with Eq. (5) for U we see that the two expressions are of the same form, with the charge neutrality now assuming the form

$$\sum_{n\tau} q_{n\tau} = 0 . \qquad (97)$$

If we introduce the lattice structure factor

$$\sigma(\vec{k}) = \sum_{n\tau} q_{n\tau} \exp(i\vec{k} \cdot \vec{R}_{n\tau}) . \qquad (98)$$

we can immediately write the expressions for E_{cl}, after simple manipulations starting from Eqs. (22), (25), and (38):

$$E_{cl} = E_1 + E_2 + E_3 . \qquad (99)$$

$$E_1 = \frac{\pi M^2}{A_0 k_2} \left(\sum_{n\tau} q_{n\tau}^2 \right) F_2(\alpha, t) . \qquad (100)$$

$$E_2 = \frac{\pi M^2}{A_0 k_2} \sum_{\substack{n\tau \\ n'\tau'}} q_{n\tau} q_{n'\tau'} P(x_1, x_2, y; \alpha t) . \qquad (101)$$

$$E_3 = -\frac{\pi M^2}{A_0} \sum_{\substack{n\tau \\ n'\tau'}} q_{n\tau} q_{n'\tau'} |\hat{z} \cdot (\vec{R}_{n\tau} - \vec{R}_{n'\tau'})| . \qquad (102)$$

In Eqs. (100) and (101) the arguments of the functions F_2 and P are the same as those used in the previous text and the Appendix.

IX. EXAMPLES: APPLICATION TO POINT-IONIC FILMS

Table I presents results for the lattice-structure-constant evaluation according to Eq. (33). The angle θ is measured either between $\vec{h}_1$, $\vec{h}_2$ (not between $\vec{k}_1$, $\vec{k}_2$). When θ is $\pi/2$, results may be compared with those of Table I of Harris. Agreement is found in every such case. The unit cell formed in the case $|\vec{h}_1| = 1$, $|\vec{h}_2| = \sqrt{2}$, and $\theta = \pi/4$ actually spans the same lattice as that spanned by $|\vec{h}_1| = 1$, $|\vec{h}_2| = 1$, $\theta = \pi/2$. Agreement is exact, although the sums are evaluated differently. The time required on the University of Utah College of Science DEC system 20/60 to compute F_2 ranges from about 0.19 sec when $N = 5$ to 6.3 sec when $N = 100$ and varies as N^2.

Madelung constants are presented in Table II for a layer of the NaCl structure. The parameter z represents the displacement of one sublattice relative to the other in the direction perpendicular to the plane. Normally, when the Evjen method is used to compute the Madelung constant, the nearest-neighbor distance is set to 1. This means that the nearest neighbor on the same sublattice is at a distance of $\sqrt{2}$. When this is taken into account, the results of the two calculations agree.

As the angle θ between $\vec{h}_1$ and $\vec{h}_2$ decreases, the Madelung energy becomes more and more negative as the ions of opposite sign come together. For lattice spacing a, as $\theta \to 0$, the sum correctly tends to the one-dimensional limit

$$E_{cl} \to \frac{4 \ln 2}{a \theta} . \qquad (103)$$

When one sublattice is displaced relative to the other, the layer is separated into oppositely charged sheets. Thus the energy begins to increase, and work must be done as z becomes larger. The increase in the E_3

TABLE I. Lattice structure constants.

$|\vec{h}_1|, |\vec{h}_2|, \theta$	α, t	N	$F_2(\alpha, t)$
1, 1, $\pi/2$	1.0	5	−3.900 169 466
1, 1, $\pi/2$	1.0	10	−3.900 250 582
1, 1, $\pi/2$	1.0	50	−3.900 264 802
1, 1, $\pi/2$	1.0	100	−3.900 264 905
1, 1, $\pi/2$	1.0	150	−3.900 264 916
1, 1, $\pi/2$	1.0	200	−3.900 264 918
1, $\sqrt{2}$, $\pi/4$	$\sqrt{2}, 1/\sqrt{2}$	100	−3.900 264 905
1, 1, 0.40π	1.0,0.30902	100	−4.011 7104
1, 1, 0.45π	1.0,0.15643	100	−3.927 9820
1, 1, 0.50π	1.0	100	−3.900 2649
1, 1, $\pi/3$	1, $\sqrt{3}/2$	100	−4.213 4226
1, $\sqrt{8/3}$, $\pi/2$	$\sqrt{8/3}, 0$	100	−2.926 6791

TABLE II. Madelung energy of distorted NaCl layer. I_{max} and $\pm J_{max}$ are ranges of n and m summations for Eq. (43).

$\lvert \bar{h}_1 \rvert, \lvert \bar{h}_2 \rvert, z, \theta$	N, I_{max}, J_{max}	E_{cl} value	Time in seconds on DEC system 20/60
$\sqrt{2}, \sqrt{2}, 0, \pi/2$	5,5,5	-1.61547	0.118
$\sqrt{2}, \sqrt{2}, 0, \pi/2$	25,5,5	-1.61554	0.482
1,1,0, $\pi/2$	25,5,5	-2.28472	0.482
1,1,0,0.45π	25,5,5	-2.32845	0.479
1,1,0,0.40π	25,5,5	-2.46338	0.476
1,1,0,0.35π	25,5,5	-2.702192	0.488
1,1,0,0.30π	25,5,5	-3.071875	0.476
1,1,0, $\pi/4$	25,5,5	-3.627312	0.482
1,1,0.1, $\pi/2$	25,5,5	-2.203007	0.481
1,1,0.2, $\pi/2$	25,5,5	-1.967742	0.478
1,1,0.3, $\pi/2$	25,5,5	-1.604450	0.476
1,1,0.4, $\pi/2$	25,5,5	-1.145134	0.478
1,1,0.5, $\pi/2$.	25,5,5	-0.619819	0.482
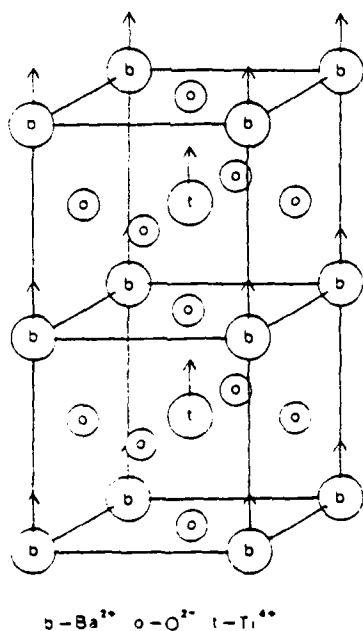
FIG. 2. Example of a double layer of barium titanate. The arrows indicate the motion of the positive ions under a distortion z of Table III. Notice that when $z = 0.5$, Ti^{4+} ions will coincide with O^{2-}.

$b - Ba^{2+} \quad o - O^{2-} \quad t - Ti^{4+}$

term is responsible for most of this energy.

As a final example, consider two layers of the barium titanate structure as illustrated in Fig. 2. Ti^{4+} ions are located at the body centers of each cube, while Ba^{2+} ions are at the face corners. O^{2-} ions are at the face centers. In all, there are two Ti^{4+}, two Ba^{2+}, and six O^{2-} ions or a total of ten ions.

The total electrostatic energy in this configuration is -134.117, in units of electronic charge squared divided by the distance between neighboring barium ions. Table III shows the variation in the contributions to this energy and to the total as the charge arrangement is distorted. The distortion is one in which the positive ions move up together in the direction perpendicular to the base plane of the thin film, while the negative ions remain fixed. Such a displacement would be associated with a ferroelectric transition in the bulk. Distortion is also measured in units of the lattice parameters.

Originally, the energy goes up with the displacement, as it did in the NaCl case, but eventually it would diverge in the negative direction by the time $z = 0.5$, since at that point, the Ti^{4+} ions would touch the O^{2-} ions. Thus, there is a maximum in the electrostatic energy of about -109 near $z = 0.3$.

A better way to treat the electrostatics of systems of point charges would be to present potential coefficients $\phi_{n\tau n'\tau'}$ such that the total energy is expressed as

$$E = \frac{1}{2} \sum_{\substack{n\tau \\ n'\tau'}} \phi_{n\tau n'\tau'} q_{n\tau} q_{n'\tau'} . \tag{104}$$

This is planned to be done for both thin films and semi-infinite geometries in a subsequent publication.[6]

TABLE III. Madelung energy for double layer of $BaTiO_3$. In each case, $E_1 = -171.6116$, and time = 18 sec on DEC system 20/60.

Distortion z	E_2	E_3	$E_{cl} = E_1 + E_2 + E_3$
0.00	37.4944	0.0000	−134.1171
0.05	21.1070	17.5929	−132.9117
0.10	6.9702	35.1858	−129.4555
0.15	−5.4024	52.7788	−124.2353
0.20	−16.8694	70.3717	−118.1093
0.25	−28.8401	87.9646	−112.4871
0.30	−43.8401	105.5575	−109.9024
0.35	−67.4202	123.1504	−115.8814

ACKNOWLEDGMENTS

APPENDIX

We will summarize the working formulas for the evaluation of the classical electrostatic part of the total energy for a film of atoms with two-dimensional *periodicity*.

Geometry definitions

(1) The two-dimensional lattice is spanned by the vectors $\vec{h}_1$ and $\vec{h}_2$. An arbitrary lattice vector is

$$\vec{R}_m = m_1 \vec{h}_1 + m_2 \vec{h}_2 . \tag{A1}$$

where the index m stands for the pair of indices (m_1, m_2), each ranging over M values.

(2) n is the layer index and τ specifies a nonprimitive displacement for an atomic site. Then the complete specification of an atomic site is given by

$$\vec{R}_{mn\tau} = \vec{R}_m + \vec{R}_{n\tau} . \tag{A2}$$

(3) The nuclear charge at the site $\vec{R}_{mn\tau}$ is denoted by $Z_{n\tau}$.

(4) The period area is denoted by A_0, and it is given by

$$A_0 = \hat{z} \cdot (\vec{h}_1 \times \vec{h}_2) , \tag{A3}$$

with $\hat{z}$ the unit vector perpendicular to the layer plane spanned by $\{\vec{R}_m\}$.

(5) Reciprocal basis vectors are

$$\vec{k}_1 = \frac{2\pi}{A_0} (\vec{h}_2 \times \hat{z}) , \tag{A4a}$$

$$\vec{k}_2 = \frac{2\pi}{A_0} (\hat{z} \times \vec{h}_1) . \tag{A4b}$$

Reciprocal-lattice vectors are denoted by

$$\vec{K}_l = l_1 \vec{k}_1 + l_2 \vec{k}_2 . \tag{A5}$$

(6) The electronic number distribution throughout the film is denoted by $\rho(\vec{r})$. This quantitiy is periodic in the lattice vector

$$\rho(\vec{r} + \vec{R}_m) = \rho(\vec{r}) . \tag{A6}$$

Its Fourier transform is expressed

$$\hat{\rho}(\vec{k}) = \frac{1}{M^2} \int \rho(\vec{r}) e^{-i\vec{k} \cdot \vec{r}} d^3 r . \tag{A7}$$

$\rho(\vec{r})$ satisfies the relationship

$$\int_{period} \rho(\vec{r}) d^3 r = Q , \tag{A8}$$

where the period nuclear charge Q is defined as

$$Q = \sum_{n\tau} Z_{n\tau} . \tag{A9}$$

(7) The centroid of the nuclear charge distribution $\vec{P}_+$ is given by

$$\vec{P}_+ = \sum_{n\tau} Z_{n\tau} \vec{R}_{n\tau} . \tag{A10}$$

(8) The centroid of the electron charge distribution $\vec{P}_-$ is given by

$$\vec{P}_- = \int_{-\infty}^{\infty} dz \int_{period} dx \, dy \, \rho(\vec{r}) \vec{r} . \tag{A11}$$

(9) The nuclear structure factor $s(\vec{k})$ is defined by

$$s(\vec{k}) = \sum_{n\tau} Z_{n\tau} \exp(i\vec{k} \cdot \vec{R}_{n\tau}) . \tag{A12}$$

Partitioning of electrostatic energy

(1) The classical Coulombic energy E_{cl} arising from the electrostatic interaction among the nuclei and electrons can be written as

$$E_{cl} = U + \langle V \rangle + C . \tag{A13}$$

(2) U is the nuclear-nuclear repulsion energy given

$$U = \frac{1}{2} \sum_{\substack{mn\tau \\ m'n'\tau'}}' \frac{Z_{n\tau}Z_{n'\tau'}}{|\vec{R}_{mn\tau} - \vec{R}_{m'n'\tau'}|} .$$ (A14)

where the prime to the summation indicates the omission of the self-energy terms.

(3) $\langle V \rangle$ is the electron-nuclear attraction energy given by

$$\langle V \rangle = -\int d^3r \, \rho(\vec{r}) \sum_{mn\tau} \frac{Z_{n\tau}}{|\vec{r} - \vec{R}_{mn\tau}|} .$$ (A15)

(4) C is the electron-electron repulsion energy given by

$$C = \frac{1}{2} \int d^3r \int d^3r' \frac{\rho(\vec{r})\rho(\vec{r}')}{|\vec{r} - \vec{r}'|} .$$ (A16)

(5) Following the analysis of the main text we partition the respective energies as follows:

$$U = U_{\mathfrak{e}} + U_1 + U_2 + U_3 .$$ (A17)

$$\langle V \rangle = \langle V \rangle_{\mathfrak{e}} + \langle V \rangle_{12} + \langle V \rangle_3 .$$ (A18)

$$C = C_{\mathfrak{e}} + C_{12} + C_3 .$$ (A19)

(6) If $\hat{z} \times (\vec{P}_+ - \vec{P}_-) = \vec{0}$, i.e., no net dipole moment parallel to the $\vec{R}_m$ plane, we have

$$U_{\mathfrak{e}} + \langle V \rangle_{\mathfrak{e}} + C_{\mathfrak{e}} = 0 .$$ (A20)

Otherwise the present method should be modified.

(7) U_1 is given by

$$U_1 = \frac{\pi M^2}{A_0 k_2} \left[\sum_{n\tau} Z_{n\tau}^2 \right] F_2 \left(\frac{k_1}{k_2}, \frac{\vec{k}_1 \cdot \vec{k}_2}{k_1 k_2} \right) .$$ (A21)

where

$$F_2(\alpha, t) = \sum_{i \in I}'' f(l_1, l_2) - 2L \left[\ln \left| \frac{\alpha t + 1 + (\alpha^2 + 2\alpha t + 1)^{1/2}}{\alpha t - 1 + (\alpha^2 - 2\alpha t + 1)^{1/2}} \right| + \frac{1}{\alpha} \ln \left| \frac{(\alpha^2 - 2\alpha t + 1)^{1/2} + \alpha - t}{(\alpha^2 + 2\alpha t + 1)^{1/2} - \alpha - t} \right| \right]$$

$$- \frac{2}{\alpha} \sum_i g_i \left(\frac{\partial}{\partial v} \right)^i \ln \left| \frac{(\alpha^2 L^2 + 2\alpha t L v + v^2)^{1/2} + \alpha L + t v}{(\alpha^2 L^2 - 2\alpha t L v + v^2)^{1/2} - \alpha L + t v} \right|_{v=L}$$

$$- 2 \sum_i g_i \left(\frac{\partial}{\partial u} \right)^i \ln \left| \frac{(\alpha^2 u^2 + 2\alpha t u L + L^2)^{1/2} + L + \alpha t u}{(\alpha^2 u^2 - 2\alpha t u L + L^2)^{1/2} - L + \alpha t u} \right|_{u=L} - 2 \sum_{i,j} g_i g_j [f_{i,j}(L,L) - f_{i,j}(L,-L)] .$$ (A22)

with

$$f_{i,j}(u,v) = \frac{\partial^{i+j}}{\partial u^i \partial v^j} f(u,v) .$$ (A23)

$$f(u,v) = (\alpha^2 u^2 + 2\alpha t u v + v^2)^{-1/2} .$$ (A24)

$$g_i = B_{i+1}/(i+1)! .$$ (A25)

The i and j summations are over odd integers, and the double primes on the I sum indicate (a) deletion of $l_1 = l_2 = 0$, (b) weights $(\frac{1}{2})$ on the edges of the inner summation region I (see Fig. 1), (c) weights $(\frac{1}{4})$ on the corners of I.

(8) U_2 is given by

$$U_2 = \frac{\pi M^2}{A_0 k_2} \sum_{\substack{n\tau \\ n'\tau'}}' Z_{n\tau} Z_{n'\tau'} P(x_1, x_2, y; \alpha, t) .$$ (A26)

with

$$x_1 = \vec{k}_1 \cdot (\vec{R}_{n\tau} - \vec{R}_{n'\tau'}) .$$ (A27)

$$x_2 = \vec{k}_2 \cdot (\vec{R}_{n\tau} - \vec{R}_{n'\tau'}) .$$ (A28)

$$y = k_2 |\hat{z} \cdot (\vec{R}_{n\tau} - \vec{R}_{n'\tau'})| .$$ (A29)

and P is partitioned according to

$$P(x_1, x_2, y; \alpha, t) = P_1(x_2, y) + P_2(x_1, x_2, y; \alpha, t) .$$ (A30)

with

$$P_1(x_2, y) = -\ln(\cosh y - \cos x_2) + y - \ln 2 .$$ (A31)

$$P_2(x_1, x_2, y; \alpha, t) = 4 \sum_{n=1}^{\infty} \sum_{m=-\infty}^{\infty} \cos[(x_1 - x_2\alpha t - 2\pi m \alpha t)n] K_0(\alpha(1-t^2)^{1/2} n [(x_2 + 2\pi m)^2 + y^2]^{1/2}) .$$ (A32)

(9) $\langle V \rangle_{12}$ and C_{12} can be most conveniently combined to give

$$\langle V \rangle_{12} + C_{12} = \frac{M^2}{A_0} \int_{-\infty}^{\infty} dk_z \sum_{l \neq 00} \hat{\rho}(\vec{R}_l + k_z \hat{z}) \left[\frac{\hat{\rho}^*(\vec{R}_l + k_z \hat{z}) - 2s(\vec{R}_l + k_z \hat{z})}{K_l^2 + k_z^2} \right] . \tag{A33}$$

(10) U_3, $\langle V \rangle_3$, and C_3 can be combined to give

$$U_3 + \langle V \rangle_3 + C_3 = \frac{M^2}{A_0} \oint_{-\infty}^{\infty} \frac{|s(k_z \hat{z}) - \hat{\rho}(k_z \hat{z})|^2}{k_z^2} \, dk_z . \tag{A34}$$

---

*Permanent address: Physics Department, University of Florida, Gainesville, Fla. 32611.

[1]F. E. Harris, Theor. Chem. 1, 147 (1975).

[2]See for example, M. Abramowitz and I. Stegun, *Handbook of Mathematical Functions* (Dover, New York, 1965), p. 806, Eq. (23.1.30); also Ref. 1, p. 165, Eq. (34).

[3]W. J. Olver, *Asymptotics and Special Functions* (Academic, New York, 1974), p. 306.

[4]F. E. Harris, H. J. Monkhorst, and W. A. Schwalm, J. Vac. Sci. Technol. 16, 1318 (1979).

[5]F. E. Harris and H. J. Monkhorst, Phys. Rev. B 2, 4400 (1970).

[6]W. A. Schwalm and H. H. Monkhorst (unpublished).

Distribution List

Office of Naval Research
800 N. Quincy Street
Arlington, Virginia 22217
Attention: Dr. George Wright

ONR Branch Office
1030 E. Green Street
Pasadena, California 91106

Elmer G. Keith
ONR Resident Representative
239 Campbell Hall
University of California
Berkeley, California 94720

NRL Code 2627 (6 copies)
Naval Research Laboratory
Washington, D. C. 20375

ONR Code 102IP (6 copies)
800 N. Quincy Street
Arlington, Virginia 22217

Defense Documentation Center (12 copies)
Bldg. 5, Cameron Station
Alexandria, Virginia 22314

Office of Research Administration
University of Utah
Salt Lake City, Utah 84112

Frank E. Harris
Department of Physics
University of Utah
Salt Lake City, Utah 84112

DATE FILMED

8